University of Reading

Accelerating innovations in C-H activation/functionalization through intricately designed magnetic nanomaterials: from genesis to applicability in liquid/regio/photo catalysis

Article

Published Version

Creative Commons: Attribution 4.0 (CC-BY)

open access

Dutta, S., Kumar, P., Yadav, S., Sharma, R. D., Shivaprasad, P., Vimaleswaran, K. S., Srivastava, A. and Sharma, R. K. (2023) Accelerating innovations in C-H activation/functionalization through intricately designed magnetic nanomaterials: from genesis to applicability in liquid/regio/photo catalysis. Catalysis Communications, 175. 106615. ISSN 1566-7367 doi: https://doi.org/10.1016/j.catcom.2023.106615 Available at https://centaur.reading.ac.uk/109987/

It is advisable to refer to the publisher's version if you intend to cite from the work. See Guidance on citing.

To link to this article DOI: http://dx.doi.org/10.1016/j.catcom.2023.106615

Publisher: Elsevier

All outputs in CentAUR are protected by Intellectual Property Rights law,

University of Reading

including copyright law. Copyright and IPR is retained by the creators or other copyright holders. Terms and conditions for use of this material are defined in the End User Agreement.

www.reading.ac.uk/centaur

CentAUR

Central Archive at the University of Reading

Reading's research outputs online

Catalysis Communications 175 (2023) 106615

Contents lists available at ScienceDirect

Catalysis Communications

journal homepage: www.elsevier.com/locate/catcom

Accelerating innovations in C—H activation/functionalization through intricately designed magnetic nanomaterials: From genesis to applicability in liquid/regio/photo catalysis

Sriparna Dutta [a,b], Prashant Kumar [c], Sneha Yadav [a], Ruchi Dubey Sharma [d], Parimala Shivaprasad [e], Karani S. Vimaleswaran [f,g], Anju Srivastava [b], Rakesh K. Sharma [a,*]

[a] Green Chemistry Network Centre, Department of Chemistry, University of Delhi, Delhi, India
[b] Hindu College, Department of Chemistry, University of Delhi, Delhi 110007, India
[c] Department of Chemistry, SRM University, Delhi-NCR, Sonepat, Haryana, India
[d] Department of Chemistry, Career College, Bhopal, Madhya Pradesh, India
[e] Department of Chemical Engineering, University of Bath, Claverton Down, Bath BA2 7AY, UK
[f] Department of Food and Nutritional Sciences, Hugh Sinclair Unit of Human Nutrition, University of Reading, Reading, UK
[g] The Institute for Food, Nutrition, and Health (IFNH), University of Reading, Reading, UK

ARTICLE INFO

Keywords:
Magnetic nanocatalysts
C—H functionalization
Heterocycles
Sustainable synthesis
Magnetic retrievability

ABSTRACT

Selective functionalization of highly inert and ubiquitous C—H bonds that would provide a ready access to synthetically valuable motifs has perplexed the chemists since long. Also, environmental benignity and economic viability have been the prime factors driving tremendous interest in C—H functionalization. This has led to many inspiring discoveries infuriating the development of potent catalytic systems that enable the facile replacement of the C—H bonds with conventional functional groups, allowing the construction of C-C, C-N, C-O, C-S, C-B and C-halogen bonds at both sp^2 as well as sp^3 centres. In fact, catalytic C—H functionalization strategies integrating the benefits of magnetic recovery have emerged as sustainable gateway for affording a diverse array of transformations. This review sheds light on the remarkable advancements witnessed in this area as a consequence of integrating the inherent magnetism of catalysts with the cutting-edge direct C—H functionalization strategy. Also, the promising future perspectives comprehensively covered in this review is anticipated to motivate the academic and industrial researchers, arousing their creativity for designing competent sustainable strategies to generate a plethora of pharmaceutically active molecules.

1. Introduction

Catalysis has emerged as a pinnacle technology for engineering a more sustainable world [1]. It is undeniably the virtual force behind all the chemicals we use today. Capturing a snapshot of the events and developments that took place in this field, we find that most of the innovations have been accredited with noble prizes that have indeed changed the entire landscape of organic synthesis. The constant urge to meet the challenges of energy and sustainability have paved the pathway for green catalysis; key goals of a green catalyst have been outlined which include high activity, facile recovery and excellent selectivity [2]. Thus, the search for such a kind of ideal catalyst that can display the inherent capability to control the synthesis of architecturally complex molecules has continued to infuriate immense enthusiasm and interest amongst researchers. Notably, with the introduction of magnetic nanocatalysts that offer bright prospects of facile recovery *via* attraction with an external magnet, whilst offering exceptional activity in terms of catalyst performance, a myriad of organic reactions have already been benefitted [3]. Amongst these, the C—H activation and functionalization that allows the direct activation of highly inert/unreactive C—H bonds and formation of new C-X bond (where X=O, N, S, C, B or halogen) leading to the synthesis of industrially significant molecules has witnessed a rapid economic and environmental boost with the utilization of magnetically recoverable nanocatalysts [4]. This novel reactivity concept has given promising direction to researchers for accomplishing the straightforward derivatization of diverse organic molecules with improved selectivity. Indeed the historical developments of the catalytic C—H functionalization have truly enthused both

* Corresponding author at: Green Chemistry Network Centre, Department of Chemistry, University of Delhi, Delhi 110007, India.
E-mail address: rksharmagreenchem@hotmail.com (R.K. Sharma).

https://doi.org/10.1016/j.catcom.2023.106615
Received 29 November 2022; Received in revised form 7 January 2023; Accepted 16 January 2023
Available online 20 January 2023
1566-7367/© 2023 The Authors. Published by Elsevier B.V. This is an open access article under the CC BY license (http://creativecommons.org/licenses/by/4.0/).

academia and industries. Despite the unquestionable significance, initially most of these protocols invariably suffered from limitations of requirement of high boiling point organic solvents, poor regioselectivity, longer reaction times, etc; however, with time and discovery of novel catalysts, these challenges have also been combatted [5]. Also, there has been an expansion from functionalization of simple hydrocarbons to complex molecules and today it has matured to a point where it can be contemplated as a viable strategy for synthesis of a broad spectrum of targets; leading to the publication of more than 400 papers in renowned journals. The idea of utilizing magnetic separation of catalysts has further added to the credentials of this category of reaction from a green chemistry perspective. Also, one of the most magical facts associated with these nanocatalysts is that they allow the fine tuning/tailoring of their catalytic activity and help in meeting the unresolved challenges of C—H functionalization [6].

Henceforth, the cocktail of C—H functionalization with magnetic recovery is being perceived as the most promising tool to generate pharmaceuticals and natural products, replacing many of the classical waste generating processes. Till date, a variety of such catalysts have been employed for efficient catalytic conversion of C(sp^3)–H and C(sp^2)–H bonds which have laid the foundation of sustainable industrial applications [7]. This review attempts to assimilate the literature reports wherein use of magnetic nanocatalysts have been wondrously integrated with C—H activation/functionalization for drawing utmost monetary as well as environmental benefits. A diverse set of C—H functionalization is chosen encompassing the C-C, C-N, C-O, C-S and C-halogen bonds. Also, the latest innovative techniques such as photochemistry and flow chemistry are being highlighted with special coverage being given to their futuristic aspects/perspectives that would open the doors for further research in this area. In addition, the future challenges have also been outlined that indicate the need to develop catalytic materials for the regioselective and enantioselective synthesis of drug moieties. Due attention has also been devoted towards critical analysis on the use of the MNPs based catalysts by shedding light on their toxicological aspects and the inferences drawn clearly signify that these NPs are not hazardous for human health and environment and lie under the umbrella of green chemistry.

2. Scope of review

C–H activation was given top priority in the list of aspirational reactions by the ACS GCI Pharmaceutical Roundtable way back in 2005, fueling the research interest of the scientific community [8]. Considering the immense significance, massive efforts have been directed towards profitably exploiting this strategy which has been covered in a few review articles published earlier. However, none of reviews focused on the impressive breakthroughs achieved in this field with the introduction of magnetic nanocatalysts. This review article attempts to comprehensively summarize the remarkable advancements encountered in the design and development of novel potent magnetically retrievable nanocatalysts for expediting the direct formation of C-X bonds *via* C—H activation, leading to sustainable synthesis and selective functionalization of industrially significant organic molecules including therapeutic agents. It is anticipated that it will serve as a guide to inspire both academic as well as industrial researchers to push the boundaries of the classic C—H functionalization.

3. Fabrication of magnetically recoverable nanocatalysts

3.1. Latest innovative synthetic methodologies for magnetic NPs

Magnetic nanoparticles have entranced the fields of science and technology spanning the biotechnology sector, medical imaging, drug delivery, data storage, catalysis, environmental remediation, etc. with their revolutionary properties such as controllable size and shape, robustness, high surface area to volume ratio, high dispersability, etc. [9]. But most importantly, it is their riveting superparamagnetic properties which assist in ready separation, adding a sustainable feature to their potential [10]. Also, they offer exceptional recyclability which is the bottleneck for any industrial application. Although there are wide range of MNPs including pure metal based (Fe, Co), alloys, spinels (AB_2O_4 where A=Co, Mg, Fe, Mn and B= Fe) however Fe_3O_4 NPs which are commonly known as magnetite or ferrite have particularly acquired paramount importance due to their high saturation magnetization (Ms) value [11]. It has an inverse spinel structure wherein Fe (II) and Fe(III) ions occupy octahedral sites while half of the Fe (III) ions occupy the tetrahedral holes. Owing to their significance, a plethora of reports have been documented on the synthesis of Fe_3O_4 NPs. Conventionally, co-precipitation, thermal decomposition, microemulsion and solvothermal techniques have been employed extensively for synthesizing the magnetite NPs with a variable size range which have been given due coverage in reviews [12]. However, these principle preparative methods suffer from a few setbacks which limit their large scale industrial applicability including poor crystallinity, problems of aggregation, requirement of longer reaction time, high temperature and pressure, larger volumes of solvents, low yield and poor reproducibility. Apart from these, a number of other approaches/pathways have been utilized for fabricating these NPs, some of which offer great prospects of controlling their size, uniformity and crystallinity and durability. The possibility to tune their size and shape by bringing a notable change in the reaction conditions has particularly proven highly useful for the catalytic sector. Polshettiwar *et. al* had demonstrated the possibility of producing six diverse, captivating morphologies by altering the iron precursor and synthetic conditions [13]. Table 1 summarizes the latest techniques adopted for their synthesis:

3.2. Surface modification/functionalization of Fe_3O_4 NPs

Despite proving its widespread utility in a myriad of organic transformations, bare Fe_3O_4 NPs suffer from critical issues of agglomeration occurring due to high surface energies associated with their large surface area to volume ratio, resulting in loss of their magnetism and catalytic activity [22] Also, they are highly susceptible to oxidation and get readily oxidized in the physiological environment that hampers their dispersibility as well as magnetic properties. Henceforth, it is important to incorporate effective surface modification strategies to impart protection and restore the stability of the MNPs. This is usually accomplished *via* the use of an appropriate coating strategy wherein the surface of the naked MNPs are coated with either organic molecules such as surfactants, polymers and biomolecules or inorganic layers such as silica [23,24] carbon [25,26]. precious metals (Ag, Au) [27,28], metal oxide [29], metal sulphides [30] metal hydroxides [31,32]. Successful coating (protective layer around MNPs) not only prevents the aggregation and oxidation of the NPs, but also offers prospects of further functionalization which is a key step followed for improvement in their physicochemical properties such as wetting, adhesion and friction. In this way surface modification (coating and functionalization) can aid in engineering of the iron oxide NPs suited for the desired catalytic application (Fig. 1).

3.2.1. Coating of MNPs

Synthesis of MNPs while maintaining the long term stability has been a real challenge for the chemists. Thankfully, with the help of effective coating strategies, this problem has been resolved to a great extent [33]. The non-magnetic protective shell formed around the surface of the naked MNPs suppresses the magnetic bipolar interactions, preventing them from aggregating. In the list of the various coating agents employed, silica (SiO_2) has proven to be the material of choice as it has a high binding strength with the iron oxide core, possesses exceptional thermal stability, exhibits chemical inertness showing resistance to various organic solvents and does not affect the redox reaction at the core which is the reason for the naked MNPs maintaining a high

Table 1
Recent synthetic approaches for formation of Fe_3O_4 NPs.

S. No	Method adopted	Description	Examples	Reaction temperature and Time Period	Morphology obtained (Size Distribution and Shape Control)	Advantages
1.	Template Mediated Synthesis	Involves the use of a sacrificial template of chemical, biological or polymeric origin to enable shaping of the initial structure. After use, the template is removed using an acid or base.	The template solvothermal strategy was adopted by Polshettiwar *et al.* for obtaining six distinct shaped iron oxide NPs by altering the iron precursor employed [13].	80-180°C	Nanorods, nanohusks, distorted cubes, nanocubes, porous spheres and self-oriented flowers.	Leads to the fabrication of nanomaterials with well-defined morphologies
2.	Sonochemical Method	Ultrasonic irradiation leads to the creation of extremely high temperature and pressure conditions within a very short time period that cannot be realized by other traditional energy sources.	-Wang and co-workers synthesized Fe_3O_4 NPs using a sonochemical co-precipitation method [14]. -Abu Much *et al.* accomplished the synthesis of Fe_3O_4 NPs using this method [15].	Very high temperature	-NPs of smaller size and narrow size distribution could be synthesized. -Extreme conditions resulted in the formation of rod shaped particles, instead of spheres.	Provides precise control over size, morphology, composition, magnetic and surface properties of the developed nanostructures
3.	Continuous Flow Synthesis	Use of continuous flow reactors involve an array of chemical processes that are performed in continuous flowing streams within micro-reactors.	Togashi and team achieved the synthesis of water dispersable Fe_3O_4 NPs with the aid of a continuous tubular flow reactor under conditions of high temperature and pressure using 3,4-dihydroxyhydro-cinnamic acid [16].	Very high temperature and residence time of 1.8 s	Particle morphology was spherical for all reaction temperatures employed during synthesis.	-Aligns the goals of Green Chemistry -Enhanced thermal management, improved mass transfer, mixing control, scalability, rapid chemical reactions and ability to withstand harsh reaction conditions.
4.	Microwave assisted synthesis	Microwave irradiation incorporates the concepts of dipolar polarization and ionic conduction effects.	Using the microwave assisted oxidation technique, Fe_3O_4 nanocrystals possessing five different morphologies were prepared by Yu and team [17].	Very high temperature	Nanospheres, nanocubes, nanorods, nano-octahedrons and nanoplates	-Uniform heating, fast reaction under a controlled environment, products with high purity, yield - Leads to the formation of nanostructures that possess a narrow size distribution and a higher degree of crystallinity.
5.	Bio-inspired co-precipitation Method	Emulating nature's best biological ideas (biomineralization strategies) and integrating it with the co-precipitation technique.	Lenders and co-workers elucidated the synthesis of Fe_3O_4 NPs by using a biologically derived M6A peptide additive that worked as nucleation and growth controller [18]. The inspiration was drawn from the mineralization strategy adopted by the magnetotactic bacteria. Initially a slow co-precipitation using Fe(II)/Fe(III) salts in presence of ammonia is effectuated during which ferrihydrate gets precipitated at low pH and there is an eventual conversion to Fe_3O_4 crystals on increasing the pH.	r.t. and 2-12 h	-Small crystals with superparamagnetic properties. -17 ± 8 nm in size (as determined *via* the TEM analysis).	As compared to the conventional co-precipitation methodology, this strategy allows the fine tuning of crystal size *via* manipulation in the iron concentration and NH_3 influx.
6.	Green Sustainable Method	Eco-friendly synthesis of MNPs using plant extracts which work as reducing and capping agents	Yew *et al.* reported the rapid sustainable synthesis of Fe_3O_4 NPs using seaweed (kappaphycus alvarezii) extract [19]. The synthesis was initiated by taking a solution of Fe^{3+} and Fe^{2+} in a 2:1 M ratio and adding it into the seaweed extract for the formation of a yellowish solution. To this, 1.0 M of NaOH was added drop-wise.	Ambient temperature for 1 h	TEM images revealed the formation of agglomerated NPs size ranging between 11.0 and 20.0 nm.	-Greener approach; no requirement of addition of external reducing agent. -Mild conditions
7.	Controllable self-assembly involving the combination of Pickering emulsions approach and polymer grafting	Pickering emulsions are those which are stabilized by solid particles that adsorb onto the interface between the two phases named after S.U. Pickering. ARGET ATRP are activators that are generated *via* the electron transfer process leading to the formation of reducing agents for the regeneration of a metal (I).	Ampiphillic Fe_3O_4 NPs were fabricated by Wu *et al.* using the cocktail of pickering emulsions approach and activators regenerated by electron transfer for atom transfer radical polymerization (ARGET-ATRP) [20]. The hydrophilic Fe_3O_4 NPs were prepared using polyol method, followed by preparation of Fe_3O_4/ wax composite microspheres wherein paraffin wax and ultrapure	70 °C for 12 h	The synthesized NPs had a size ranging between 30 nm-150 nm in water.	-High saturation magnetization -Exhibits highly controllable self-assembly behaviour in different solvents

(*continued on next page*)

Table 1 (*continued*)

S. No	Method adopted	Description	Examples	Reaction temperature and Time Period	Morphology obtained (Size Distribution and Shape Control)	Advantages
			water were added to Fe_3O_4 suspension under stirring. The composite was dispersed in ethanol and reacted with bromoacetic acid. Finally ARGET-ATRP process lead to the synthesis of the desired NPs.			
8.	Solution based dehydration process	Oleic acid crowned Fe_3O_4 nanoparticles were synthesized on an ultra-large –scale.	Ultra large scale synthesis of Fe_3O_4 NPs was accomplished by Su and team using a solution based dehydration process in autoclave reactor [21] Oleic acid and NaOH were dissolved in toluene, ethanol and water under vigorous stirring conditions to which Fe (II) and Fe (III) salts were added and refluxed at 70 °C for 4 h under vigorous stirring conditions.	70 °C for 4 h	Formation of irregular cubic shape particles with the size range of 50-200 nm	Facile synthetic procedure that can be upscaled easily for industrial applications.

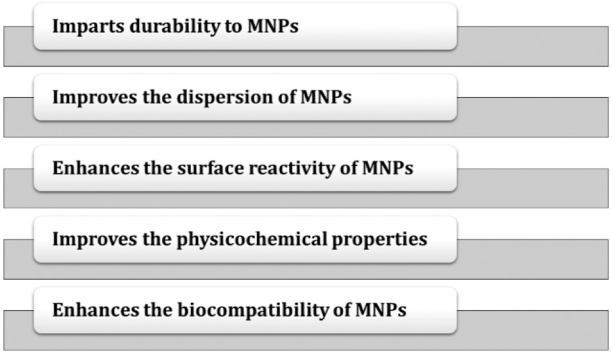

Fig. 1. Advantages of surface modification of MNPs.

saturation magnetization value [34]. In addition to this, silica also has terminal silanol groups present on its surface which can be utilized for further attachment of functionalities. Sol gel, micro-emulsion and silicic acid solution mediated approaches have been commonly employed for the silica coating of MNPs using sodium silicate or TEOS (Tetraethylorthosilicate) as silica precursors. These strategies have integrated the desirable advantages of coating (i) stability and (ii) providing sites for covalent linkage of functional groups. On the other hand, for the carbon coating of the MNPs, hydrothermal, sonochemical and flame spray pyrolysis based methods have been incorporated using glucose and cellulose as carbon precursors. The carbon coated MNPs have displayed good chemical and thermal stability as well as excellent biocompatibility [35]. Polymers have also been employed as coating agents and to accomplish the polymeric coating, inversion microemulsion and oxidative polymerization techniques have been adopted with the use of polyesters, polyaniline and polyethylene glycol as reaction precursors [36]. Polymers have helped in enhancing colloidal stability of the MNPs. Recently, Neamtu *et al.* encapsulated nano magnetite within an eco-friendly polymeric matrix (PEG) and used it for the purpose of photodegradation of Bisphenol-A (BPA) [37]. Metal, metal oxide and metal hydroxides have been also utilized for the purpose of coating by using micro-emulsion, redox metalation, iterative hydroxylamine seeding, sonochemical, sol-gel, homogeneous co-precipitation and seed assisted hydrothermal methods.

3.2.2. *Functionalization of MNPs*

The prime objective of functionalization is to introduce functionalities on the surface of the MNPs which allow binding of other metals, polymers or biomolecules so that they can lead to the fabrication of advanced catalytic systems. The strategy adopted for the process of functionalization varies depending on the interaction of the linker with the MNPs. Fig. 2 highlights the two prime approaches commonly employed for functionalizing the MNPs.

The functional group may be directly introduced onto the surface of bare MNPs or silica coated magnetic nanoparticles (SMNPs) which comprise of abundant hydroxyl groups. These can be covalently attached to organic molecules that work as functionalizing agents (FA). Popular examples of functionalizing agents include silane agents such as 3-amino-propyltriethoxysilane (APTES), p-aminophenyltrimethylsilane (APTS), mercaptopropyltriethoxysilane (MPTES) [38]. The reaction between MNPs and silanes leads to the formation of Si-O bonds. For instance: Sharma *et al.* utilized APTES for the purpose of incorporating amine groups onto the surface of SMNPs which lead to the formation of ASMNPs [39]. Thereafter, a suitable ligand was grafted onto the surface of the amine functionalized NPs *via* a Schiff's base condensation process and finally the ligand grafted ASMNPs were metallated using a desired metal salt. Apart from silanes, phosphonates, carboxylates, sulphonates, sulfamates etc. have also been used for the purpose of functionalization [40] In the application part, there is an extensive focus on illustration of how functionalization has been achieved for the purpose of fabricating robust catalysts that have boosted various C—H functionalization/activation reactions.

3.3. *Approaches for catalyst design*

The beauty of C—H functionalization process lies in the controlled functionalization of specific C–H bonds even in the presence of apparently more reactive functional moiety. With the advent of nano-magnetite based catalytic systems, new opportunities have been

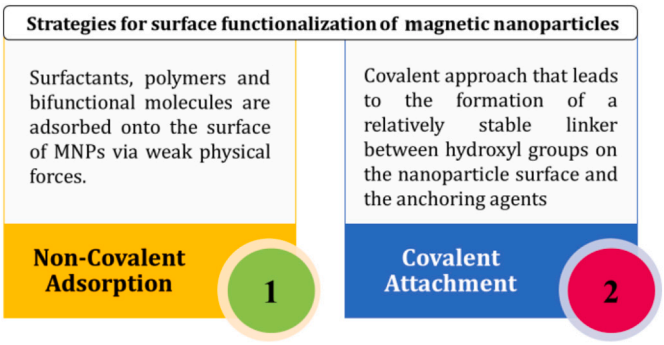

Fig. 2. Prime approaches for functionalization of MNPs.

unravelled in achieving site selective C—H functionalization. Thus, catalyst designing stands as a crucial step for affording this transformation. The previous subsections have described how the MNPs can be synthesized and functionalized. For the purpose of catalyst design, four prime approaches have been utilized: (i) Dispersion of metal NPs onto the surface of MNPs using wet impregnation approach [41] (ii) Covalent immobilization approach wherein a ligand is chosen which is grafted onto the surface of functionalized MNPs and thereafter metalation is done [42] (iii) Functionalization of MNPs wherein the functionalized MNPs are used as catalysts [43] (iv) Direct one-pot synthesis of metal loaded MNPs [44]. Ensuing subsections would help readers in gaining an insight into these incorporation of these approaches for designing a magnetic nanocatalyst.

3.3.1. *Dispersion of metal NPs onto the surface of MNPs using wet impregnation approach*

Wet impregnation is one of the most well-known techniques used for the fabrication of heterogeneous catalysts [45]. It involves the dissolution of active metal precursor in aqueous or organic solution followed by addition of the metal solution to catalyst support comprising of same pore volume as the volume of the solution that was added. The solution gets drawn into the pores *via* capillary action, while the excess of the solution then causes the transport of solvent to get transformed from the capillary action to a slow diffusion process. Finally, the catalyst is dried and calcined to remove any volatile component if present in the solution. The method has been named as wet impregnation because the impregnated substance maintains a dry nature at a macroscopic scale [46]. Lately, this approach has gained an increasing momentum in the synthesis of Fe_3O_4 supported catalysts (Scheme 1). There are several examples wherein such catalysts have been fabricated by adopting the wet impregnation methodology enlisted in Table 2. Apart from Fe_3O_4, other magnetic nanoparticles based catalysts have also been projected.

3.3.2. *Covalent immobilization approach*

Covalent immobilization approach has emerged as one of the best synthetic methods for fabricating active and durable catalysts. This is based on a heterogenization approach wherein a homogeneous metal complex/enzymatic complex is covalently tethered/anchored onto the surface of a solid support material [52,53]. Owing to covalent bond formation between the support matrix and complex, the final catalyst is stable and does not suffer from any leaching/sintering issues. This approach has been exploited over the years for designing MNPs supported catalyst that have proven to be highly promising in their action towards diverse industrially significant reactions. For instance: Sharma *et al.* accomplished the covalent immobilization of a quinoline-2-carboimine copper complex onto the surface of amine functionalized silica encapsulated Fe_3O_4 nanoparticles which was utilized as a catalyst for expediting the C—H activation of formamides [6a]. This catalyst offered notable advantages of high activity (in terms of conversion percentage and TON), facile recovery and outstanding recyclability. The detailed description (schematic illustration as well as other details) has been provided in the application section. Table 3 projects examples of catalysts fabricated using this approach that has shown unparalleled activity in various reactions of industrial significance.

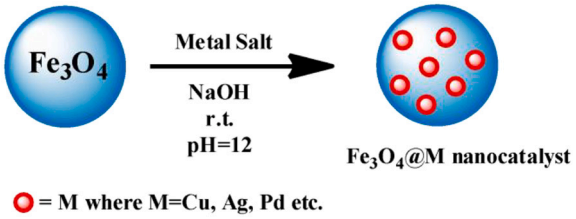

Scheme 1. Wet impregnation method for synthesis of magnetic nanocatalysts.

Table 2
Examples of wet impregnation strategy employed for the fabrication of Fe_3O_4@M nanocatalyst.

Sl. No	Catalyst Prepared	Morphology	Advantages	Ref
1.	Nanocat-Fe-CuO	-Spherical NPs with size ranging between 20−30 nm -Uniform distribution of Cu, Fe, and O on the surface of magnetite (evidenced by elemental mapping images)	-Facile and sustainable preparative method -Use of inexpensive precursors -Excellent catalytic activity in the synthesis of 4-methoxyaniline, pyrazole derivatives, and Ullmann-type condensation. -Appreciable catalytic recyclability upto six runs	[47]
2.	Nano-Fe_3O_4−CoO_x	-Spherical morphology with nanosized dimensions -Some aggregates of individual Fe_3O_4−CoO_x NPs were observed	-Good catalytic performance for the conversion of 5-hydroxymethylfurfural into 2,5-furandicarboxylic acid (FDCA)	[48]
3.	Cu/$CuFe_2O_4$ @C	- TEM analysis revealed the presence of black colored mixed oxide having spherical morphology with size distribution of 6.3 ± 0.4 nm (distributed well over nanoporous carbon support)	-Displays high selectivity (100%) in the hydrodeoxygenation (HDO) of biomass-derived furfural (FFR) to 2-methyl furan (MF) - Catalyst displayed high stability upto 5th run without any drastic loss of the active component (Cu).	[49]
4.	NiO/Co_3O_4 and Fe_2O_3/Co_3O_4	-Small clusters (ca. 5 nm) of Fe_2O_3 were found to wet the surface of Co_3O_4, whereas in case of the nickel nanocatalyst, NiO grew as distinct isolated particles having big diameter (35-45 nm).	-High durability	[50]
5.	Fe_3O_4@Au/TiO_2 catalyst	-Fe_3O_4@Au NPs i. e. the unsupported NPs displayed size distribution of 5.34 ± 0.71 nm (core of about 4.9 nm and shell thickness of about 0.5 nm). - Particle size of final nanocatalyst (TiO_2-supported Fe_3O_4@Au NPs) was found to be about 5.96 ± 0.71 nm.	-High catalytic activity in CO oxidation due to the synergistic integration of Fe and Au.	[51]

3.3.3. *Functionalization of MNPs and use of Functionalized MNPs as Catalysts*

The functionalized MNPs can also be directly used as catalyst for some of the reactions and has been given due coverage in the previous surface modification section.

3.3.4. *Direct one-pot synthesis of metal loaded MNPs*

In this technique, the metal precursor as well as the key ingredients required for preparation of MNPs are taken in one pot and reacted together, leading to the in situ generation of MNPs and deposition of

metal over the MNPs. An example illustrating this process was provided by Park and co-workers who prepared hybrid nanocomposites of Cu-doped Pd–Fe_3O_4 using a controlled thermal decomposition approach [63]. For this, firstly sodium oleate (0.3 g) and 1-octadecene (ODE) (10 mL) were reacted in a three necked flask at 200 °C under Ar and continuous stirring. To the same reaction vessel, $Pd(OAc)_2$, oleylamine and $Fe(CO)_5$ were added sequentially. Finally, $Cu(acac)_2$ was added drop-wise into the resulting mixture and allowed to undergo heating at 240 °C (Scheme 2). Finally the product precipitated *via* the addition of ethanol and hexane, and separated by centrifugation. The catalyst proves its efficacy in the tandem synthesis of 2-phenylbenzofurans.

Another one pot procedure was reported for the fabrication of Pd/Fe_3O_4/charcoal nanocatalyst using the combination of solid state grinding and thermal decomposition [64]. The catalyst showed good

Table 3
Magnetic nanoparticles supported catalysts fabricated using covalent immobilization methodology.

Sl. No	Catalyst	Structure of catalyst	Preparative Method and Reaction Conditions	Catalytic Activity and Recyclability	Ref.
1.	Second-generation Hoveyda–Grubbs catalyst immobilized over MNPs *(MNPs were coated with orthoisopropoxystyrene ligands by covalent bonds)*	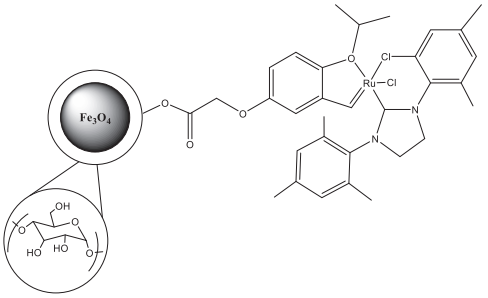	Commercially available MNP support was reacted with second generation Grubb's catalyst followed by metallation with Ru catalyst.	High activity for both self- and cross-metathesis of methyl oleate (MO)	[54]
2.	Magnetically retrievable ruthenium–arene–PTA (RAPTA) complex	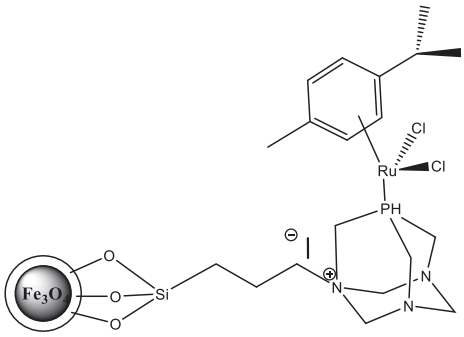	Fe_3O_4 nanoparticles were prepared using a co-precipitation method followed by coatinf of the MNPs with silica using a sol-gel approach. Thereafter, silica coated MNPS were functionalized with PTA functionalized magnetic nanoferrites and finally metallated with Ru complex.	High efficiency for the hydration of nitriles and various isomerization reactions in aqueous media	[55]
3.	Pd-NHC catalyst immobilized on core/shell super paramagnetic NPs *(consisted of a highly crystalline γ-Fe_2O_3 core and a very thin polymeric shell wall)*	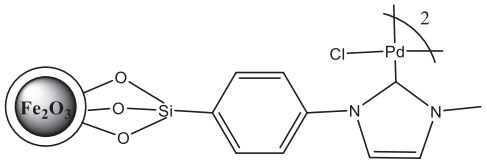	Emulsion polymerization approach was utilized and methylimidazole was loaded onto the surface of core/shell NPs by reacting MNPs with 1-methylimidazole in a refluxing toluene solution Then, Na_2CO_3 was used as a base for deprotonation of the imidazolium group to generate N-heterocyclic carbenes (NHCs) that could form strong complex with Pd catalyst.	More than 97% of Pd-iron oxide NPs could usually be recovered. - An average isolation yield of biphenyl product (82%).	[56]
4.	Magnetic nanoparticle-supported (β-oxoiminato) (phosphanyl) palladium catalyst	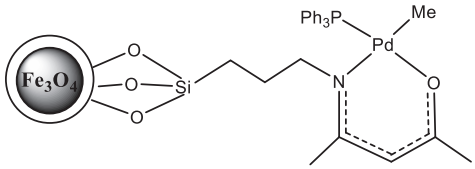	Triethoxysilyl-functionalized palladium complex immobilized on the surface of core-shell SiO_2/Fe_3O_4 in refluxing toluene	High catalytic activity (upto 95% yield) and excellent recyclability upto 10 runs	[57]
5.	Nano-FeDOPA Cu bimetallic catalyst	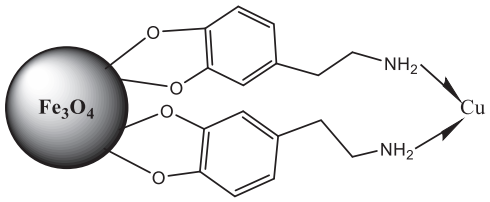	(β-oxoiminato)(phosphanyl) palladium complex was immobilized on the surface of silica coated Fe_3O_4 nanoparticles.	Microwave irradiation	[58]
6.	MoO_2 salpr-immobilized silica-coated nanocatalyst.		Covalent binding of a Schiff base ligand (N,N′-bis(3-salicylidenaminopropyl)amine) (salpr) onto the surface of silica-encapsulated magnetite nanoparticles (Si-MNPs)	Activity and selectivity remained persistent upto two catalytic runs	[59]

(*continued on next page*)

Table 3 (*continued*)

Sl. No	Catalyst	Structure of catalyst	Preparative Method and Reaction Conditions	Catalytic Activity and Recyclability	Ref.
		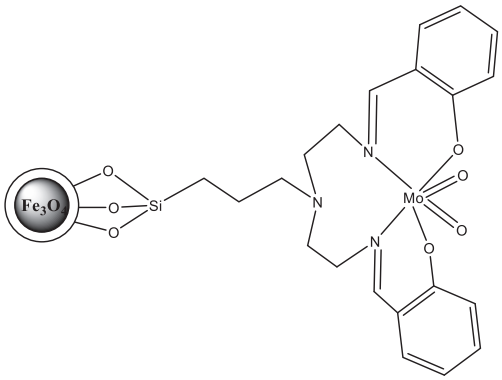			
7.	$Fe_3O_4/SiO_2–NH_2–M$ (M=Cu or Co).	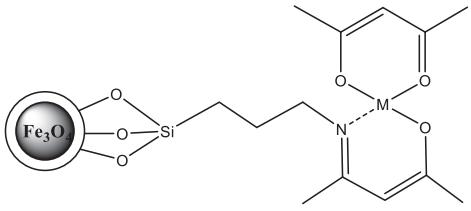 M = Co or Cu	Covalent anchoring of cobalt(II) or copper(II) acetylacetonate complexes ([$Co(acac)_2$] or [$Cu(acac)_2$]) onto core–shell structured Fe_3O_4/SiO_2 previously functionalized with 3-aminopropyl-triethoxysilane (APTES)	Good catalytic activity as evident through high styrene conversion upto 90% and reusability upto four runs	[60]
8.	Fe_3O_4 magnetic nanoparticle-supported gold dipyridine complex	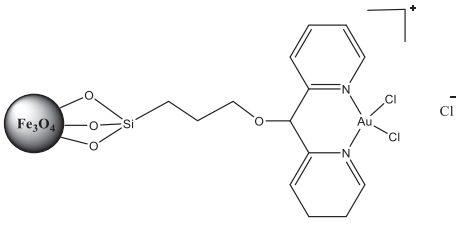	Prepared by sonicating nanoferrites with dipyridine (which acts as a robust anchor and avoids Au(III)) in absolute MeOH, followed by addition of sodium tetrachloroaurate (III) hydrate.	Excellent Yield	[61]
9.	Cu-BPy@Am-SiO_2@Fe_3O_4 Core−Shell Nanocatalyst	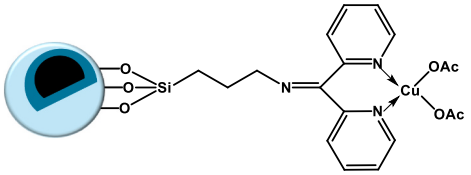	Am-SiO_2@Fe_3O_4 nanoparticles were reacted with BPy (4 mmol, 0.736 g) in ethanol for 10 h for the covalent immobilization.	-Catalyst reusable upto 8 catalytic cycles, and highly durable. -Excellent TON (upto 400)	[39b]
10.	Fe_3O_4@SiO_2-supported acetate-based butylimidazolium ionic liquid nanocatalyst	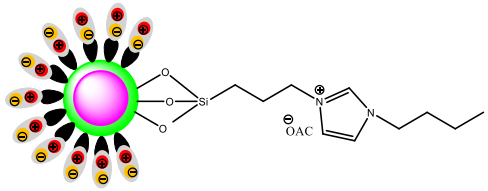	acetate-based butylimidazolium ionic liquid immobilized silica-coated magnetic nanoparticles (IL-OAc@FSMNP)	Exhibited conversion and selectivity (>99%) in reaction of aniline and its derivatives with ethylene carbonate to form bioactive N-aryl oxazolidin-2-ones	[62]

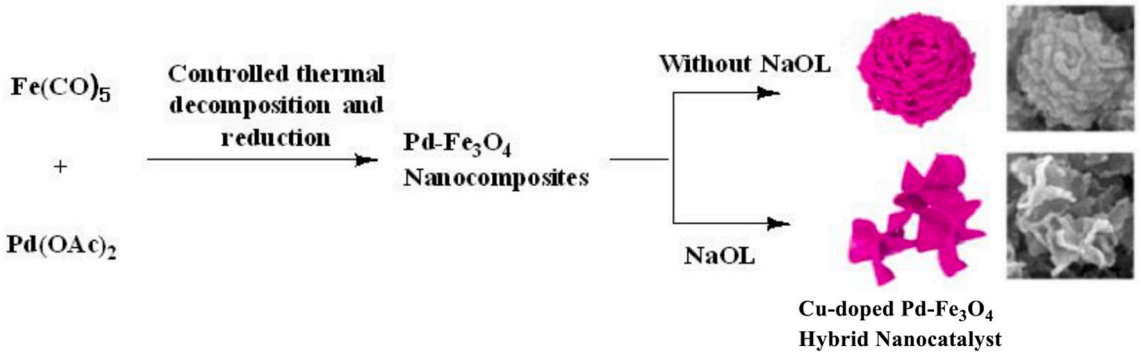

Scheme 2. Synthetic strategy for one-pot synthesis of Cu-doped Pd-Fe_3O_4 nanocomposites. Adopted from ref. [63]

activity in the Suzuki Miyaura coupling of substituted aryl halides and aryl boronic acids. For synthesizing the catalyst, firstly a mixture of Pd $(NO_3)_2 2H_2O$ and $Fe(NO_3)_3 9H_2O$ were concurrently melt-infiltrated into mesoporous charcoal by grinding well at r.t. and subsequent kept in oven for a day at 50 °C. Next, the infiltrated salt was decomposed into Pd and Fe_3O_4 nanoparticles *via* thermal decomposition at 400 °C under N_2 atmosphere.

4. Application of MNPs in C—H functionalization/activation

In an attempt to achieve completely green and sustainable organic transformations, over the past decades, there has been an explosive growth in the use of superparamagnetic MNPs based catalysts. Interestingly, these magnetically driven catalysts have shown remarkable efficacy in leveraging C—H functionalization/activation reactions owing to advantages of ready recovery facilitated by their superparamagnetic properties, good recyclability, high yield and selectivity, etc. [46,5b,65]. The size and shape of the NPs have been found to play a significant role in influencing the efficacy, selectivity and reusability of these catalysts. As expected, smaller NPs enhance the reactivity and selectivity due to larger surface area to volume ratio, while the shapes of the nanocatalysts favour the formation of catalytic active sites in specific surface planes. In addition to this, the choice of the MNP support also affects the catalytic performance *via* interaction with the other components decorated on the surface of the MNPs. Careful manipulation of these governing factors has permitted the design and development of superior magnetic nanocatalysts for gaining a ready access to important heterocyclic motifs, many of which form the core of marketed drug molecules *via* the effective exploitation of C—H functionalization/activation strategy. This section of the review enlightens the readers about the seminal studies focusing on synthesis of the magnetically retrievable nanocatalysts employed for boosting a wide set of C—H functionalization/activation reactions including C—H arylation, cyanation, alkylation, multicomponent reactions (MCRs) etc.

4.1. Direct C—H arylation of heteroarenes

Heterocyclic compounds constitute the largest and one of the most vital classes of organic compounds used in many biological fields due to their importance in the treatment of multiple illnesses and industries [66,67]. They play a crucial role in almost all the fields of science such as medicinal chemistry, biochemistry and synthetic chemistry, and are widely distributed in natural products, biomolecules and other bioactive molecules. Considering their multifaceted uses, pharmacists and organic chemists have been devoting extensive efforts toward the construction and functionalization of heterocyclic molecules using versatile, atom- and step-economical efficient synthetic strategies.

Imidazo[1,2-*a*]pyridine scaffold is of high significance as it is widely distributed in natural products, pharmaceuticals and an integral part of many marketed drugs. Molecules bearing imidazo[1,2-*a*]pyridine moiety display fascinating biological properties [68] and therefore continuous efforts have been directed towards the synthesis of C-2 and C-3 functionalized imidazo[1,2-*a*]pyridine [69]. In order to develop a greener approach for the direct C-3 C—H functionalization of imidazo [1,2-*a*]pyridine, Lee *et al.* designed a magnetically recoverable Pd-Fe_3O_4 bimetallic heterodimer nanocatalyst [70]. A two-step thermal decomposition method was used to prepare Pd-Fe_3O_4 bimetallic nanocatalyst by adding solid $Pd(acac)_2$ and solid $Fe(acac)_3$ to a solution of oleylamine and oleic acid. The synthesized nanoparticles were found to have 1:1 hybrid bimetallic system composed of a single Pd nanosphere with diameter of ~6 nm and a faceted Fe_3O_4 nanocrystal of ~30 nm in dimension. The application of this bimetallic hybrid nanocatalyst was investigated in the C—H arylation of imidazo[1,2-*a*]pyridine using wide range of aryl bromides. Aryl bromides bearing various functional groups such as CN, CHO, COMe, Cl, Me, OMe participated well in the reaction to give exclusively C-3 arylated product in moderate to excellent (42-95%) yield (Scheme 3). Electron rich aryl bromides provided inferior product yields in comparison of electron poor aryl bromides. However, the positions of substituents had no significant effect on the reaction outcomes, as comparable yields were obtained with *para*- and *meta*-substituted aryl bromides. Hindered aryl bromides such as 1- and 2-bromonaphthalenes, 9-bromoanthracene were also suitable for this reaction, endowing 70%, 75% and 58% product yield, respectively. Wondrously, the catalyst could be recovered readily with the aid of an external magnet and reused for 10 consecutive catalytic runs.

Moghaddam *et al.* prepared three different mixed metal oxide ferrite nanoparticles *viz.* $NiFe_2O_4$, $CuFe_2O_4$ and $CoFe_2O_4$ catalysts using co-precipitation method and compared their catalytic activity towards α-arylation of oxindoles with aryl halides [71]. The efficiency of these catalysts was exploited by studying the scope of reactions between various differently substituted aryl halides (iodo-, bromo- and chlorobenzenes) and oxindole derivatives (Scheme 4). The reaction showed good functional group tolerance in case of aryl halides by furnishing monoarylated oxindole derivatives in high yield with good selectivity. Similarly, the scope of several *N*-substituted oxindole (*N*-methyl, *N*-ethyl, *N*-phenyl, *N*-benzyl etc.) was also investigated in presence of these mixed metal oxide ferrite nanoparticles. Excellent product yields were obtained in short reaction time. Although, nickel and copper ferrite nanoparticles ($NiFe_2O_4$ and $CuFe_2O_4$) displayed comparable yield and selectivity towards monoarylated oxindole. However, in case of cobalt ferrite nanoparticles ($CoFe_2O_4$) an increase in the probability of formation of diarylated oxindoles were seen. To investigate the reusability of catalysts, reactions were carried out between bromobenzene and *N*-methyloxindole and deterioration in the catalytic efficacy of $NiFe_2O_4$ and $CuFe_2O_4$ NPs was found however, the catalytic activity of $CoFe_2O_4$ decreased after the fifth run.

Moving a step further, Frank Glorius and his team impregnated copper on magnetite to develop a reusable nanocatalyst (CuO/Fe_3O_4) for the direct C—H arylation of heteroarenes such as thiophenes, indoles, benzofurans, etc. under mild reaction conditions [72]. The catalyst was prepared by stirring the alkaline mixture of $CuCl_2$ and Fe_3O_4 at room temperature for 24 h. Initially, the applicability of this catalyst was examined for the scope of heteroarenes. It was found that electron-rich as well as electron poor thiophenes provided good reaction outcomes and 2-substituted thiophene resulted in regioselective C-5 arylation. 2,3-Dimethulfuran gave the corresponding C-2 aryl product in low yield with high regioselectivity (C5/C4> 99:1). Unprotected indole and *N*-methylindole also reacted with high selectivity delivering the good product yields. Afterwards, the scope of diaryliodonium salt was exploited. Experimental results revealed that electronically diverse diaryliodonium salt could react efficiently resulting in good to excellent yields of arylated products (Scheme 5). The catalyst could be recovered easily using a magnet and no loss in catalytic activity was seen even after five consecutive runs.

Shariatipour *et al.* fabricated a modified magnetic reduced graphene oxide supported palladium catalyst (MRGO@DAP-AO-Pd^{II}) by a multi-step approach and reported its applicability in selective C-5 arylation of

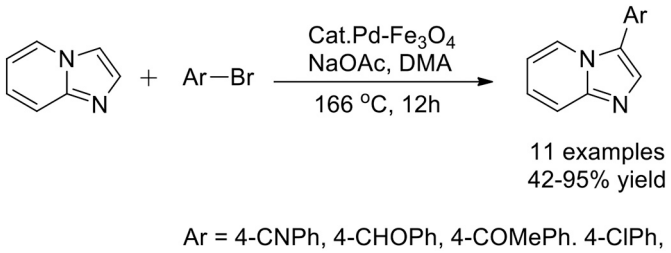

Scheme 3. Pd-Fe_3O_4 catalyzed selective C-3 arylation of imidazo[1,2-*a*]pyridine.

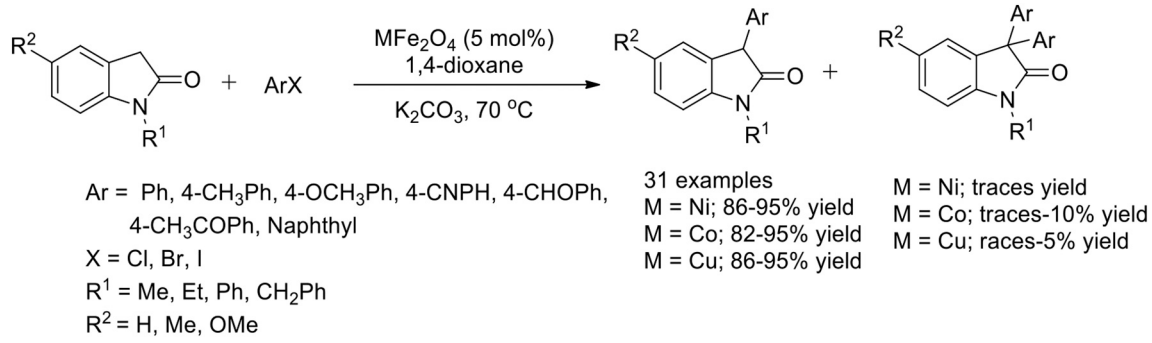

Scheme 4. Mixed metal oxide ferrite nanoparticles catalyzed α-arylation of oxindoles.

imidazoles using alkaline deep eutectic solvent (potassium carbonate in glycerol) under aerobic conditions [73]. During the preparation of catalyst, initially magnetic reduced graphene oxide (MRGO) was formed through *in situ* preparation of ferrite (Fe_3O_4) nanoparticles on the surface of graphene oxide (GO) by chemical co-precipitation process followed by subsequent reduction using 80% hydrazine hydrate. Then the modification of MRGO was carried out to prepare MRGO@DAP by treating MRGO with (3-chloropropyl)trimethoxysilane (CPTMS) and subsequent reaction with 2,6-diaminopyridine (DAP). Next, MRGO@DAP was functionalized with 2-chloroacetonitrile to afford cyanomethyl group which then converted into amidoxime to get MRGO@DAP-AO. Lastly, MRGO@DAP-AO was treated with $Pd(CH_3CN)_2Cl_2$ to accomplish MRGO@DAP-AO-Pd^{II} catalyst (Scheme 6a). The scope of the catalyst was explored in C-5 arylation of the imidazole using 0.3 mol% of MRGO@DAP-AO-Pd^{II} and it was found that the reaction proceeds smoothly to give good product yields. Aryl bromides either having electron-releasing (OMe, Me) groups or electron-donating (CHO, CO_2Me, F) groups resulted in better product yields. Sterically hindered α−naphthylbromide and heteroaryl bromide such as 2-brompyridine also afforded the desired products in good yields (Scheme 6b). The recyclability test of catalyst revealed that it could be reused seven times with no adequate loss in its catalytic activity, however drastic loss of product yield was seen in 8th run. The supremacy of MRGO@DAP-AO-Pd (II) catalyst was checked with previously reported catalysts in C—H arylation of 1,2-dimethylimidazole using 4-bromobenzaldehdye (Table 4). This catalyst was found to be more efficient in terms of low reaction time, good yield and reusability.

Likewise, Wang and co-workers used the Click chemistry concept to prepare a highly efficient and magnetically recoverable catalyst which involved the immobilization of 1,2,3-triazole-Pd^{II} complex on Fe_3O_4 magnetic nanoparticles that was subsequently utilized for the C-2 arylation of indoles using arylboronic acid [74]. The preparation of catalyst was done in a stepwise manner starting with the incorporation of thin layer of silica over Fe_3O_4 to synthesize Fe_3O_4@SiO_2 nanoparticles *via* sol-gel method. The Fe_3O_4@SiO_2 NPs were functionalized under refluxing conditions with (4-(azidomethyl)phenethyl)trimethoxysilane to introduce azide group on its surface. Afterwards, Click reaction was carried out between azide functionalized magnetic core-shell and phenylacetylene to generate triazole loaded MNPs. Finally, triazole functionalized MNPs were metallated using $Pd(OAc)_2$ solution (Scheme 7a). The efficacy of developed catalyst was examined in the C-2 arylation indoles with arylboronic acids. Both the substrates indoles and arylboronic acids reacted well in presence of Fe_3O_4@SiO_2 immobilized palladium catalyst to provide the corresponding products in good yields. Indoles containing electron-withdrawing groups such as F, CN, CO_2Me afforded slightly lower product yields in comparison to the ones containing electron-releasing Me and OMe groups. However, presence of electron-releasing groups (Me, OMe, *t*-Bu, biphenyl) and electron-withdrawing groups (F, Cl, CN, CO_2Me) on arylboronic acid had no considerable effect on product yield (Scheme 7b). Steric effect was seen in case of *ortho*-, *meta*- and *para*-methoxy phenylboronic acid which resulted in 65%, 82% and 71% yield of respective products. While examining the scope of recovery and reusability of the catalyst, it was found that the catalyst could be recycled and reused for 8 times without any substantial loss in its catalytic activity and product yield.

4.2. Cyanation of amines

The bifunctional α-aminonitrile compounds constitute a versatile class of intermediates used for the synthesis of several important organic

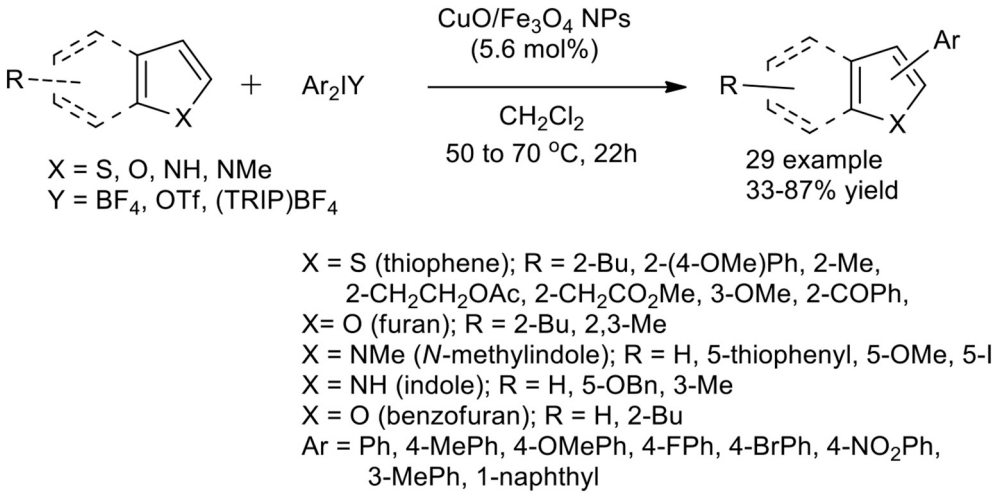

Scheme 5. CuO/Fe_3O_4 NPs catalyzed arylation of thiophene, furan and indoles.

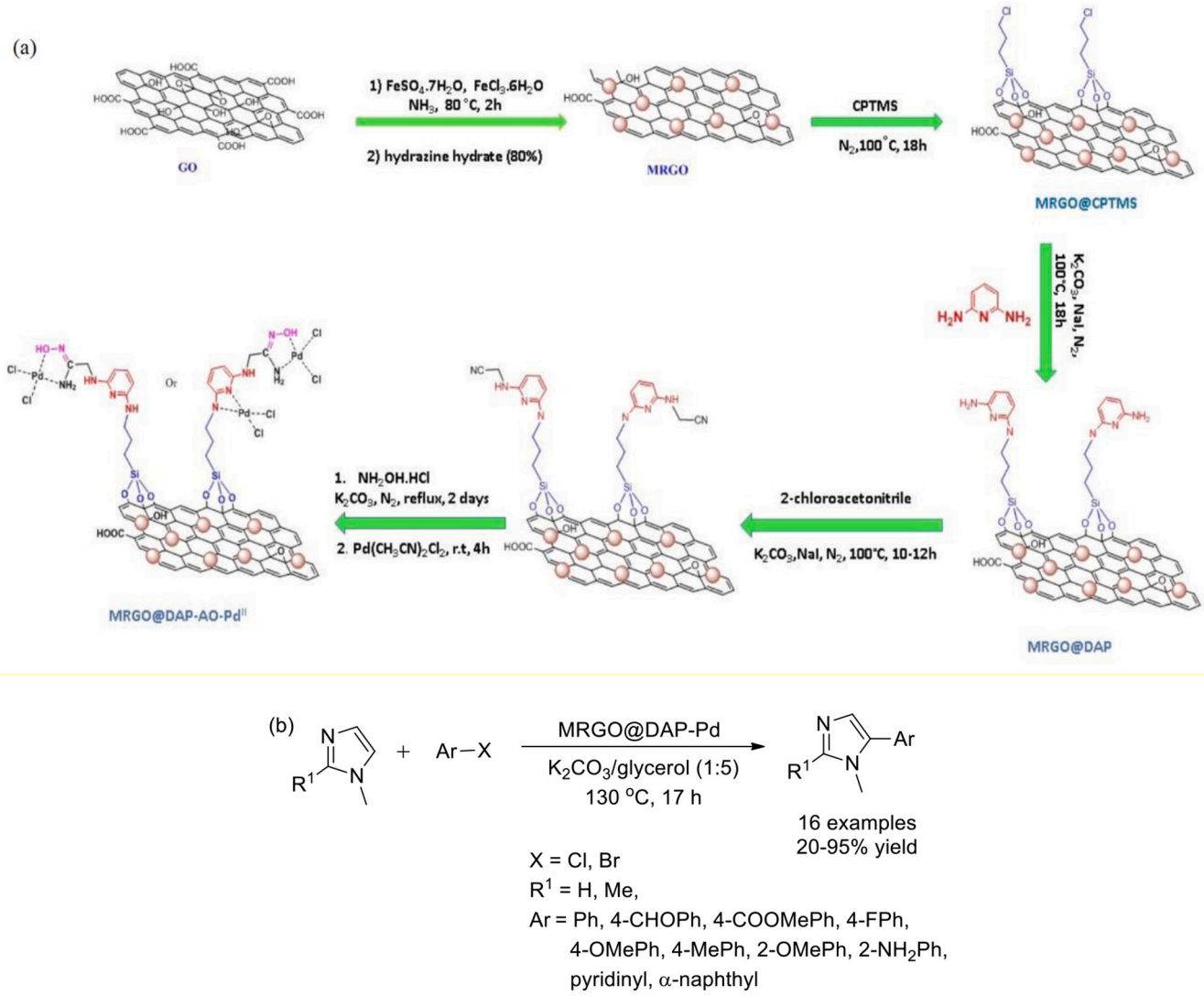

Scheme 6. (a) Preparation of MRGO@DAP-AO-Pd(II) catalyst; (b) C-5 arylation of imidazole using MRGO@DAP-AO-Pd(II). Adopted from ref. [73]

Table 4
Comparison of catalytic activity of MRGO@DAP-AO-Pd(II) with some literature reports for C—H arylation.

S. No.	Catalyst (mol%)	Solvent	Base	Temperature (°C)	Time (h)	Yield (%)
1	$Pd(OAc)_2$ (0.5-0.1 mol%)	DMA	KOAc	150	17	77
2	Bis(imino)acenaphthene (BIAN)-supportedPd-PEPPSI (0.5-0.1 mol %), PivOH (30 mol %	DMA	K_2CO_3	130	12	99
3	Pd-PEPPSI-IPr (1 mol %), PivOH(30 mol %)	DMA	K_2CO_3	130	12	98
4	Palladium(II) Complexes of *N*-Heterocyclic Carbene Amidates Derived from Chalcogenated Acetamide-Functionalized 1*H*-Benzimidazolium Salts (0.5 mol %), PivOH (30 mol %)	DMA	K_2CO_3	110	20	71
5	Pd@PPy (0.5 mol %)	DMA	KOAc	150	17	93
6	$Pd(OAc)_2$ (5 mol %), P(2-furyl)$_3$ (10 mol %)	DMF	K_2CO_3	110	24	80
7	$Pd(OAc)_2$(5 mol%) PPh_3(10 mol %)	DMF	K_2CO_3	140	48	93
8	MRGO@DAP- AO-Pd^{II} (0.3mol %)	K_2CO_3/ glycerol	-	130	17	95

molecules such as carbonyl compounds, α-amino acids, diamines, natural products and alkaloids, etc. [75]. Therefore, several synthetic strategies have been developed for the synthesis of these α-aminonitrile derivatives using stoichiometric amount of reagents [76] and lately transition-metal-catalyzed *via* C—H activation has also been profitably exploited for accomplishing these types of compounds [77]. To overcome the limitations of these methods which include increased waste generation, use of expensive and toxic metals, difficulty in recycling of catalysts, etc. Varma and co-workers in 2015, synthesized an iron based magnetically retrievable magnetic graphite carbon nitride (Fe@γ-C_3N_4) catalyst for α-cyanation of secondary and tertiary amines *via* C—H activation using sodium cyanide as effective source of cyano group and H_2O_2 as oxidant [78]. The synthesis of Fe@γ-C_3N_4 catalyst started with the preparation of graphitic carbon nitride (γ- C_3N_4) by calcination of urea, then dispersing in a 10% aqueous solution of PEG-400 followed by further stirring with $FeSO_47H_2O$ solution. Finally, iron sulfate was reduced to magnetic ferrites using $NaBH_4$ as the reducing agent (Scheme 8a). Synthetic applicability of Fe@γ-C_3N_4 was explored in selective

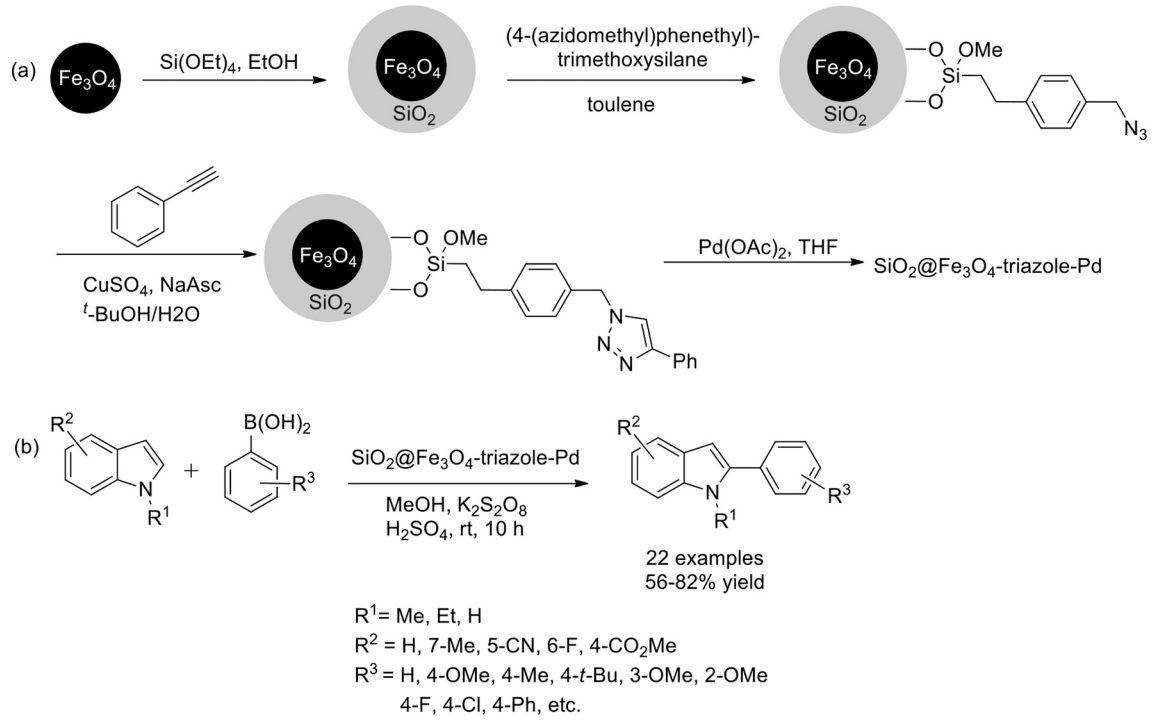

Scheme 7. (a) Preparation of SiO_2@Fe_3O_4-triazole-Pd nanocatalyst; (b) SiO_2@Fe_3O_4-triazole-Pd catalysed C-2 C—H functionalization of indoles using boric acid.

α-cyanation of amines. Applied amines (secondary and tertiary) reacted adequately to deliver the respective α-amino nitriles in good to excellent yields. Electronic behaviour of substituents present on amines display a crucial role in altering the reaction outcome, as the electron-releasing group (Me) provided slightly higher yield in comparison to electron-withdrawing groups (Br, NO_2) (Scheme 8b). The prepared catalyst could be recovered from the reaction mixture with the help of an external magnetic force and recycled for five times without any loss in its activity. The plausible reaction mechanism for this transformation is depicted in scheme 8c. The mechanism shows that the reaction proceeds through the formation of a reactive oxo-iron(IV) species which leads the formation of iminium ion upon reaction with tertiary amine. The iminium intermediate finally provided the α-aminonitrile product on reaction with in-situ generated HCN.

In the same year Panwar *et al.* developed PEG functionalized magnetic (PEG@Fe_3O_4) based nanocatalyst for the cyanation of tertiary amines using NaCN as source of cyanide group and H_2O_2 as the oxidant [65]. The catalyst (PEG@Fe_3O_4) was prepared in three steps: firstly, Fe_3O_4 nanoparticles were prepared using co-precipitation method by adding a mixture of acidic solution of Fe^{2+}, Fe^{3+} in a weak alkaline solution of NH_4OH. In the second step, prepared ferrite (Fe_3O_4) nanoparticles were functionalized with succinic acid and then finally PEG@Fe_3O_4 nanocatalyst was obtained by treating succinic acid modified ferrite nanoparticles with polyethylene glycol (PEG_{300}) in presence of *N*-(3-dimethylaminopropyl)-*N*-ethylcarbodiimidehydrochloride (EDC) and an ion-exchanger (Indion 130) (Scheme 9a).

The efficacy of the catalyst was explored in the selective oxidative cyanation of tertiary amines that involved the C—H activation approach. The amines bearing both electron-releasing groups as well as electron-withdrawing groups could be selectively converted into corresponding cyanation products in good to excellent yields in the presence of PEG@Fe_3O_4 as the catalyst. Cyclic amines such as tetrahydroisoquinolines and piperidine also afforded the targeted products in good yields, however aliphatic amines could not furnish fruitful results (Scheme 9b). The recyclability of this catalyst was explored in the cyanation of *N,N*-dimethylaniline; the nanocatalyst could be recovered after completion of reaction using an external magnetic and recycled six times without significant deactivation.

4.3. Alkynylation of aryl halides

Alkynes are known as versatile key building units in organic synthesis as they work as efficient pharmaceuticals, agrochemicals, polymers, feedstock commodity chemicals and material science [79]. Since the last few years, alkynylation of aryl halides have gained wider attention as Ar-X serves as a great substrate to produce a variety of products with acetylenic moiety which finds extensive application in industries. In this regard, a lot of studies have been conducted to explore the substrate scope of aryl halides towards alkynylation [80,81]. Within this context, Liu *et al.* reported iron-copper co-catalysis, i.e. the use of [$Cu(acac)_2$] (acac = acetylacetonate) catalyst along with Fe_2O_3 to yield the desired heterocyclic alkyne derivatives in good to excellent yields (Scheme 10) [82]. A broad range of substrates (aliphatic alkynes, substituted aryl alkynes, heterocyclic alkynes, and aryl or heterocyclic aryl iodides) effectively participated in this process to afford the targeted products under the optimized reaction conditions. Further, the developed protocol was highly efficient, cost-effective, environment friendly, displayed good versatility and practibility to create the C(sp)-C (sp^2) bond for the coupling of terminal alkynes with aryl iodides.

Panda *et al.* reported a heterogeneous magnetic catalytic system without ligand for the reaction between terminal alkynes and aryl halides. The system contained Fe_3O_4 and various MFe_2O_4 type substituted ferrite nanoparticles where, M could be Cu (II), Co (II) & Ni (II). Amongst all the tested materials, $CuFe_2O_4$ nanoparticles were found to catalyze the alkynylation of aryl halides with 70% yield at 110 °C in 1,4-dioxane and Cs_2CO_3 (Scheme 11). The synergistic effects of Cu and Fe in $CoFe_2O_4$ nanoparticles played a key role towards enhancing the overall catalytic performance in the alkynylation reaction. Moreover, the magnetic characteristics of cobalt ferrite nanoparticles not only facilitated their easy and expedient separation but also permitted quantitative catalyst recovery as negligible leaching of Cu and Fe was observed [83].

Firouzabadi *et al.* [84] reported the use of superparamagnetic nanoparticles, magnetite (Fe_3O_4) (<30 nm) as an efficient catalyst for C-

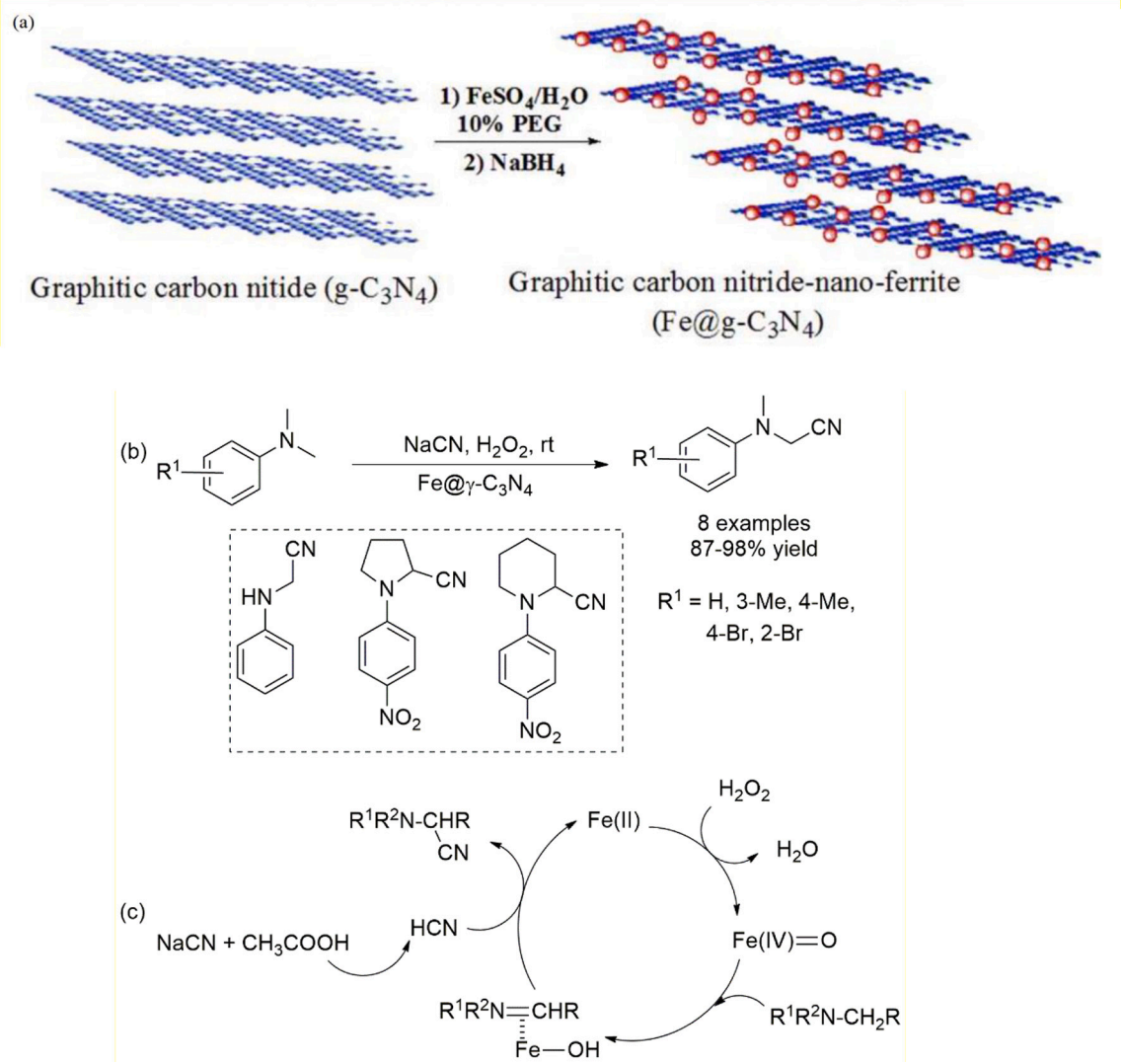

Scheme 8. (a) Preparation of magnetic graphitic carbon nitride-nano-ferrite; (b) α-cyanation of secondary and tertiary amines using magnetic graphitic carbon nitride-nano-ferrite; (c) Plausible reaction mechanism. Adopted from ref. [78]

C bond formation *via* ligand free Sonogashira-Hagihara reaction using K_2CO_3 as a base and ethylene glycol (EG) as a solvent (Scheme 12). By taking phenylacetylene and 4-iodotoluene as representative substrates, authors studied different ratios of Pd and Cu impurities along with Fe_3O_4 nanocatalyst as catalytic entities for the cross-coupling reaction. A change in amount of Pd and Cu impurities in absence of catalyst to the reaction mixture, did not considerably affect the product yield. The addition of Pd resulted in 35-42% desired product while, the extra amount of Cu resulted 10-12% yield only, thereby signifying the crucial role of magnetite nanoparticles. Further, a broad range of substituted aryl iodides and activated heteroaryl bromides efficiently reacted with substituted alkynes under the optimized reaction parameters to furnish the anticipated arylalkynes in good to excellent yields.

Gholinejad *et al.* [85] synthesized Pd@bisindole@SiO_2@Fe_3O_4 catalyst (Scheme 13a) and utilized it for catalysing a reaction between aryl halides and terminal alkynes (Scheme 13b). The presence of uniform and small sized Pd NPs possessing size 2 nm was revealed through the high resolution transmission electron microscopy (HTEM) images (Fig. 3). The reactants i.e. aryl halides and terminal alkynes were taken in an equivalent molar ratio of 1.0 to 1.5 respectively; along with 0.18 mmol/ 20 mg of Pd@bisindole@SiO_2@Fe_3O_4, DABCO and 2 mL DMA. The resulting mixture was stirred at 60 °C (in case of aryl bromides and aryl iodides) or 120 °C (in case of aryl chlorides along with 1 mmol TBAB). Pd@bisindole@SiO_2@Fe_3O_4 was found to catalyse the alkynylation of diverse aryl halides under air, copper and phosphane free environment with high turnover numbers and reproducibility, i.e. showing recyclability upto seven cycles with negligible decrease in catalytic efficiency. Further, the developed Pd@bisindole@SiO_2@Fe_3O_4 was also explored for large scale industrial applicability and it was observed that it could be scaled upto 10 mmol under the optimized reaction conditions.

In another report, magnetic nanoparticles supported palladium 'catalyst i.e. CPS-MNPs-NNN-Pd [86] was fabricated (Scheme 14a) and applied in the Sonogashira coupling reaction for the alkynylation of aryl halide with phenylacetylene.

A step by step assembly strategy was employed to synthesize the desired catalyst wherein Fe_3O_4 nanoparticles prepared *via* co-precipitation route were coated with silica and further functionalized with (3-chloropropyl)-trimethoxysilane (CPTMS) to render chloro-functionalized magnetic nanoparticles (CPS-MNPs). Simultaneously, NNN Schiff base ligand was synthesized which underwent substitution reaction with CPS-MNPs to form CPS-MNPs-NNN ligand. Finally palladium species were immobilized onto CPS-MNPs-NNN to produce the anticipated CPS-MNPs-NNN-Pd nanocatalyst. Microscopy techniques revealed the presence of palladium in the range of 8-15 nm in the catalyst. The Sonogashira coupling was also explored using various aryl

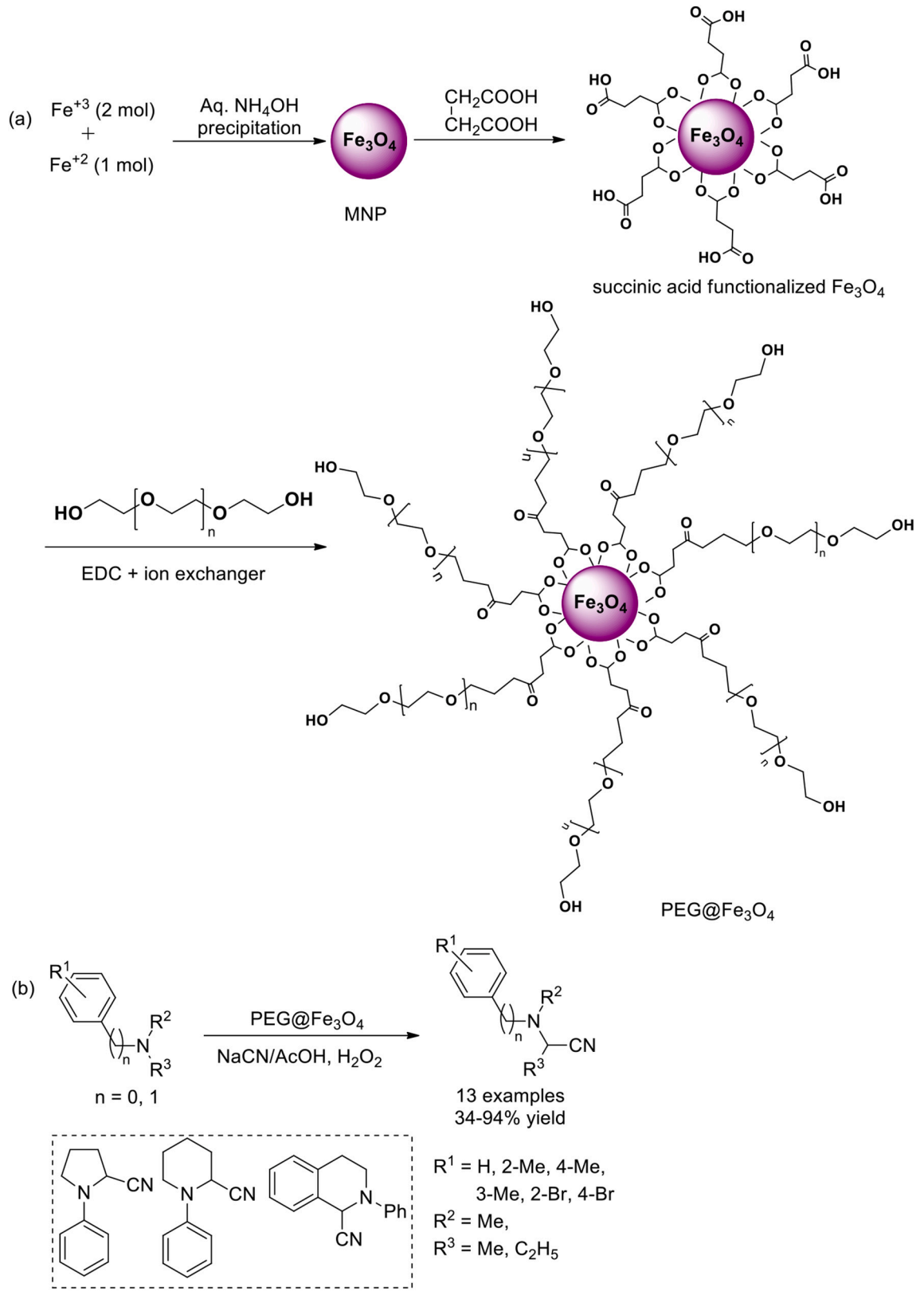

Scheme 9. (a) Synthesis of PEGylated magnetic nanoparticles (PEG@Fe_3O_4) catalyst; (b) PEG@Fe_3O_4 catalysed cyanation of tertiary amines.

halides with phenylacetylenes and desired diarylethyneproducts were obtained in good to excellent yields (Scheme 14b).

Comparative account of some reported Pd catalysts with proposed CPS-MNPs-NNN-Pd catalyst for Heck coupling reaction of iodobenzene with n-butyl acrylate has been summarized in Table 5. The CPS-MNPs-NNN-Pd has more efficiency than the other Pd catalyst in terms of time, percent yield and reaction conditions.

On similar grounds, Zhang *et al.* demonstrated the applicability of Pd NPs supported on branched/linear polyethylenimine-grafted magnetic Fe_3O_4/SiO_2/P(GMA-co-EGDMA) composite (Scheme 15a) for

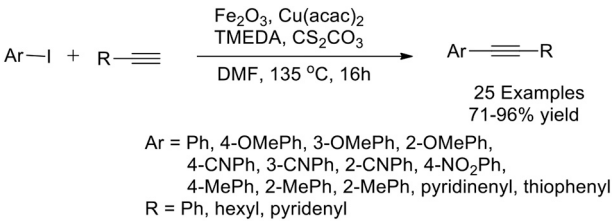

Scheme 10. Cu-Fe catalysed alkynylation of aryl iodides with terminal alkynes

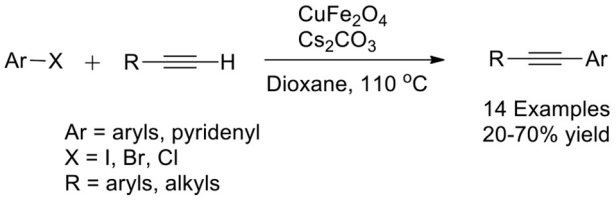

Scheme 11. $CuFe_2O_4$ catalysed alkynylation of aryl halides with terminal alkynes.

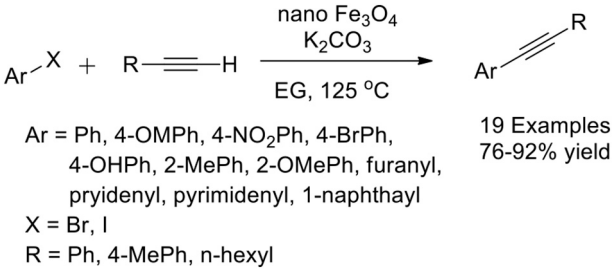

Scheme 12. Alkynylation of aryl halide *via* nano Fe_3O_4.

alkynylation of aryl halides with aryl acetylenes (Scheme 15b) [87]. A series of aryl halides such as iodobenzene, bromobenzene, chlorobenzene, 4-chloroacetophenone, 4-nitrochlorobenzene and 4-chlorotoluene effectively cross coupled with phenylacetylene, 3-aminophenylacetylene and 4-(ethynyl)phthalic anhydride to generate desired products in excellent yields. The observed product yields revealed high activity of iodobenzene in comparison to bromobenzene followed by chlorobenzene. High stability, superior catalytic performance (inhibiting formation of 1,3-diyne as by-product), magnetic retrievability, good recyclability for eight runs without any significant loss in its catalytic efficiency were some of the additional noteworthy attributes of the developed nanocomposite. The mechanism for Fe_3O_4/SiO_2/P(GMA-co-EGDMA)-PEI-Pd (0) catalysed Sonogashira reaction is depicted in Scheme 15c. The superiority of catalyst lies in zero valent Pd to escape unnecessary addition of CuI as co-catalyst and hence formation of 1, 3-diyne as by-product can be significantly averted to a considerable extent.

Phan *et al.* reported the synthesis of $CoFe_2O_4$ NPs [88] through a microemulsion approach and functionalized it further with 2-acetyl pyridine to generate immobilized Schiff base bidentate ligand which then underwent complexation with palladium (Scheme 16a). The catalytic efficacy of resulting nanomaterial was investigated in the alkynylation of aryl halides and phenylacetylene in presence of CuI as the co-catalyst, K_3PO_4 as the base and DMF as the solvent. Experimental results revealed that electron withdrawing functionalities on aryl halides favored the Sonogashira coupling reaction and furnished the targeted moieties in high yields as compared to the electron donating functionalities that rather slowed down the rate of coupling reaction (Scheme 16b). Besides, the prepared nanocatalyst could be reused and recovered for at least 10 cycles without showing any significant reduction in its catalytic efficiency.

Ali Elhampour *et al.* synthesized tetrazole functionalized palladium catalyst supported on magnetic nanoparticle ($Fe_3O_4@SiO_2$–T/Pd) through a (2+3) cycloaddition pathway (Scheme 17a) and successfully evaluated its catalytic activity for alkynylation of aryl halides in the presence of Et_3N and DMF at 120 °C [89]. It was found that substituted phenylacetylenes and aliphatic alkynes successfully underwent reaction with halobenzenes (iodo-, bromo- and chloro-benzene) to afford corresponding products in remarkable yields (Scheme 17b). Further, the palladium based catalyst being magnetic in nature permitted easy recovery and reusability of palladium thereby eliminating the chances of palladium contamination of the isolated product.

The dominance of present protocol in comparison to other literature reports can be seen in Table 6. This $Fe_3O_4@SiO_2$–T/Pd catalyst is superior being reusable, lesser time to synthesize the target entity and easily separable.

Likewise, another research group reported the fabrication of a Schiff base complex of Pd (II) supported on $Fe_3O_4@SiO_2$ nanoparticles (Scheme 18a) and subsequently utilized it in the copper and phosphine ligand free coupling of aryl halides with phenylacetylene [90]. In addition to Pd^{2+} complex of $Fe_3O_4@SiO_2$/Schiff base, various complex of metal ions such as Fe^{2+}, Ni^{2+}, Cu^{2+}, Co^{2+}, Cd^{2+}, Mn^{2+} and Zn^{2+} were synthesized and their potential was tested in the coupling of iodobenzene with pehnylacetylene (Scheme 18b). It was concluded that though metal complexes of iron, copper, nickel and cobalt displayed promising activity, but it was the palladium catalyst which exhibited highest catalytic activity in the concerned coupling reaction. Additional notable advantages of the designed protocol included true heterogeneous nature of the catalyst, excellent yield of products, facile catalyst separation using external magnet, easy work up, shorter reaction times and reusability up to six cycles.

Sobhani *et al.* reported the synthesis and application of Pd-BIP-γ-$Fe_2O_3@SiO_2$ (a Pd complex of bis(imino)pyridine as an NNN pincer ligand supported on γ-$Fe_2O_3@SiO_2$ magnetic nanoparticles) (Scheme 19a) towards alkynylation of aryl halides which generated the targeted products in good yields (71-96%) (Scheme 19b) [91]. The heterogeneous nature of the Pd nanocatalyst was further affirmed through the hot filtration test which demonstrated that the Pd-BIP-γ-$Fe_2O_3@SiO_2$ could be reused for ten consecutive runs without showing any appreciable reduction in its catalytic activity, thus making it an attractive potential material for large scale coupling reactions in industrial settings.

Owing to the noteworthy catalytic activities and great significance for transformation of aryl halides for alkynylated products, it can be concluded that magnetic nanoparticles are highly valuable for organic synthesis especially when recovery is concerned. However, still broader applicability based catalytic systems which provide better yields with aryl chloride as a substrate are needed to be explored as greener, low cost and environmentally benign tools.

4.4. *Synthesis of carbamates via C—H activation of formamides*

Organic carbamates are highly significant structural elements of many marketed drugs used for the treatment of various diseases such as asthma, AIDS, seizures, arrhythmias, etc. [92]. Therefore, several traditional methods have been developed for the construction of carbamate skeleton of bioactive molecules using toxic starting materials which includes chloroformate, isocyanates, and phosgene [93]. Other methods have also been developed to overcome the issues associated with previously used toxic reaction substrates, which include cross coupling reactions using transition metals [94], carbonylation of amines [95], use of CO_2 [96], rearrangement reactions [97]. In 2015 Sharma *et al.* disclosed a method for the synthesis of organic carbamates *via* C—H activation of formamides under solvent free conditions using magnetically retrievable Cu-2QC@Am-$SiO_2@Fe_3O_4$ catalyst [6a]. The

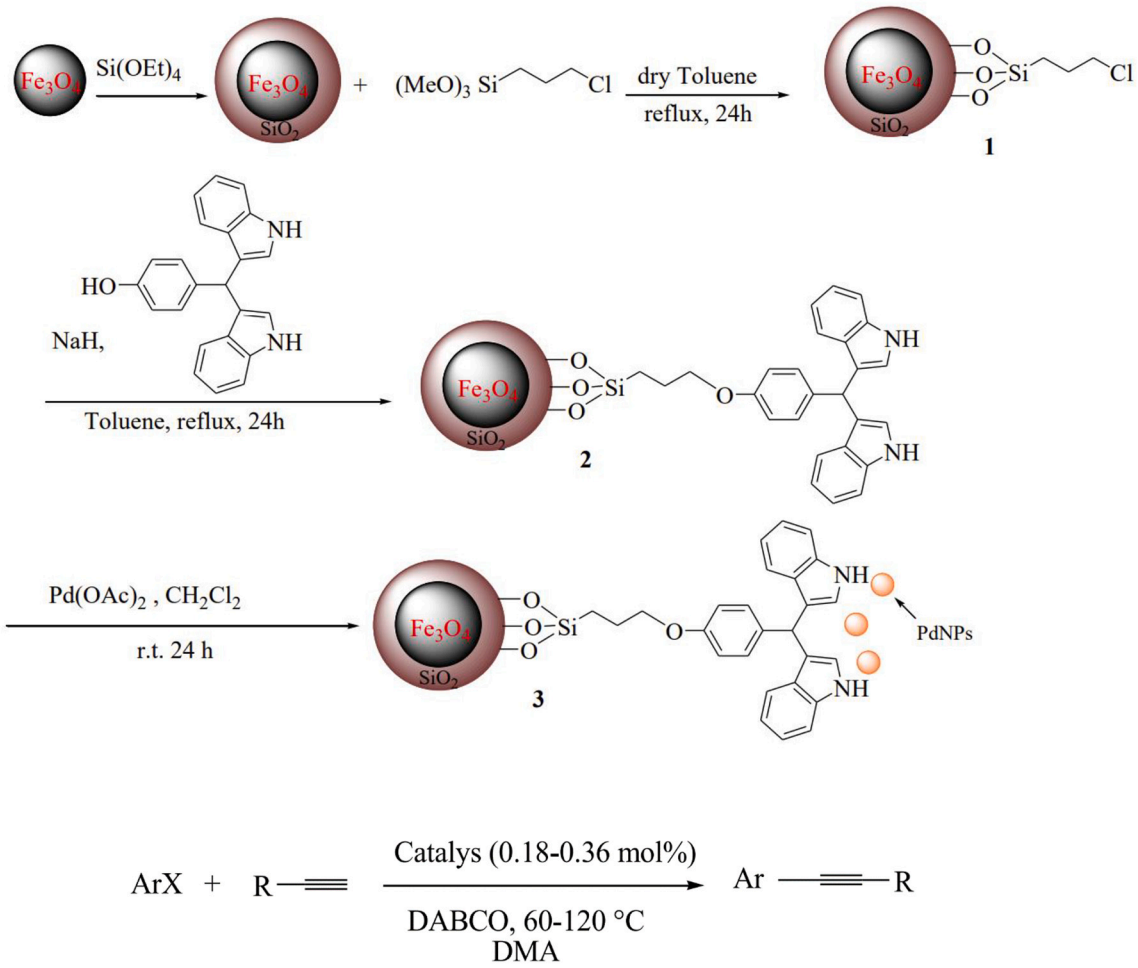

Scheme 13. (a) Synthesis of Pd@bisindole@SiO_2@Fe_3O_4; (b) Alkynylation of aryl halide *via* Pd@bisindole@SiO_2@Fe_3O_4.

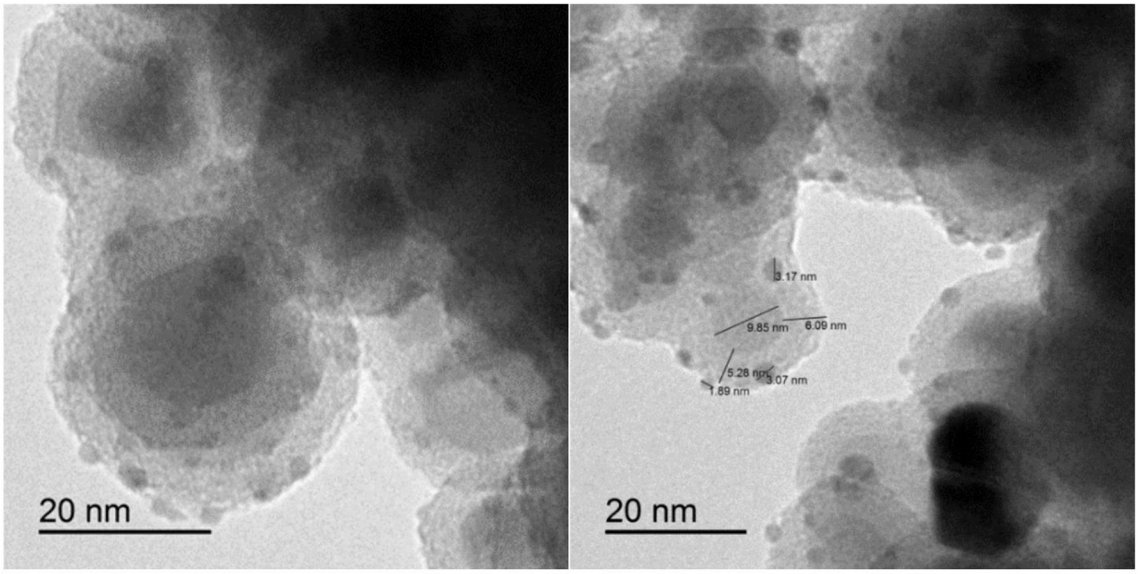

Fig. 3. HTEM images of Pd@bisindole@SiO_2@Fe_3O_4. Adopted from ref [85]

preparation of nanocatalyst initiated with the synthesis of ferrite (Fe_3O_4) nanoparticles using co-precipitation method followed by sol-gel encapsulation of Fe_3O_4 over silica to achieve SiO_2@Fe_3O_4 and then treated with APTES to introduce amine groups over the surface of SiO_2@Fe_3O_4 to obtained amine functionalized silica coated magnetite (Am-SiO_2@-Fe_3O_4) nanoparticles. Finally Cu-2QC@Am-SiO_2@Fe_3O_4 catalyst was prepared through the immobilization of quinoline-2-carboimine on amine functionalized silica coated magnetite nanoparticles and

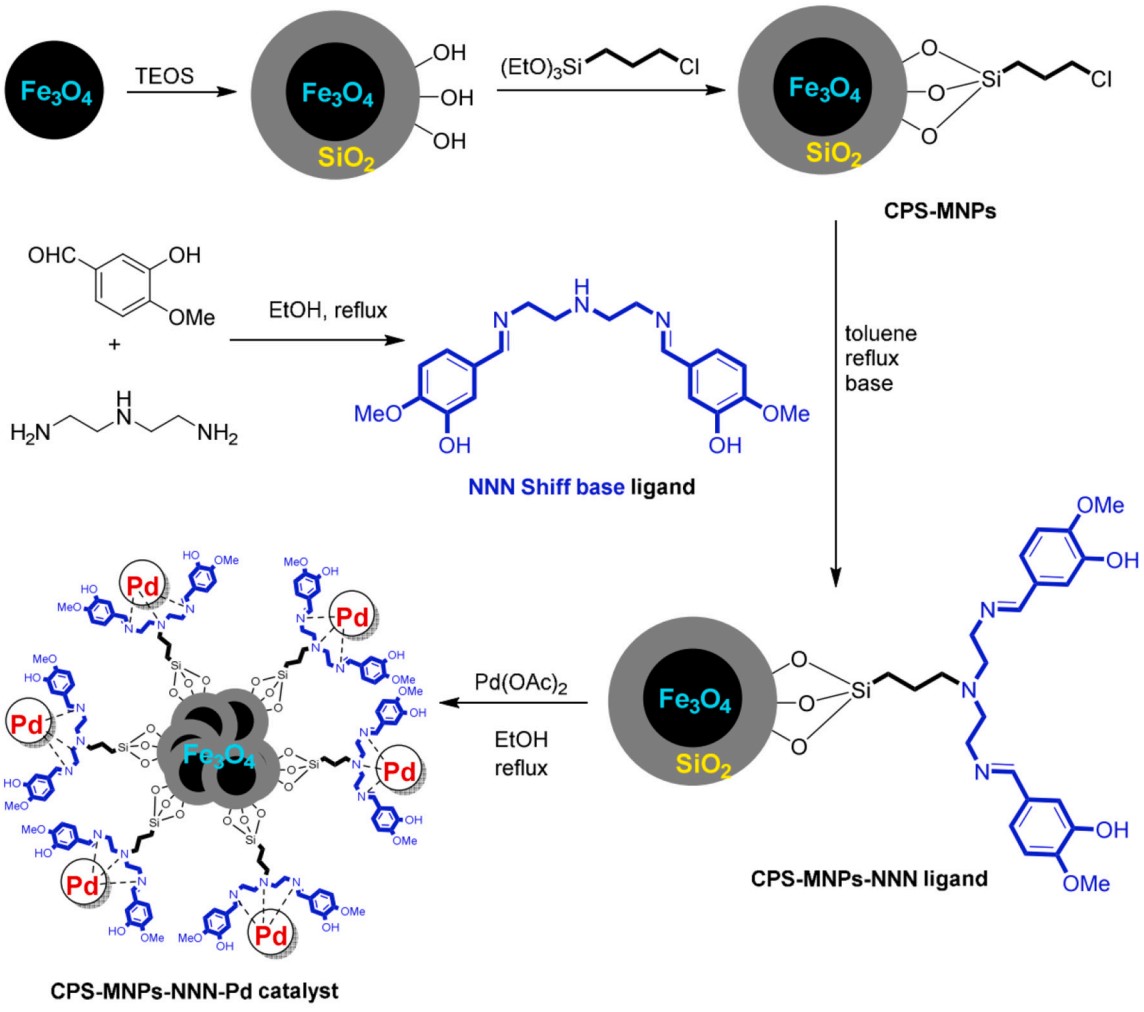

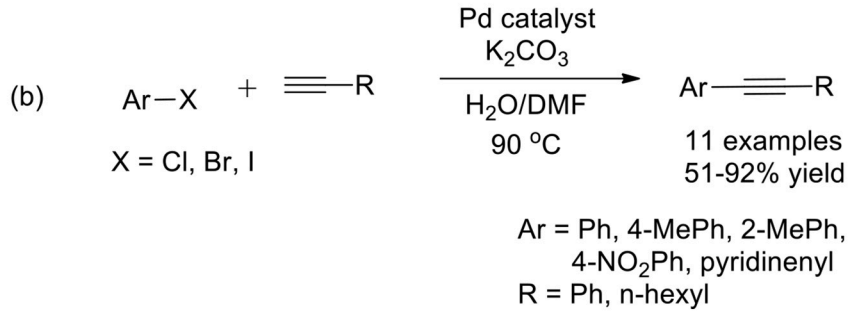

Scheme 14. (a) Preparation of CPS-MNPs-NNN-Pd catalyst; (b) Sonogashira coupling reaction for the alkynylation of aryl halide with phenylacetylene. Adopted from ref. [86]

subsequent treatment with copper acetate (Scheme 20a). The catalytic activities of the developed nanocatalysts were evaluated in the reaction between β-ketoesters/*ortho*-carbonyl substituted phenols and formamides to synthesize carbamates *via* C—H activation of formamides (Scheme 20b). All the substrates reacted effectively to give the desired carbamates with good to excellent conversion percentages and very high turnover numbers (TONs). The recyclability test of the catalyst was done in the phenol carbamate synthesis and observed that the catalyst can be reused eight times without any appropriate loss in its activity. A plausible free radical mechanism for the synthesis of targeted carbamates was proposed as shown in scheme 20c, which was also ascertained by the addition of a radical scavenger (TEMPO).

The effectiveness of the present methodology was established by comparing the results obtained with those of the previously reported protocols. The Cu-2QC@Am-SiO_2@Fe_3O_4 nanocatalyst showed promising results in terms of product yield and reaction time in comparison to the literature precedents (Table 7).

Table 5
Comparison of CPS-MNPs-NNN-Pd catalyst with other reported catalysts for the coupling reaction of iodobenzene and *n*-butyl acrylate.

S. No.	Catalyst	Reaction conditions	Time (h)	Yield[a] (%)	TON[b]	TOF[c] (h^{-1})
1	CPS-MNPs-NNN-Pd	K_2CO_3, H_2O/ DMF, 90^0 C, 0.5 mol% Pd	0.4	95	190	475
2	Pd-dendr	Bu_3N, THF, 60 °C, 2 mol% Pd	24	96	48	2
3	$PdCl_2$	K_2CO_3, H_2O, 80-100 °C, 1.5 mol % Pd	8	92	61.3	7.7
4	Tetraimine Pd(0)	K_2CO_3, H_2O, 90 °C, 0.4 mol% Pd	1	94	235	235
5	Pd/Fe_3O_4	K_2CO_3, NMP, 130 °C, 5 mol% Pd	5	99	19.8	4
6	TiO_2@Pd NPs	Et_3N, DMF, 140 °C, 1 mol% Pd	10	92	92	9.2
7	Pd-SiO_2	Et_3N, MeCN, 130 °C, 2 mol% Pd	3	97	48.5	16
8	Pd-SMTU-boehmite	Na_2CO_3, PEG, 120 °C, 2.56 mol % Pd	0.3	97	37.9	114.8
9	Pd-Zn Fe_2O_4 MNP	Et_3N, DMF, 120 °C, 4.62 mol% Pd	3	90	19.5	6.5

[a] Isolated yield.
[b] TON = mol product per mol cat.
[c] TOF = (mol product per mol cat) per h.

4.5. Multicomponent reactions for propargylamines synthesis

Propargylamines belong to a highly substantial class of organic compounds and have versatile applications in several fields of chemistry. Due to unique structure of propargylamines because of the presence of amine group in β-position of alkyne bond, they haveenzy been extensively used as synthetic precursors for the production of important pharmaceutically active organic molecules, natural products and drugs. Therefore significant advancements have been made in past several years in the synthesis of propargylamines using transition metal catalysts, biocatalysts and also using metal-free conditions [98].

In 2013 Huo *et al.* reported a three-component coupling reaction for the synthesis of propargylic amines using magnetically separable graphene-ferrite (graphene@Fe_3O_4) nanoparticles as catalyst [99]. The magnetite nanocatalyst (graphene@Fe_3O_4) was prepared by carrying out the thermal decomposition reaction of $Fe(CO)_5$ in a graphene oxide (GO) dispersion system. The effectiveness of the catalyst was explored in A^3 coupling reaction between various aldehydes, amines and alkynes for the synthesis of propargylic amines. All used aliphatic aldehydes smoothly participated in coupling reactions affording the high yield of the desired products. Unfortunately, in case of aromatic aldehyde (benzaldehyde), only traces of product could be observed by NMR. Several cyclic dialkylamines and phenylacetylenes were also coupled effectively to give the respective propargylamines in good yields (Scheme 21). The recyclability test of catalyst revealed that the catalyst can be reused 8 times without substantial loss of catalytic activity.

Nguyen *et al.* synthesized superparamagnetic $CuFe_2O_4$ nanoparticles for the aldehyde free synthesis of propargylic amines through sequential methylation and C—H activation approach [100]. $CuFe_2O_4$ nanoparticles were prepared by stirring a mixture of $CuCl_2.2H_2O$ and Fe $(acac)_3$ in triethylene glycol at room temperature for 60 min followed by ultrasonication and subjected to stirring for another 30 min. Finally, after heating the obtained dark red mixture at 270 °C for 8 h desirable superparamagnetic $CuFe_2O_4$ nanoparticles were formed. Then the catalytic performance of $CuFe_2O_4$ nanoparticles was tested through a sequential methylation and C-C coupling reaction between *N*-methylanilines and phenylacetylenes in TBHP (*tert*-butyl hydroperoxide). Good yields of propargylic amines were obtained by treating substituted phenylacetylenes with *N*-methylaniline derivatives (Scheme 22a). Electron-releasing groups such as Me, OMe were well tolerated on phenylacetylene. *N*-methylaniline bearing electron-withdrawing group Cl provided highest product yield. The recovery and reusability test for superparamagnetic $CuFe_2O_4$ nanoparticles suggested that it can be reused several times without any significant decrease in catalytic activity. The proposed mechanism for this tranfomation is given in Scheme 22b. Oxidant TBHP in presence of copper catalyst produced a tert-butyl radical which on decomposition in unimolecular fashion generated methyl radical. Methyl radical on raction with *N*-methylaniline over Cu-catalyst delivered *N,N*-dimethylaniline or an iminium in presence of TBHP oxidant. Finally, the nucleophilic attack of phenylacetylide to iminium reseulted the desired product.

In 2015 Tajbaksh *et al.* reported the magnetite supported 2,2'-biimidazole complex of metal ions (Cu(I), Cu(II), Ni(II), Co(II)) (MNP@BiimM) as catalysts for the synthesis of propargylic amines by three-component coupling between aldehyde, amine and alkyne in water [101]. Authors prepared the nanocatalyst by a multi-step approach; initially magnetite (Fe_3O_4) nanoparticles were prepared by co-precipitation method and then coated with layer of silica (SiO_2) to form Fe_3O_4@SiO_2 nanoparticles. Afterwards, Fe_3O_4@SiO_2 (MNP) nanoparticles were functionalized by CPTES (3-(chloropropyl)triethoxysilane) to prepare CPTES coated MNPs, which then reacted with biimidazole and subsequently with metal salts to furnish magnetically separable MNP@BiimM nanoparticle catalyst (Scheme 23a). Finally, the catalyst was used in A^3 coupling reaction of aldehydes (aromatic, aliphatic and heterocyclic), amines and phenylacetylene, and corresponding propargyl amines were obtained in good to excellent yields (Scheme 23b). The recoverability test suggested that catalysts could be easily separated with the help of external magnet and can be reused several times without any substantial loss in catalytic activities. The proposed reaction mechanism for the formation of propargyl amines in presence of MNP@BiimM nanoparticle catalyst has also been given scheme 23c.

Moreover, to show the importance of this newly developed catalyst for the A^3 coupling reaction, the results obtained were also compared with some literature reports using other catalysts (Table 8). Interestingly, the results of present protocol were found to better in terms of reaction yield, separation of catalyst from reaction mixture, reaction time and sustainability.

With the similar objective in mind, Nemati and co-workers in 2016 synthesized Ag-doped nano magnetic γ-Fe_2O_3@DA core shell hollow spheres to accomplish A^3 and KA^2 coupling reactions for the construction of propargylic amines [102]. The catalyst was prepared in a systematic way starting with hydrothermal synthesis of Fe_2O_3 hollow sphere followed by functionalization with dopamine to form Fe_2O_3@DA hollow sphere and finally $Ag(NH_3)_2NO_3$ was supported on the surface of magnetic Fe_2O_3@DA to accomplish the synthesis of Ag-doped nano magnetic γ-Fe_2O_3@DA core shell hollow spheres (Scheme 24a). After successful synthesis of the nanocatalyst, its applicability in C—H activation was evaluated through A^3 (coupling among aldehyde, amine and alkyne) and KA^2 (coupling among ketone, amine and alkyne) coupling reactions. Investigation of A^3 coupling reaction of aromatic aldehydes, cyclic amines and aryl acetylenes using the synthesized magnetite nanocatalyst revealed that aromatic aldehydes and aryl acetylenes having either electron-releasing groups or electron-withdrawing groups delivered the desired products in very good yields (Scheme 24b). KA^2 coupling reactions between cyclic ketones, secondary amines and aryl acetylenes also furnished high product yield of targeted propargylic amines (Scheme 24c). Authors could recover the catalyst after completion of reaction using an external magnet and reused 5 times without effective loss in yields.

The proposed mechanism revealed that Ag nanoparticles acted as Lewis acid catalyst in this conversion. The immobilized Ag nanoparticles

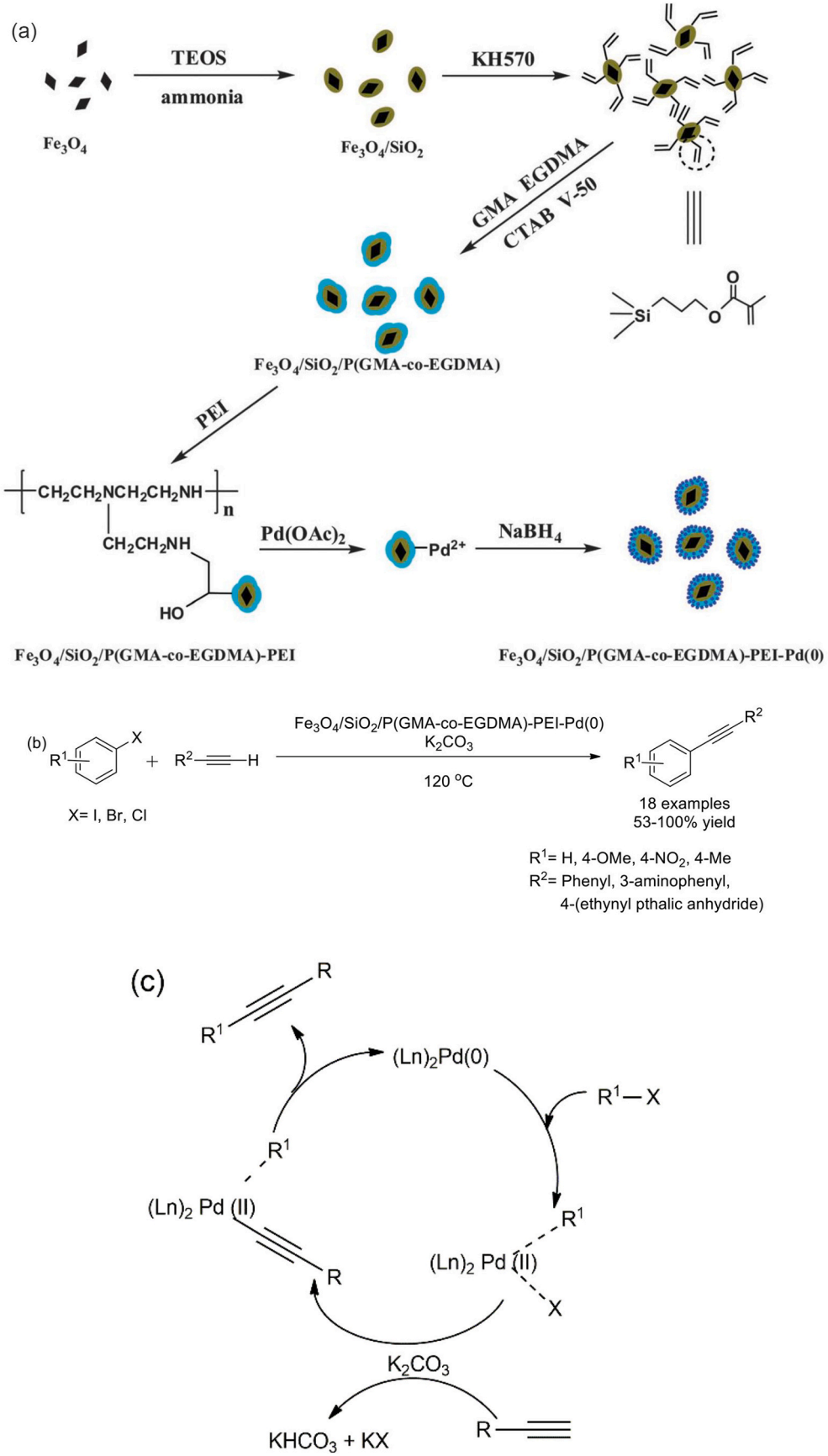

Scheme 15. (a) Preparation of catalyst; (b) Fe_3O_4/SiO_2/P(GMA-co-EGDMA)-PEI-Pd catalysed alkynylation; (c) Proposed reaction mechanism. Adopted from ref. [87]

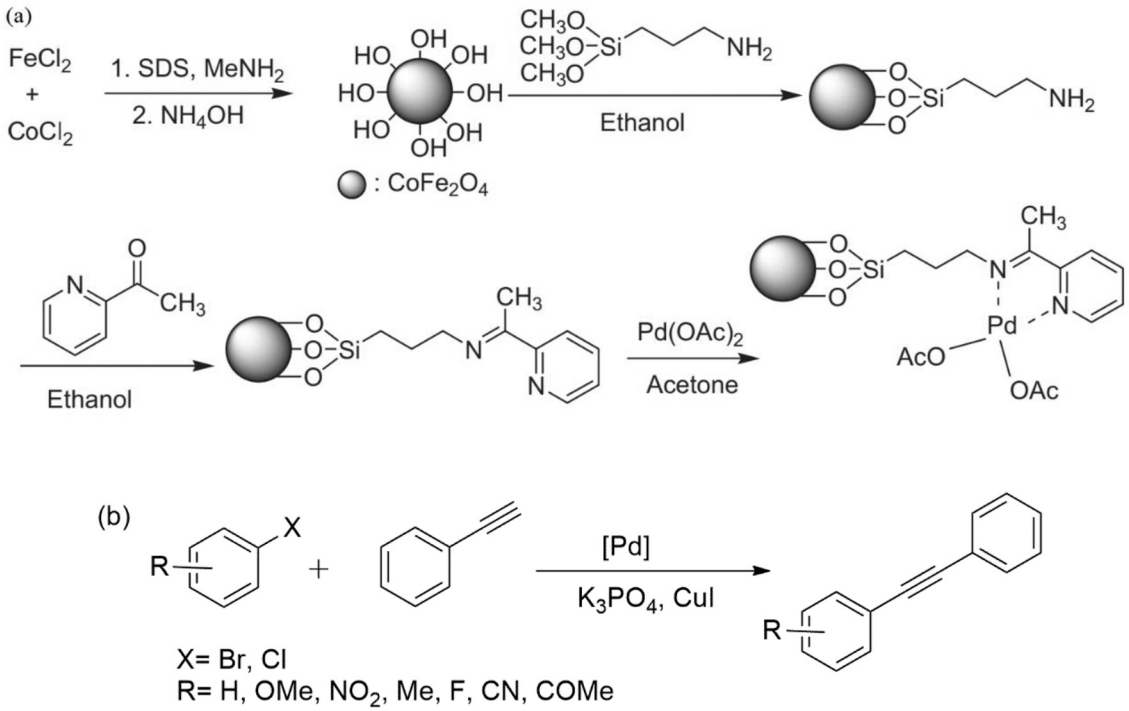

Scheme 16. (a) Preparation of $CoFe_2O_4$ NPs; (b) Superparamagnetic $CoFe_2O_4$ NPs catalysed alkynylation. Adopted from ref. [88]

insert in terminal alkyne and form the Ag acetylide intermediate through C—H activation process. In the meantime, an iminium ion get generated by the nucleophilic addition of amine to aldehyde. Finally, the attack of acetylide intermediate on iminium ion resulted the corresponding propargylamine (Scheme 24d).

On similar grounds, Zarei and Akhlaghinia reported magnetically recoverable Zn^{II}/HAP/Fe_3O_4 nanocatalyst for a one-pot three-component coupling reaction of aldehydes, secondary amines and terminal alkynes for the synthesis of propargylamines under solvent free conditions [103]. For the fabrication of Zn^{II}/HAP/Fe_3O_4 nanocatalyst, firstly natural hydroxyapatite (HAP) was extracted from cow bones and then added to acidic solution of $FeCl_3.6H_2O$ and $FeCl_2.6H_2O$ for the synthesis of magnetic HAP/Fe_3O_4 nanoparticles. Finally, synthesized HAP/Fe_3O_4 nanoparticles were added to alcoholic solution of $Zn(OAc)_2 2H_2O$ to accomplish the preparation of Zn^{II}/HAP/Fe_3O_4 nanoparticles (Scheme 25a). The catalytic performance of newly developed magnetite Zn^{II}/HAP/Fe_3O_4 nanocatalyst was evaluated in preparation of propargylic amines. For this purpose various aldehydes, secondary amines (morpholine and pyrrolidine) and aryl alkynes were coupled using Zn^{II}/HAP/Fe_3O_4 nanocatalyst under optimized reaction conditions. The corresponding products could be obtained in good to excellent yields. Benzaldehydes bearing electron-releasing groups afforded slightly higher product yields in shorter reaction time in comparison to benzaldehydes having electron-withdrawing groups. Almost similar results were obtained in case of substituted phenylacetylenes (Scheme 25b). The recyclability test of catalyst revealed that the catalytic activity of Zn^{II}/HAP/Fe_3O_4 nanocatalyst remained intact showing no remarkable loss upto 7 successive runs. The mechanism for this reaction is shown in scheme 25c, which depicts the formation of desired propargylamine through the nucleophilic addition of generated zinc acetylide intermediate on iminium ion.

The proficiency of Zn^{II}/HAP/Fe_3O_4 for the synthesis of 4-(1,3-diphenylprop-2-yn-1-yl)morpholine was checked by comparing with various literature reported catalysts and found to be more efficient and green magnetic nano-catalyst (Table 9).

In a quest to develop recyclable nanocatalyst, Munshi *et al.* disclosed the effectiveness of magnetically recoverable Fe_3O_4@Au-coated nanoparticles in A^3 coupling reaction [104]. Fe_3O_4@Au-coated nanoparticles were synthesized using a multistep approach. Initially Fe_3O_4-PEI nanoparticles were prepared and subsequent coating with Au seeds delivered fabricated Fe_3O_4-PEI-Au seeds nanoparticles. Finally, Fe_3O_4@Au-coated nanoparticles were prepared by mixing Fe_3O_4-PEI-Au seeds nanoparticles in 0.01 M NaOH solution with stirring followed by addition of $HAuCl_4$ and 0.2 M $NH_2OH{\cdot}HCl$. After successful preparation of nanocatalyst, it was used in A^3 coupling reaction of aldehydes (aliphatic, aromatic and heterocyclic), piperidine and phenylacetylene and resulted in the poor to good conversion of substrates into corresponding products (Scheme 26). Formaldehyde exhibited maximum 95% conversion and minimum conversion (7%) was obtained in case of 3-nitrobenzaldehyde.

Heravi and co-workers in 2017 synthesized Ag-doped nano magnetic h-Fe_2O_3@SiO_2-CD core shell hollow spheres (h-Fe_2O_3@SiO_2-CD/Ag) and utilized it further in ultrasonication assisted A^3 and KA^2 coupling for the synthesis of propargylic amines [105] The preparation of catalyst was started with the hydrothermal synthesis of Fe_2O_3 hollow sphere followed by coating with SiO_2 to achieve hollow Fe_2O_3@SiO_2 (h-Fe_2O_3@SiO_2) nanoparticles. Subsequent treatment of hollow Fe_2O_3@-SiO_2 nanoparticles with 3-*N*-(2-(trimethoxysilyl)ethyl)methanediamine delivered amine functionalized Fe_2O_3@SiO_2 nanoparticles, which on reaction with tosylated cyclodextrin resulted h-Fe_2O_3@SiO_2-CD. Finally, h-Fe_2O_3@SiO_2-CD/Ag nanoparticles were obtained after doping h-Fe_2O_3@SiO_2-CD with Ag(0) nanoparticles using hollyhock flower extract as a reducing agent (Scheme 27a). The catalyst was then used in A^3 coupling reactions using various aldehydes containing different functional groups, amines and phenylacetylene, and high yields of propargylic amines were obtained (Scheme 27b). Benzaldehydes having electron-releasing as well as electron-withdrawing substituents delivered excellent yields of the products. Also, the scope of catalyst was explored in KA^2 coupling by replacing aldehyde with ketone and high yields of desired products could be obtained. The recyclability experiments showed that catalyst can be recovered easily with the help of magnet and can be reused four times without any effective loss in

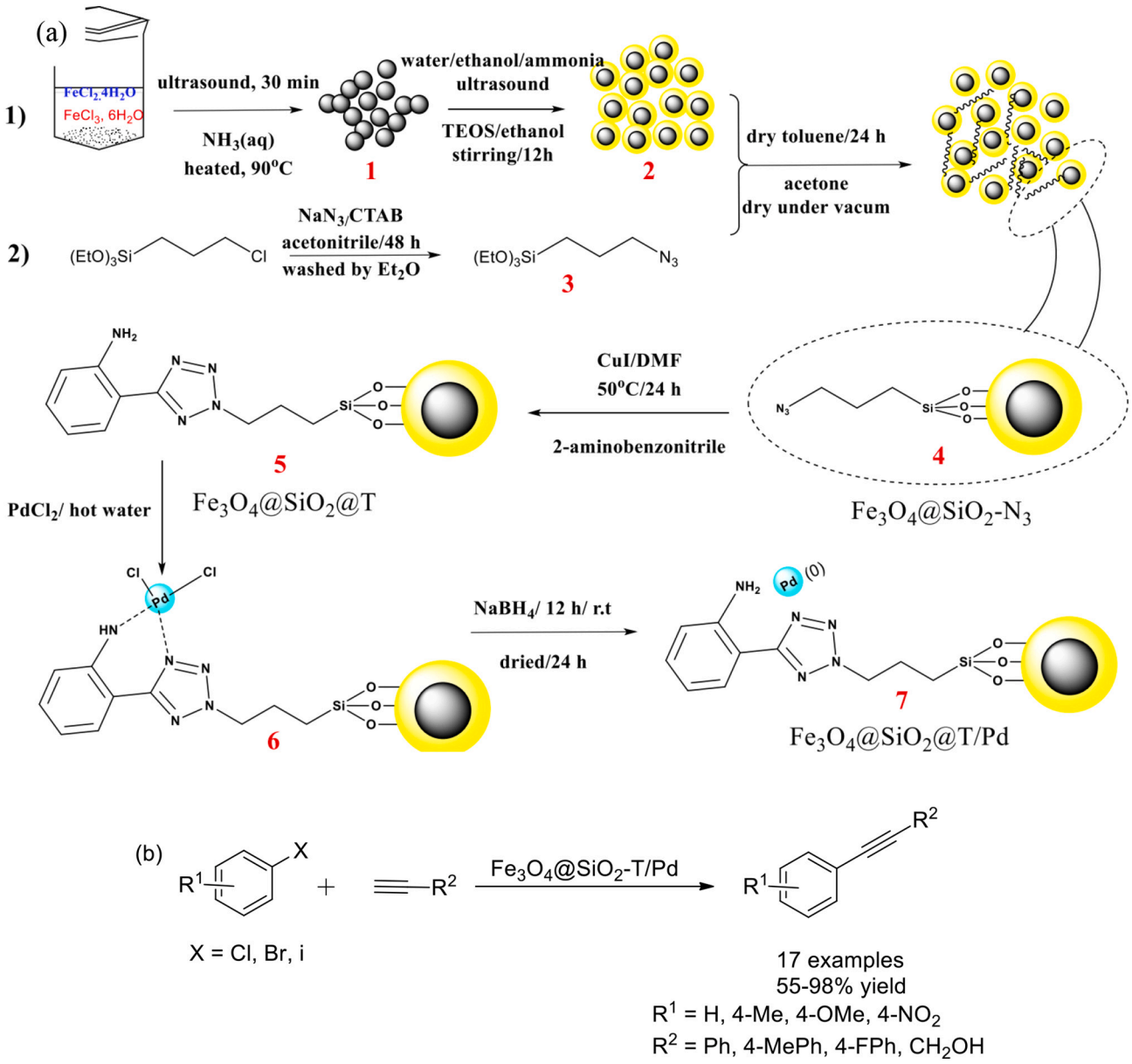

Scheme 17. (a) Preparation of Fe_3O_4@SiO_2–T/Pd catalyst; (b) alkynylation of aryl halides using Fe_3O_4@SiO_2–T/Pd catalyst. Adopted from ref. [89]

Table 6
Comparison to check the supremacy of Fe_3O_4@SiO_2–T/Pd catalyst over other reported catalysts

S. No.	Catalyst	Condition (base, solvent, temperature)	Time (h)	Yield (%)
1	Pd@bisindole@SiO_2@ Fe_3O_4 (4 mg 0.18 mol%)	DABCO, DMA, 90 °C	24	94
2	Pd-Cu Fe_2O_4@SiO_2 (10 mg, 0.3 mol% Pd)	DABCO, DMA, 50 °C	24	80
3	CS/MMT/Pd (0.3 mol%)	KOAc, DMSO, 110 °C	5	94
4	Pd@PANI (0.005 mol%)	Et_3N, MeCN, 80 °C	48	86
5	Nano Pd@Fe_3O_4 (1 mol% Pd)	DMF, piperidine, 110 °C	24	88
6	Pd^0- Mont (0.07 mol%)	Et_3N, CH_3CN, 82 °C	3	90
7	PdNPs/DNA (8 mg, 0.5 mol%)	Cs_2CO_3, MeOH, 65 °C	24	85
8	Fe_3O_4@SiO_2-T/Pd (20 mg)	Et_3N, DMF, 120 °C	2.5	97

activity. However, in the fifth run slight loss of catalytic activity was observed and in sixth run with 10% loss in catalytic activity low product yield was obtained.

The comparison for the catalytic efficiency of this newly synthesized nano-catalyst with previously reported catalyst was also determined. h-Fe_2O_3@SiO_2-CD/Ag nanoparticles catalyst was found better in several aspects such as high yield, shorter reaction time, mild reaction conditions, greener solvent, etc. (Table 10).

In 2019 Shahamat *et al.* reported magnetic mesoporous polymelamine formaldehyde/zinc oxide (Fe_3O_4-mPMF/ZnO) nanocomposite for one-pot three component propargylic amine synthesis [106]. During the preparation of catalyst, initially Fe_3O_4-mPMF nanoparticles were prepared by heating a mixture of melamine, paraformaldehyde and ethylene glycol followed by the addition of $FeCl_3.6H_2O$ and NaOAc, and heating the resulting reaction mixture in stainless steel autoclave at 200 °C for 48 h. Finally, to synthesize Fe_3O_4-mPMF/ZnO nanocomposite Fe_3O_4-mPMF nanoparticles were dispersed in alcoholic solution of Zn $(OAc)_2 2H_2O$ and subjected to sonication(Scheme 28a). Then synthesized nanocomposite was used for the synthesis of propargylamines by

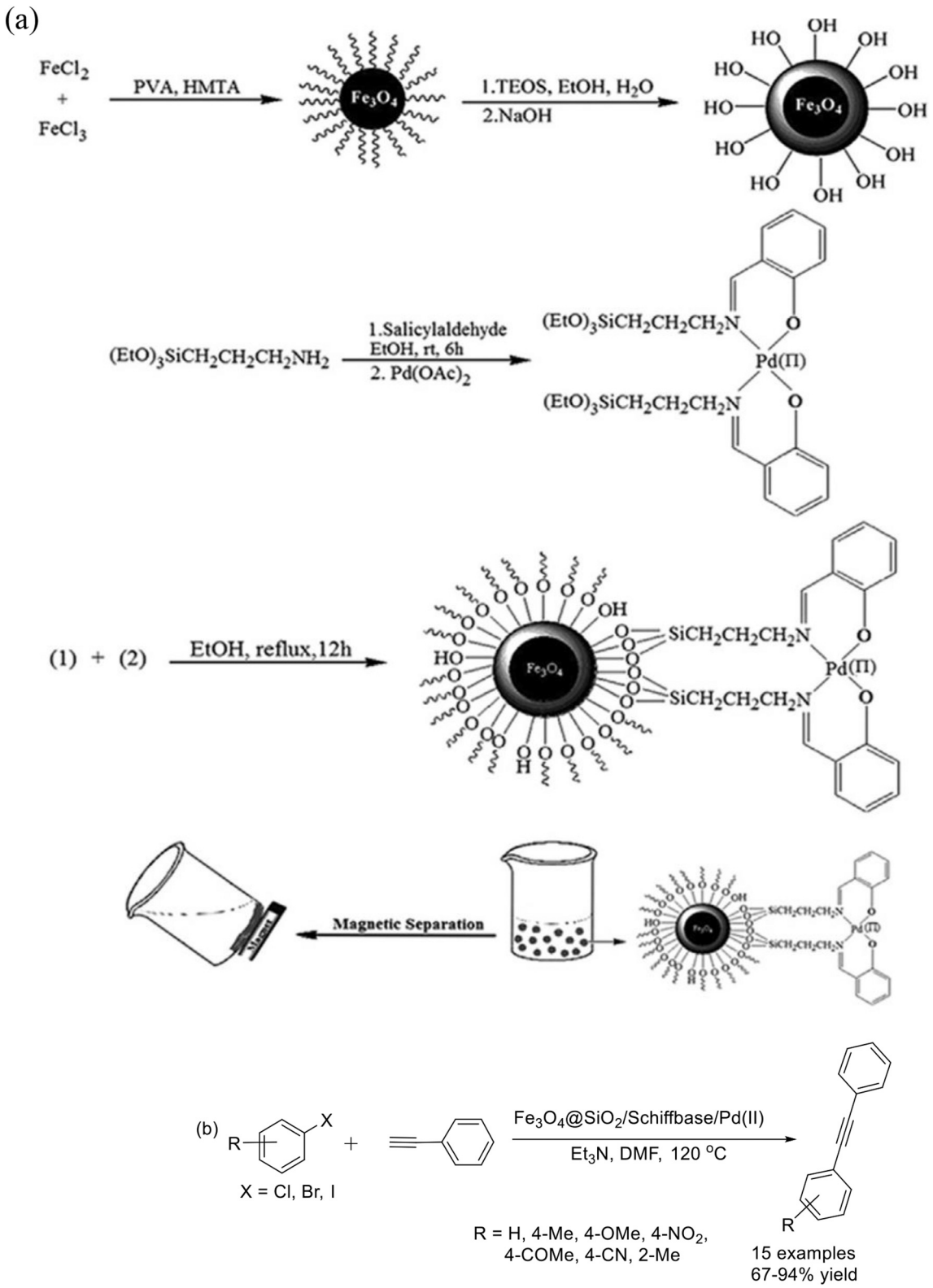

Scheme 18. (a) Preparation of Fe_3O_4@SiO_2 supported Schiff base complex of Pd (II); (b) Sonogashira coupling between aryl halides and phenylacetylene using Fe_3O_4@SiO_2/Schiffbase/Pd(II) catalyst. Adopted from ref. [90]

coupling various aromatic and aliphatic alkynes, secondary amines and aldehydes (aromatic and aliphatic) under solvent free conditions and corresponding products could be obtained in good to excellent yield (Scheme 28b). The mechanism for the Fe_3O_4-mPMF/ZnO nanocomposite catalysed propargylamine synthesis is depicted in scheme 28c. The authors proposed that ZnO nanoparticles embedded on the core Fe_3O_4 nanoparticles activate terminal C–H bond of phenylacetylene which is converted into the metal/acetylide intermediate. Thereafter, the nucleophilic addition of the amine moiety to the activate aldehyde led to the generation of iminium ion which was attacked by the metal/

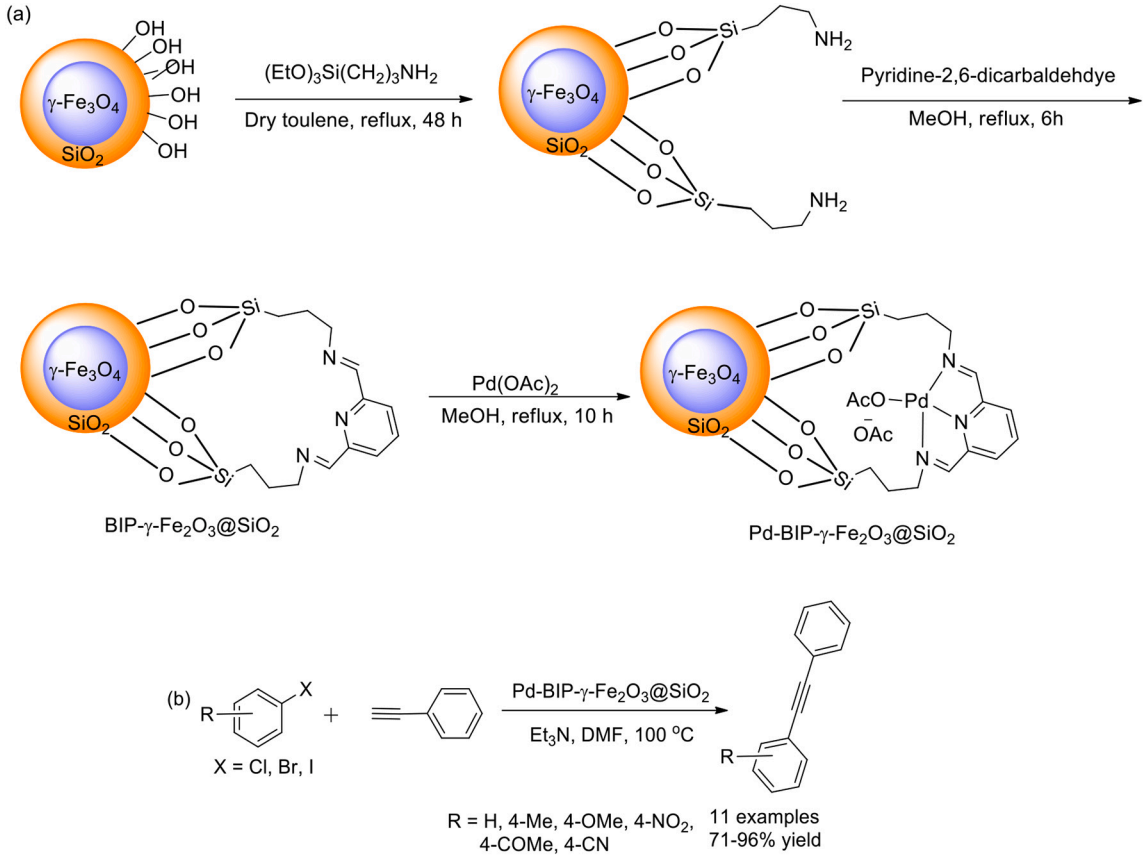

Scheme 19. (a) Synthesis of Fe_3O_4@SiO_2 superparamagnetic nanoparticle; (b) Sonogashira coupling between aryl halides and phenylacetylene using Pd-BIP-γ-Fe_2O_3@SiO_2 catalyst. Adopted from ref. [91]

acetylide intermediate, generating the corresponding propargylamine.

5. Recent breakthroughs and future perspectives in C—H activation using innovative tools/techniques

5.1. Photocatalysis

Faced with the world-wide challenges of increasing energy crisis, environmental contamination and global warming, present-day scenario demands the development of efficient environmentally friendly greener routes that could directly harness solar energy into energy of usable form. The scientific community has great desire of developing reaction systems that resourcefully harvest visible light as the energy source for driving industrially noteworthy chemical transformations. Photocatalysis is one such process that encompasses direct transformation of light energy into chemical energy through photoactive materials and has gained incredible attention in the recent years [107]. Further, inclusion of magnetic components imparts numerous excellent features such as immense chemical and thermal stability, ease of recoverability *via* external magnetic forces to the overall photocatalytic system [108]. Within this context, Sharma *et al.* [109] delineated the synthesis of a magnetically retrievable ruthenium based photoredox catalyst for the cross-dehydrogenative coupling approach involving transformation of sp^3 C—H bond adjacent to tertiary amines. The catalyst was fabricated by adopting surface functionalization strategy wherein Fe_3O_4 nanoparticles prepared *via* co-precipitation approach were coated with silica and further modified with APTES as the functionalizing agent to afford ASMNPs. A Schiff base condensation approach was further employed for grafting 4,5-diazafluoren-9-one (DAFO) onto ASMNPs which was finally metalated using $RuCl_3$ to form the desired Ru@DAFO@ASMNPs photocatalyst (Scheme 29a).

Catalytic potential of the designed photoresponsive Ru@DAFO@ASMNPs was thereafter investigated in the photooxidative Mannich reaction using *N*-phenyl-tetrahydroisoquinoline and acetone as representative substrates in the presence of *L*-proline as Lewis base and air as an oxidant under visible light irradiations (Scheme 29b). The synthesized photocatalyst successfully catalyzed the C—H activation between numerous *N*-aryl-tetrahydroisoquinolines based tertiary amines and ketones as carbon nucleophiles to furnish C-C coupled products in remarkable yields along with great regioselectivity. Impressed by the efficiency of the developed photocatalyst, the protocol was further extended to the cross dehydrogenative coupling reaction of tertiary amines with nitroalkanes (Scheme 29c).

A probable mechanistic route (Scheme 29d) was also proposed by the authors which commenced with the photoexcitation of Ru@DAFO@ASMNPs and the photoexcited Ru^{2+}*@DAFO@ASMNPs further oxidize tertiary amines to radical cationic species and gets reduced itself to Ru^{+}*@DAFO@ASMNPs. The reduced Ru^{+}*@DAFO@ASMNPs then gets oxidized by reducing O_2 to $O_2^{\cdot-}$. The deprotonation of radical cation by $O_2^{\cdot-}$ led to the generation of reactive iminium ion which then reacts with the activated nucleophile species to furnish the anticipated cross coupling product.

Bhalla and co-workers reported the synthesis of a heterooligophenylene derivative attached with thiophene moieties which formed spherical aggregates in aqueous media and further served as a reactor for preparing bimetallic Au-Fe_3O_4 hybrid in THF/H_2O media [110]. Interestingly, during the synthetic process, aggregate derivatives were oxidized to polythiophene moieties possessing fibrous morphology and underwent self-assembly to generate polythiophene-encapsulated bimetallic Au-Fe_3O_4 nanohybrid. The judiciously designed material was then evaluated as a recyclable catalytic entity for C(sp^2)-H bond activation of electron rich anilines with electron deficient alkynes under

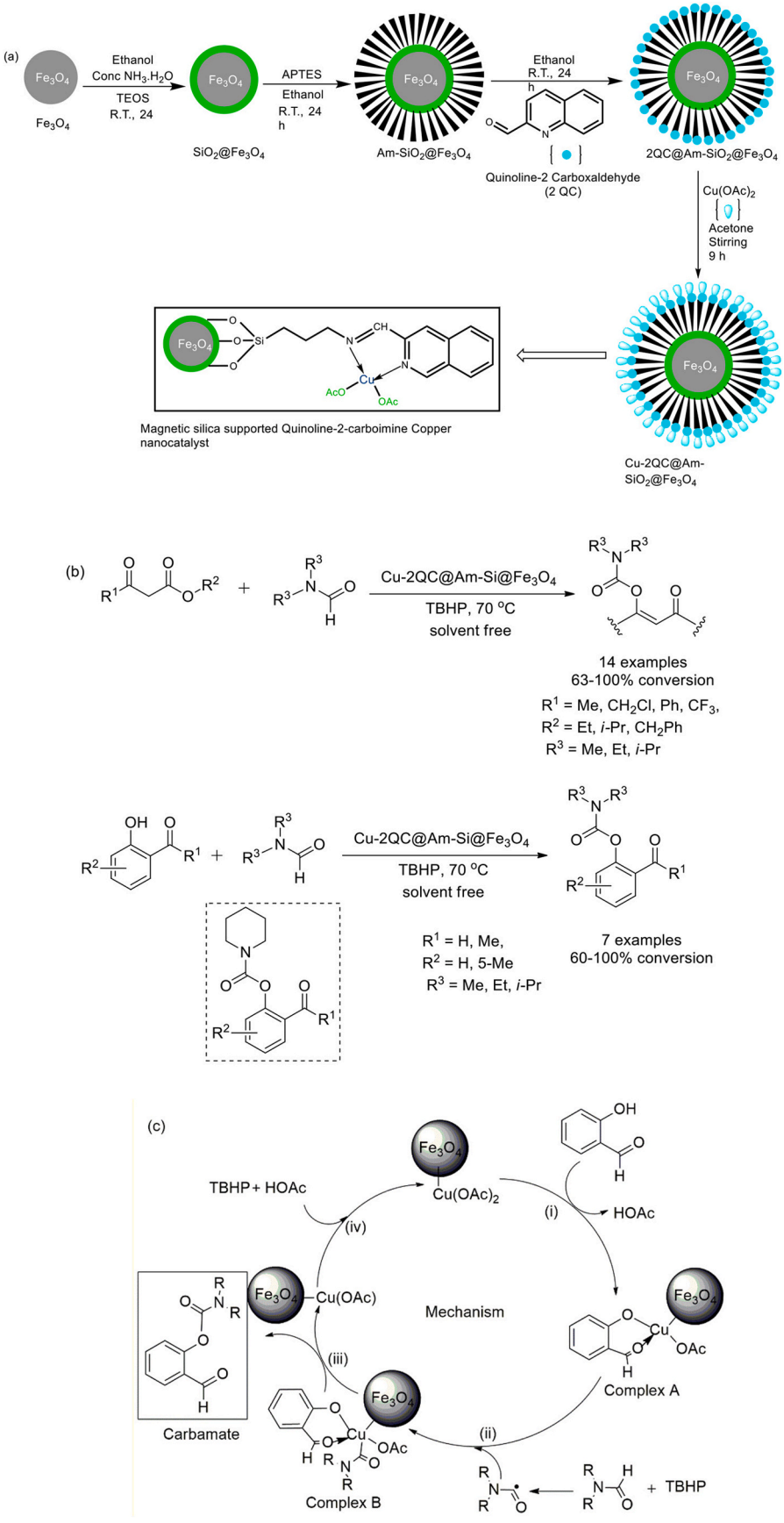

Scheme 20. (a) Preparation of Cu-2QC@Am-SiO_2@Fe_3O_4; (b) Synthesis of carbamates using Cu-2QC@Am-SiO_2@Fe_3O_4; (c) Plausible reaction mechanism.

Table 7
Comparison of the catalytic activity of the Cu-2QC@Am-SiO_2@Fe_3O_4 nano-catalyst with other catalysts reported in literature for the synthesis of carbamates.

Entry	Formamide	Phenols/β-ketoesters	Reaction Conditions	Yield (%)
1		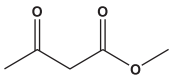	$CuBr_2$ (5 mol %) / TBHP (1.5 equiv) /80 °C/3 h	69
2		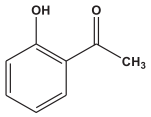	$Cu(OAc)_2$ (5 mol %)/ TBHP (1.5 equiv) / 80 °C/3 h	81
3		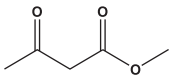	CuCl (1 mol %) / TBHP/ 70 °C/ 15-30 min	85
4		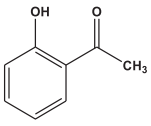	CuCl(1 mol %) /TBHP/ 70 °C/ 15-30 min	99
5		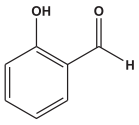	CuCl(1-2mol%)/TBHP/ 80 °C/ 15 min	96
6		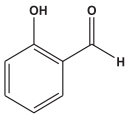	$Cu_2(BPDC)_2(BPY)$/TBHP/ 100 °C/ 120 min (n-hexane as an internal standard)	88
7		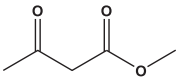	Cu-2QC@Am-SiO_2@Fe_3O_4 nanocatalyst/TBHP/ reflux at 70 °C/ 15 min	98
8		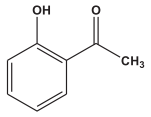	Cu-2QC@Am-SiO_2@Fe_3O_4 nanocatalyst/TBHP/ reflux at 70 °C/ 15 min	97
9		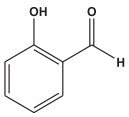	Cu-2QC@Am-SiO_2@Fe_3O_4 nanocatalyst/TBHP/ reflux at 70 °C/ 12 min	99

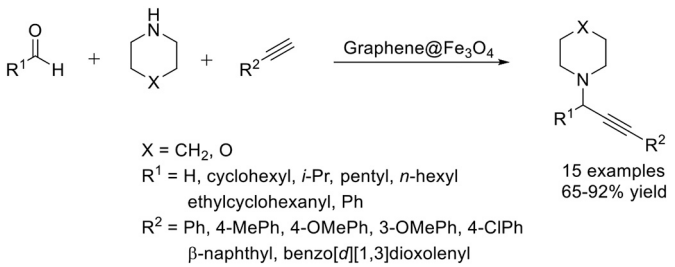

Scheme 21. Graphene@Fe_3O_4 catalyzed A^3-Coupling reaction for the synthesis of propargylic amines.

visible light irradiations for rendering synthetically demanding quinoline carboxylates (Scheme 30a).

For accomplishing desired synthesis, substituted anilines reacted with methyl propiolate in the presence of paraformaldehyde and Au-Fe_3O_4 nanohybrid as the carbonyl source and catalyst respectively to furnish 3-substituted quinolines in good to excellent yields. Further investigations divulged that switching of the alkyne from methyl propiolate to ethyl propiolate also demonstrated satisfactory results in terms of reaction rates and yields of the desired products. In order to elucidate the exact mechanism of quinoline formation, the reaction was also performed in the presence of radical scavenger 2,2,6,6-tetramethyl-1-piperidinoxyl (TEMPO). The obtained results revealed that existence of TEMPO inhibited the reaction thereby validating the formation of free radical. On the basis of results obtained, a probable radical/single electron transfer mechanism has been outlined in Scheme 31a.

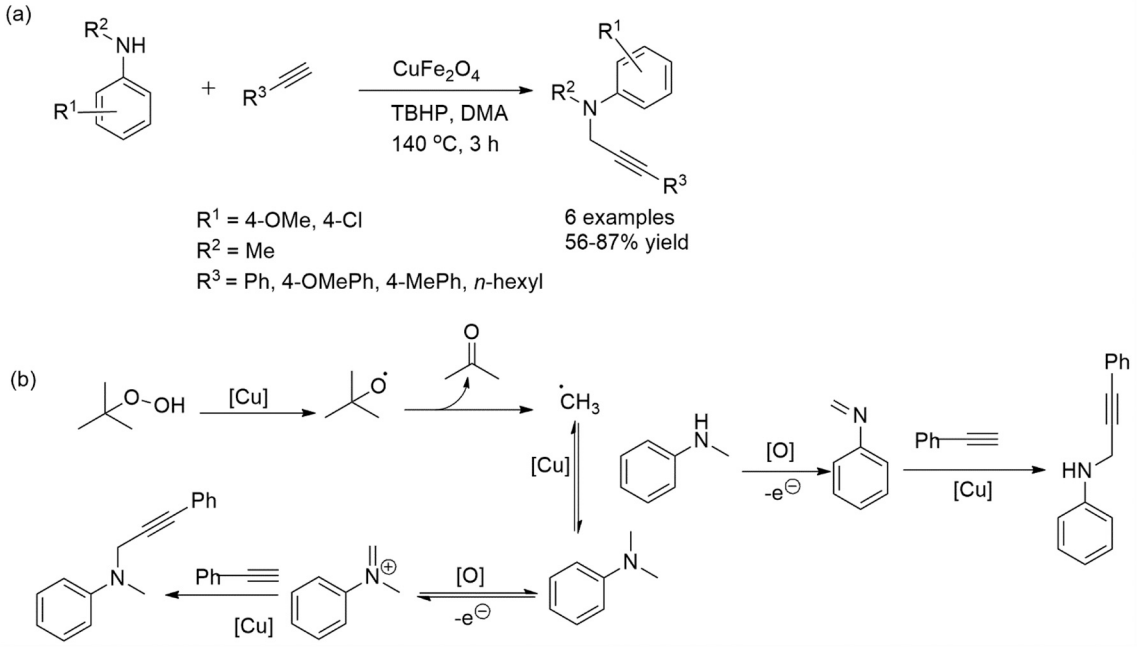

Scheme 22. (a) Superparamagnetic $CuFe_2O_4$ catalysed synthesis of propargylamines; (b) Plausible reaction mechanism.

DFT calculations and possible transition states were also carried out (Scheme 31b) in gas phase through B3LYP functional and 6-31G(d)/LANL2DZ basis sets in Gaussian 09 program. For this Au system (modeled as gold clusters) was chosen for monitoring the reaction mechanism. DFT calculations were conducted on transient electron transfer from light excited Au NPs surface to aniline molecules. The interaction between Au NPs and ortho C(sp^2)-H bond of aniline makes the bond cleavage easier. The energy of photoexcited electrons on Au NPs activates the C—H bond which then furnishes the formation of AuNP stabilized aniline radical intermediate. The subsequent step involves the interaction of π-electron cloud of alkyne and finally intermediates react to construct C-C bond. The next step involves CO insertion and finally annulation leads to the formation of desired quinoline carboxylate. These studies revealed that Au is the main reactive species and catalytic transformation occurs through C—H activation, carbonylation and consequent annulation processes.

Photocatalytic potency of synthesized materials was further assessed in the three component reaction between anilines, benzaldeydes and methyl propiolate to generate quinoline derivatives *via* C—H activation (Scheme 30b). In order to further recognize the mechanism (Scheme 31c), aniline, methyl propiolate and benzaldehyde were reacted in presence of polymer-encapsulated 4:Au-Fe_3O_4 nanohybrid materials and studied using ^{1}H NMR spectroscopy. The ^{1}H NMR spectrum revealed the formation of an alkynylated intermediate (iii) through C(sp^2)-H activation. It is further anticipated that the imine intermediate (i) formed interacted with the alkynes to form alkynylated intermediate (iii) and this imine linkage interacted with Au NPs and behaves as directing group to assist the ortho C(sp^2)-H activation. In the final step, intramolecular hydroarylation resulted in the quinoline generation.

The same research group designed fluorescent assemblies of pentacenequinone derivative with 3-theinyl groups for the subsequent formation of Ag@Fe_3O_4 nanoclusters (NCs) [111]. The synthesized polythiophene supported Ag@Fe_3O_4 NCs (1:2) hybrid assembly was then utilized as a recyclable photocatalyst in the dehydrogenative coupling reaction of benzophenone phenylhydrazones for the production of indazole motifs under ambient reaction conditions i.e. visible light and room temperature (Scheme 32a). Authors further highlighted that quinone assemblies in conjunction with Ag@Fe_3O_4 NCs acted as internal oxidant for the conversion of C—H to C-N bond. It was further revealed that in the composite material, Fe_3O_4 NCs shell acts as active catalytic center while Ag core and polythiophene served the role of visible light antenna and support material respectively to work effectively under photocatalytic conditions.

A probable mechanism of visible light mediated dehydrogenative coupling of benzophenone phenyl hydrazones has been outlined on the basis of experimental results obtained (Scheme 32b). The photocatalytic mechanism initiates with the generation of superoxide anions by the photoexcited electrons present in polythiophene supported Ag@Fe_3O_4 NCs through decomposition of dissolved O_2. The superoxide anions abstract proton from the reactant to form anionic intermediate (A) which then goes through single electron transfer process to form radical B. This intermediate B then undergoes radical addition to the aryl ring followed by subsequent oxidation, deprotonation and elimination of hydrogen peroxide to form the desired product.

The supremacy of present protocol was recognized by comparing the results of the developed catalyst with those already documented in literature (Table 11). It was further validated that the developed photocatalyst exhibited good results in terms of reaction conditions and product yield.

Working on similar lines, another supramolecular porous ensemble of hetero-oligophenylene derivative possessing amino/thiophene groups was synthesized and utilized as template for the subsequent growth of Au-Fe_3O_4 nanodots (size in range of 1.5-2.0 nm) to yield PTh-co-PANI-6:Au-Fe_3O_4 [112]. The developed material was then investigated in the photocatalytic C(sp^2)-H activation of anilines with terminal alkynes to produce quinoline carboxylates under visible light irradiation and eco-friendly conditions. The obtained results proved that the smaller size and morphology of the synthesized catalytic entity delivered superior results in terms of product yield and reaction parameters. Further, diverse substituted aryl amines possessing electron rich/electron withdrawing functionalities and electron deficient alkynes effectively reacted under the optimized conditions to furnish desired products in moderate to excellent yields *via* C—H activation strategy.

5.2. *Use of micro and macro reactors*

The last two decades have seen an increasing popularity in the use of continuous-flow microreactors due to their inherent advantages over

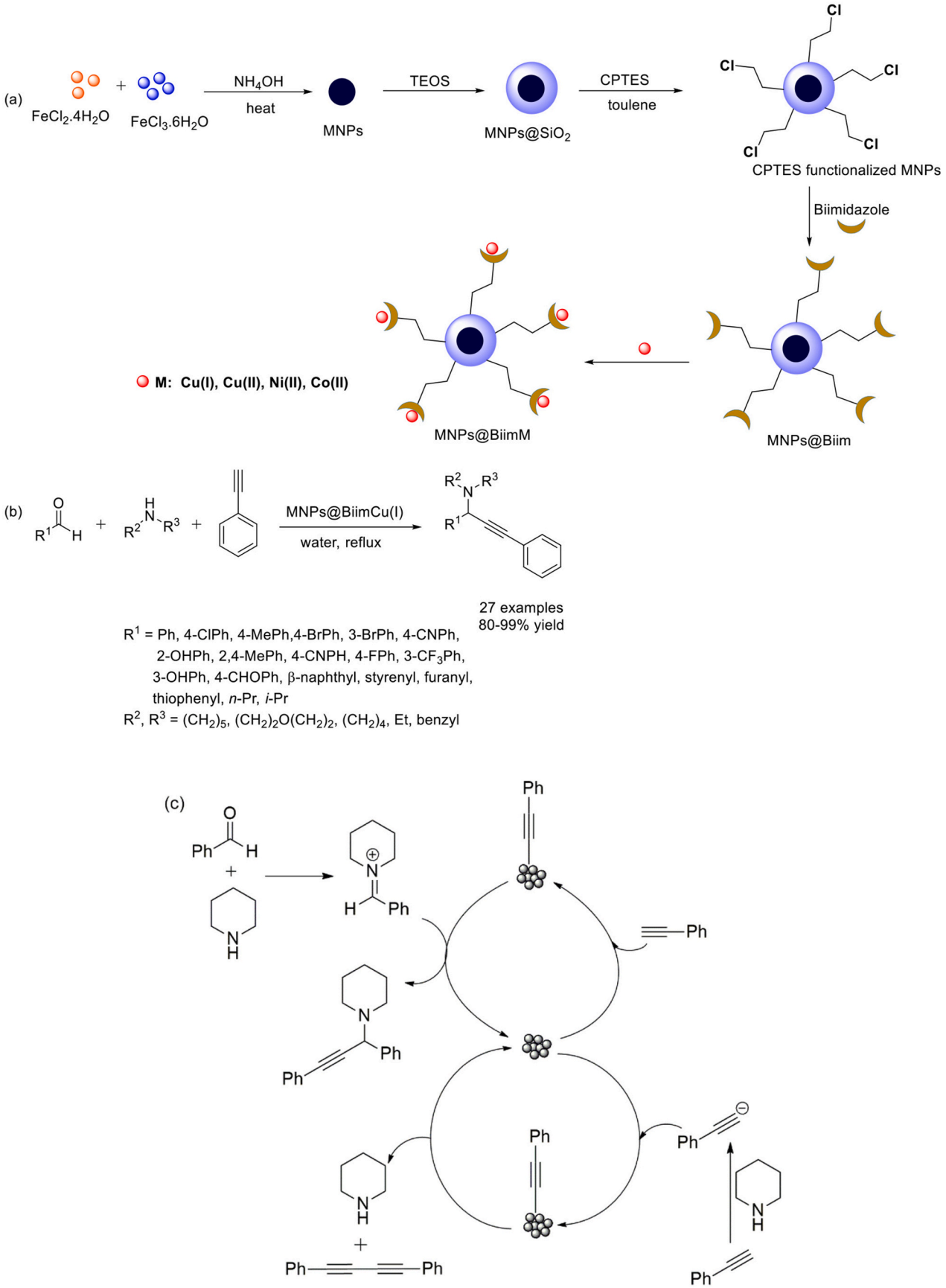

Scheme 23. (a) Schematic representation for the synthesis of MNPs@BiimM; (b) MNPs@BiimM catalyzed A^3-coupling reaction; (c) Possible reaction mechanism.

Table 8
Comparison of catalytic activity of MNP@BiimCu(I) with some literature reports for A^3 coupling reactions.

S. No.	Catalyst (mol%)	Solvent	Temperature (°C)	Time (h)	Yield (%)
1	Ag-graphene (0.1 mol%)	CH_2Cl_2	60	24	86
2	Graphene-Fe_3O_4 (5 mol%)	CH_3CN	80	24	Traces
3	Fe_3O_4 (20 mol%)	Toluene	110	16	75
4	Cu(0)-MM clay (0.05 mol%)	Toluene	110	3	94
5	Cu(OH)x- Fe_3O_4 (0.1 mol%)	Solvent-free	120	3	99
6	Au-SBA (0.04 mol%)	Solvent-free	100	8	95
7	Au/CeO_2 (0.127 mol %)	H_2O	100	6	99
8	MNP@BiimCu(I) (1.7 mol%)	H_2O	reflux	1.5	99

traditional reactor configurations [113]. The most significant benefit of reactor minimisation is the increase in surface area-to-volume ratio, which provides a large interfacial area for multi-phase heterogeneous catalytic reactions. Additionally, small channel diameter (10-100μm) allow for better mass and heat transfer properties [114]. This reduces the formation of hot spots within the reactor (for exothermic reactions) and increases the selectivity of the desired product due to narrow residence time distribution. Heterogeneous catalysis in continuous-flow microreactors offers advantages like higher reaction efficiency, less waste production, better safety, continuous product formation and easy catalyst separation and re-use [115]. Traditionally, heterogeneous catalysis in microreactors are carried out using three configurations: (i) packed bed, (ii) monolithic and (iii) wall coated [112]. However, there are limitations associated with high pressure drop, clogging of micro-channels and catalyst de-activation with these configurations. The advent of magnetic nanoparticles as catalysts and catalyst support has provided vast improvements for the traditional approach to heterogeneous catalysis. One major advantage is the ease of separation of the catalysts from the reaction mixture, reducing the number of downstream processing steps and improving the energy and cost efficiency of the process [116]. In microreactors, an external magnetic field can be used with magnetic nanoparticle catalysts to provide better mixing and carry out in-situ separation of the catalyst from the product stream. From the preceding sections, it is quite evident that the reactions involving the creation of carbon-carbon and carbon-heteroatom bonds have played a crucial role in the synthesis of pharmaceutical and biologically active compounds. However, these reactions are often limited by poor product selectivity in conventional batch technologies. Continuous flow processing has shown potential to improve selectivity through improved mixing and better control over temperature through reducing the possibility of overreaction [113]. Additionally, flow processing allows for lower catalyst loading in some cases due to improved reaction kinetics, which is a common challenge for C—H functionalisation mechanisms [117]. The synergistic potential of continuous-flow microreactors for C—H activation/functionalisation chemistry has been investigated and found to be successful on a lab scale.

Varma *et al.* [118] have demonstrated a rapid protocol for oxidative

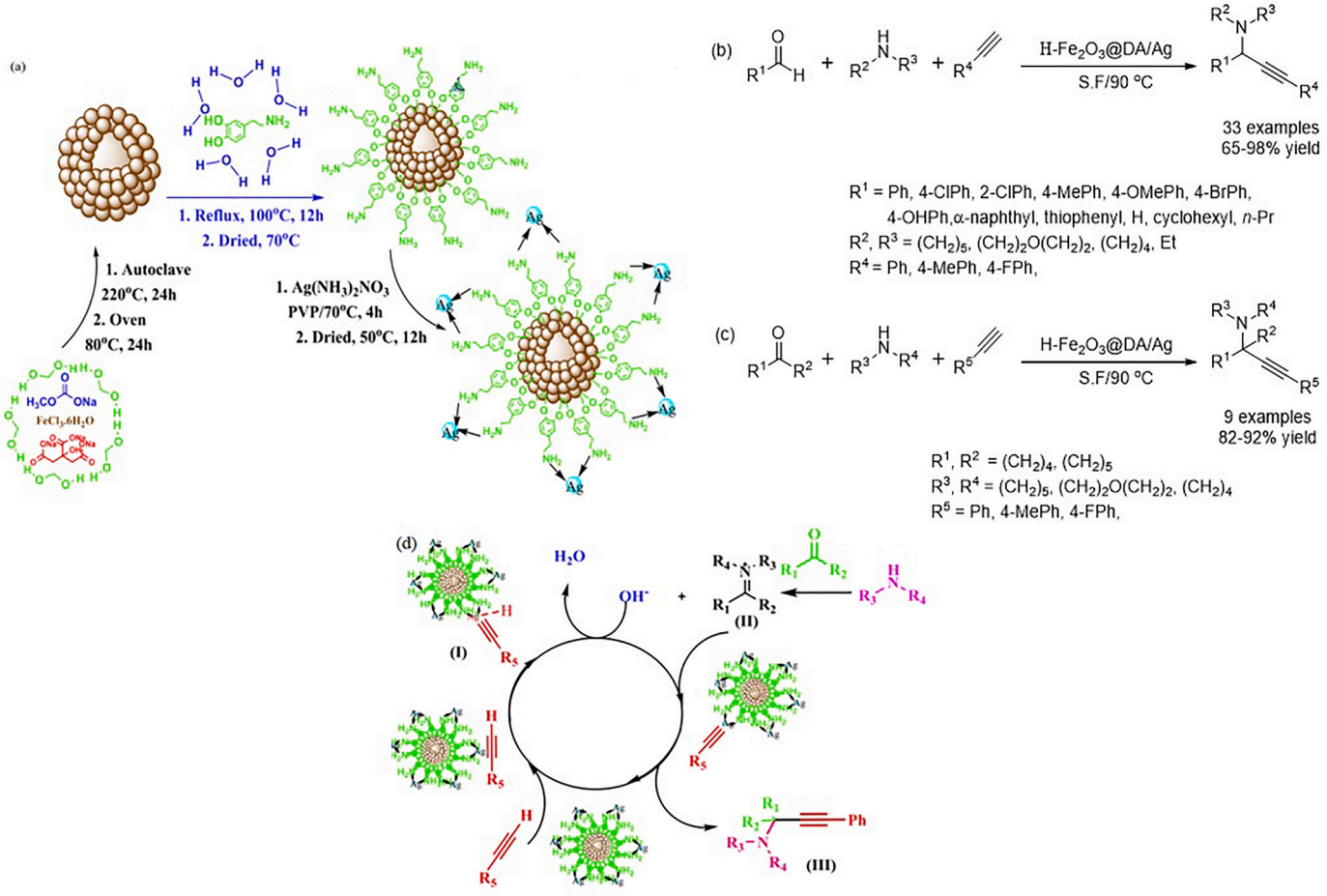

Scheme 24. (a) Synthesis of Ag-doped nanomagnetic Fe_2O_3@DA core shell hollow sphere catalyst; (b) H-Fe_2O_3@DA/Ag catalysed A^3-coupling reactions; (c) H-Fe_2O_3@DA/Ag catalyzed KA^2-coupling reactions; (d) Proposed reaction mechanism. Adopted from ref. [102]

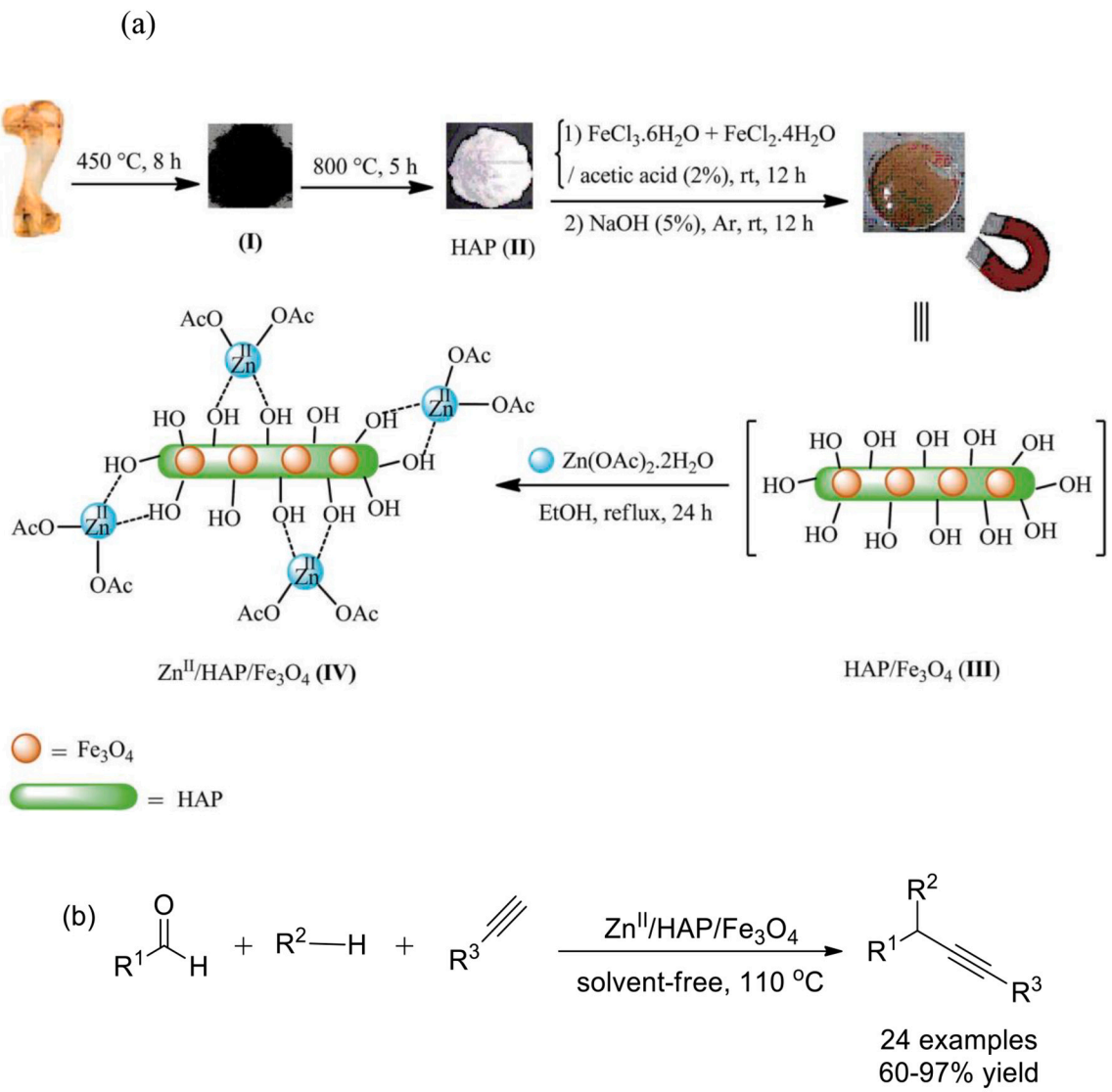

Scheme 25. (a) Preparation of Zn^{II}/HAP/Fe_3O_4 nanocatalyst; (b) Zn^{II}/HAP/Fe_3O_4 nanocatalyst catalyzed solvent free synthesis of propargylic amines; (c) Plausible reaction mechanism. Adopted from ref. [103]

cyanation of secondary and tertiary amines *via* C—H activation under flow conditions using single phase magnetic nano-ferrites as a catalyst (Scheme 33).

The coiled tube flow reactor used in this study enabled the production of thin film of the reaction mixture resulting in superior heat and mass transfer and reducing the reaction time to less than 10 minutes (Fig. 4). The catalyst was easily separated at the end of the reaction through the application of an external magnetic field, while maintaining the catalytic activity on re-use.

Reactions involving powdered and catalysts in microreactors are met with challenges associated with high pressure drop due to clogging of microchannels. To provide deep insights into reactor designing, a few other reactions involving C-C and C-hetero bond formation are also being discussed. The knowledge acquired can be fruitful in leveraging a plethora of diverse C—H functionalizations conducted using suitable micro as well as macro reactors, as ample scope remains in this field. Rehm *et al.* [119] have reported a novel mechanism to circumvent this challenge. Palladium nanoparticle catalyst was embedded within a dendron shell of a magnetic nanoparticle. The whole catalyst system was immobilised on the walls of a glass and a stainless steel microchannel reactor using external magnetic forces. This provides flexibility to the reactor system as the immobilisation is reversible, allowing for a range of catalysts to be immobilised on the microchannel walls. The two reactors were used to investigate Suzuki cross-coupling of 4-bromoanisole with phenyl boronic acid under continuous flow condition. The single pass reaction conversion from both reactors was found to be 5-fold lower

(c)

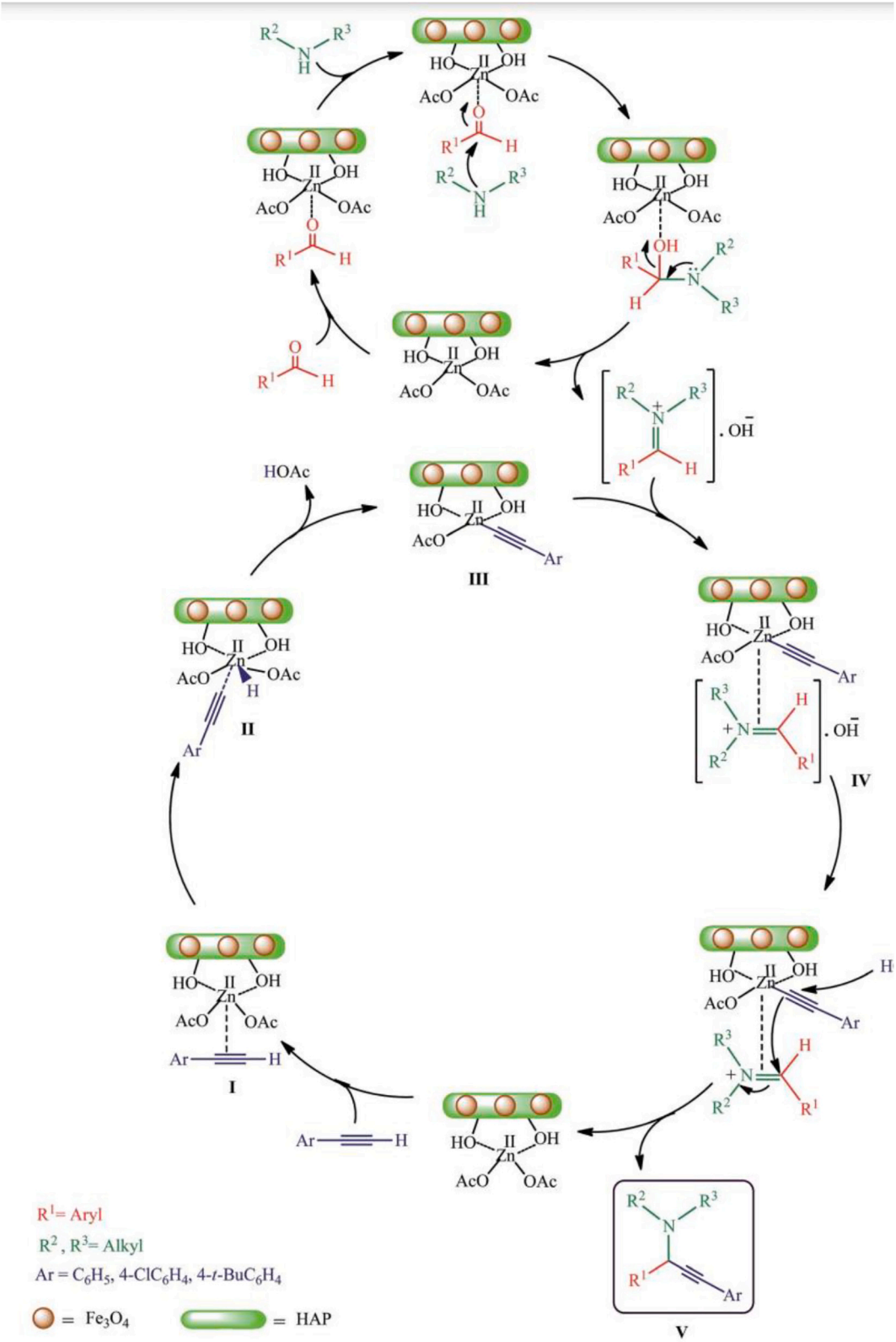

Scheme 25. (*continued*).

in comparison to the batch system. This was mainly due to lower residence time in the microreactor and loss of active catalyst surface area due to immobilisation.

Supported catalytic reactions in microreactors are met with challenges associated with catalyst immobilisation and loss of active catalyst surface area. In-situ separation of catalyst immobilised magnetic particles in flowing fluid from the reaction stream ensures a continuous recirculation of the catalyst stream. Park *et al.* [120] have developed a microchip type separator coupled with a microtube reactor to enable a coaxial flow of the product stream carrying the catalyst immobilised

Table 9
Comparison between proficiency of Zn^{II}/HAP/Fe_3O_4 and other reported catalysts.

S. No.	Catalyst (mol%)	Molar ratio	Solvent	Temperature (°C)	Time (h)	Yield (%)
1	Au/CeO_2, Au/ZrO_2 (0.10 g)	1/1.2/1.3	H_2O	100	12	83
2	Au@GO (1)	1/1.2/1.3	H_2O	100	18	90
3	Fe_3O_4 NPs/GO-CuONPs (0.02 g)	1/2/3	EtOH	90	24	87
4	Fe_3O_4@SBA-15 (5)	1/1.2/1.5	Toluene	110	8	72
5	Cu(OH)-$Fe3O_4$ (3)		Toluene	120	3	99
6	$CuFe_2O_4$ (6.5)	1/1.2/1.3	Toluene	80	4	85
7	Cu(I)-N_2S_2-salen (3)	1/1.1/1.2	Toluene	80	4	92
8	Cu-Mont (0.05)	1/1/1.2	Toluene	110	3	90
9	CuO (10)	1/1.3/1.5	Toluene	90	8	65
10	[Cu(N_2S_2)]Cl@Y-zeolite (0.68 g)	1/1.1/1.2	DCE	70	12	90
11	CuHAP (0.10 g)	1/1.2/1.3	CH_3CN	reflux	6	70
12	$NiCl_2$ (10)	1/1.2/1.5	Toluene	111	8	88
13	$Zn(OAc)_2.H_2O$ (15)	1/1.3/1.5	Toluene	reflux	7	96
14	CuCN (2)	1/1.2/1.5	[bmim]PF_6	120	2	95
15	CuI (10)	1/1.2/1.5	PEG	100	12	92
16	CuI (3)	1/1.2/1.5	Toluene	100	6	98
17	[AQ_2Cu(II)] (5)	1/1.1/1.1	Solvent-free	100	70	96
18	Cu[($CH_3CN)_n$(PPh_3)]Br (5)	1/1/1	Toluene	80	85	44
19	$CuPy_2Cl_2$ (1)	1/1.5/1.5	Solvent-Free	95	40	90
20	Cu(salen) (3)	1/1.2/1.5	Solvent-Free	80	2.5	85
21	ZnO (10)	1/1/1	Solvent-Free	100	2	95
22	Cu_2O/ZnO (0.01 g)	1/1.2/1.5	Solvent-Free	100	1	95
23	CuNPs/TiO_2 (0.50)	1/1/1	Solvent-Free	70	7	91
24	Zn^{II}/HAP/Fe_3O_4 (8)	1/1/1	Solvent-Free	110	3	95

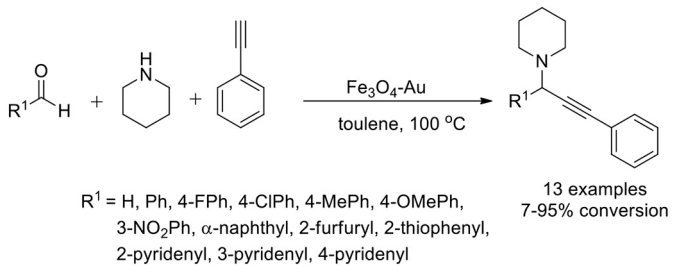

Scheme 26. Fe_3O_4@Au-coated nanoparticles catalyzed synthesis of propargylic amines.

magnetic particles along with the fresh reactant stream (Fig. 3). This ensures a complete separation of the two streams as they are directed into the reactor capillaries. External magnetic forces are applied to the separator channel, leading the product stream out of the reactor while also separating the catalyst particles from the product stream. This is the first example of a self-regulated, continuous microchannel system for supported, magnetic catalytic reactions. Palladium tridentate complex was immobilised on commercially available magnetic nanoparticles functionalised with amine groups and the catalyst system was used to investigate the dioxygenation of alkenes in the microchannel system described above. Dioxygenated product yield of 89% were achieved for a residence time of 14 minutes and was found to be comparable to the product yield from a batch system for a reaction time of 5 hours. The reaction was also carried out for an extended time period of 10 hours to test the robustness of the catalyst activity and separation efficiency in the microchannel reactor system. There was no significant loss in the product yield and no catalyst leaching was observed indicating excellent catalyst re-use properties. The microchannel reactor system can be used for a range of reactions due to easy cleaning in between reaction minimising the reactor downtime.

Lee *et al.* [121] have successfully used the microfluidic technology for fabricating platinum decorated magnetic silica nanoparticles (PMS-NP) and utilizing it furtherfor the oxidation of 4-isopropylbenzaldehyde. The PMS-NPs were then aggregated into microparticles known as PMS-supraballs with a hierarchal pore structure providing a better access to the active sites of the metal catalyst. PMS-supraballs (1 mg) and glass beads were incorporated into a packed bed microreactor for the reaction. The PMS-NP catalysts showed a selectivity of 94-95% towards the product, which was higher in comparison with two commercially available catalyst systems. The catalyst was easily recovered after the reaction using an external magnet with a significant retention of catalyst activity. This study is an example of a general approach to synthesise and incorporate magnetic nanoparticle catalysts in a microreactor and has potential to be applied for a wide range of catalyst/reaction systems.

In addition to supporting metal catalyst, magnetic nanoparticles can be utilised as an inductive source to heat the reaction mixture. Kirschning *et al.* [122] were able to generate thermal energy in the reactor by exposing the magnetic nanoparticles to a constantly changing magnetic field, resulting production of heat due to magnetic inductive hyperthermia. This requires a much simpler technical setup compared to microwave reactors and also offers uniform heating of the reagents. Magnetic nanoparticles with a silica shell coating were used in a microfluidic fixed bed reactor for transesterification and condensation reactions. Further, palladium particles were functionalised on the silica shell to enable Heck and Suzuki-Miyaura cross-coupling reactions. Both catalysts could be re-used over three consecutive cycles without any decrease in the activity.

Miao *et al.* [123] demonstrated for the first time the use of nickel coated ferrite nanoparticles as magnetic self-stirring catalysts for microreactions. The resulting catalyst was easy to fabricate with good size distribution and adaptable to any microreactor configuration. The self-stirring property of the catalyst enabled movement of reactants along narrow channels (using an external magnetic field), thus improving mixing within the microchannels. The catalyst system was tested for reduction of 4-nitrophenol in a microtube reactor. The reaction was found to follow pseudo-first order kinetics and the rate was comparable to that obtained using commercial noble metal nanocatalysts. The catalyst was successfully reused for up to five cycles without any significant loss in catalytic activity.

Schatz *et al.* [124] have successfully immobilised a transition metal complex on carbon coated cobalt nanoparticles through a tagging method involving copper catalysed azide/alkyne cycloaddition reaction. The resulting catalyst system was used to study the asymmetric benzoylation of 1,2-diols in batch and continuous flow conditions. A glass column packed with the catalyst was placed between two adjacent magnetic stir motors which ensured containment and agitation of the magnetic nanocatalyst in difference to the traditional fixed bed reactors which require a membrane to achieve this (Fig. 5). Reaction yields

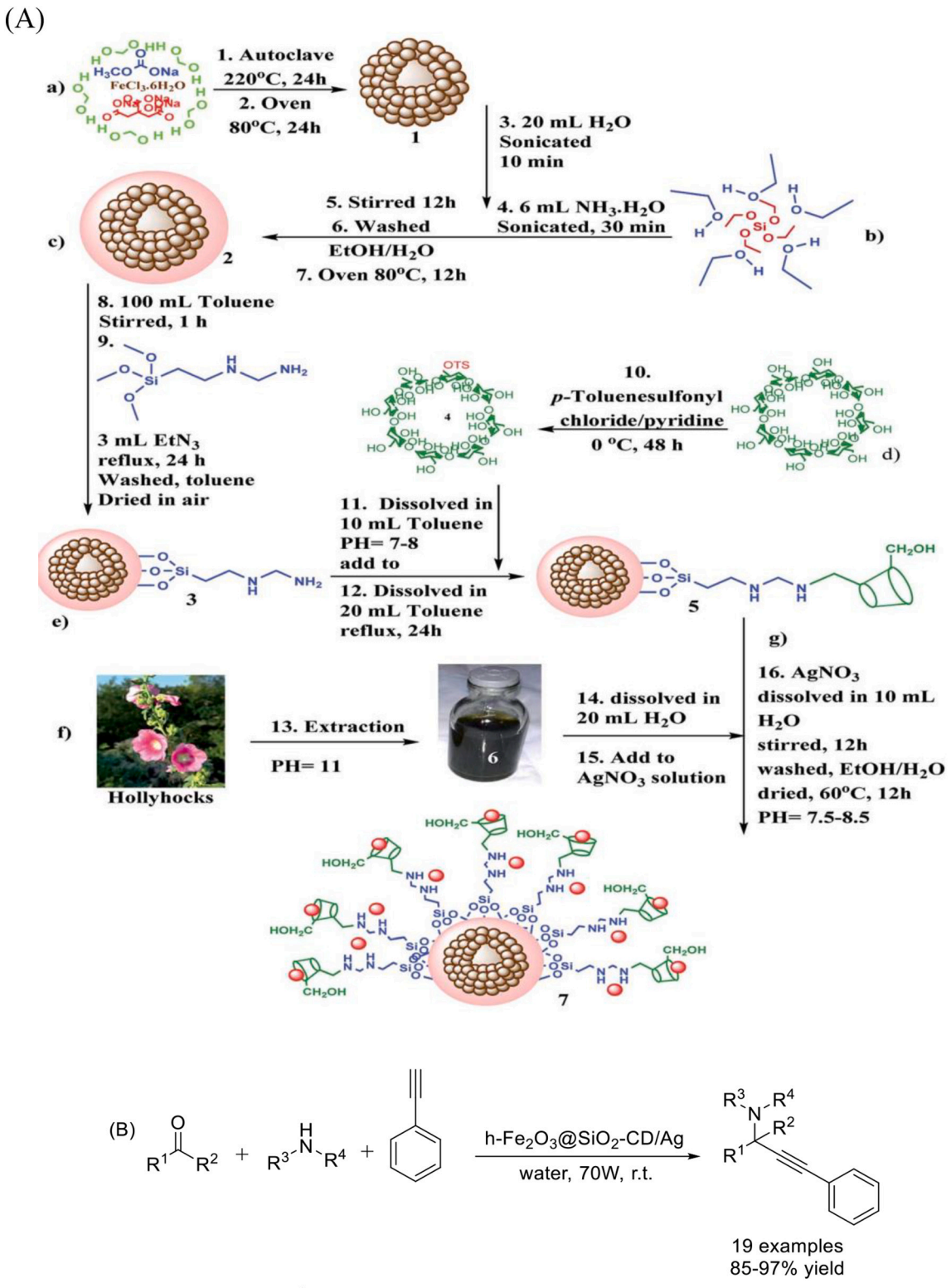

Scheme 27. (A) Synthesis of h-Fe_2O_3@SiO_s-CD/Ag nanoparticles; (B) h-Fe_2O_3@SiO_2-CD/Ag nanoparticles catalyzed synthesis of propargylic amines. Reproduced from Ref. [105] with permission from the Royal Society of Chemistry.

Table 10
Comparison of catalytic activity of h-Fe_2O_3@SiO_2-CD/Ag with other reported catalysts.

S. No.	Catalyst	Amount	Reaction Conditions	Time (min)	Yield (%)
1	CuI	15 mg	H_2O/r.t./U.S.	45	98
2	h-Fe_2O_3@SiO_2-CD/Ag	20 mg	H_2O/r.t./70 W	7	97
3	h- Fe_2O_3@DA/Ag	10 mg	S.F./90 °C	60	96
4	Gold nanocrystals stabilized on montmorillonite	20 mg	Reflux/ toluene	180	91
5	ZnO nanoparticles	10 mol %	Stirrer/ 90 °C	120	89
6	Immobolized silver on surface-modified ZnONPs	10 mol %	Reflux/H_2O	240	89
7	Cu_2O-ZnO	10 mg	S.F./100 °C	60	95
8	CuCN	2 mol%	[bmim]PF_6/S. F./120 °C	120	95
9	CuNPs/TiO_2	0.5 mol %	Neat/70 °C	420	91
10	Naflon-NR50	350 mg	CH_3CN/70-80 °C/ N_2 atm	300	85
11	ZnS	10 mol %	Reflux/ CH_3CN	270	89

between 43-47% were achieved with >99% enantioselectivity under flow conditions using a lower catalyst loading in difference to the batch system. This study demonstrates the versatility, thermal stability and chemical inertness of the carbon coated cobalt nanoparticles as scaffold for metal catalysts for future applications of organic transformations in continuous flow reactor systems.

Zhang *et al.* [125] have successfully demonstrated the synergistic catalytic effect of MOFs and magnetic nanoparticles for fast reactions in a microreactor. The Fe_3O_4 magnetic core was first pre-treated with a polyelectrolyte to modify the surface charge to enable the absorption of zinc cations, resulting in the formation of a thin film of ZIF-8 on the magnetic core shell microsphere. The Fe_3O_4@ZIF-8 catalyst was used to catalyse Knoevenagel condensation reaction in a microreactor. The catalyst was filled in the microcapillaries using an external magnetic field and the catalyst loading could be easily controlled by changing the catalyst concentration in the solvent feed. Also, the magnetic property of the catalyst ensured the microspheres remained well dispersed in the liquid feed, reducing mass transfer limitations. Under the same experimental conditions, the conversion in the microreactor was found to be 50% higher in the microreactor compared to the batch reactor for a residence time of 25 minutes. The superior reaction efficiency was attributed to the ZIF-8 nanocrystals on the shell and the microreactor configuration enhancing the reaction rate.

Environmentally benign catalysts are fast gaining importance due to increased need for sustainability in organic transformations. Nafion-H catalysts have shown superior catalytic activity while being ecologically friendly for organic transformations. Narei *et al.* [126] have developed a new catalyst system by immobilising Nafion-H on superparamagnetic iron oxide nanoparticles (SPIONs) encapsulated within a silica shell. The Nafion-H/Spion catalyst system was used in the Dakin-West reaction for the synthesis of β-Acetamido ketones in a microtube reactor. In a typical experiment, a T-shaped micromixer, microtube reactor was pumped with the feed containing the reactants and the catalyst dispersed in the reaction solvent. After a residence time of 10 minutes in the reactor, the outlet stream was collected and the catalyst was separated using an external magnet. The product yield in the microreactor was found to be 5% higher compared to the conventional stirred tank reactor under the same experimental conditions. Further, the catalyst could be re-used for up to seven times without any significant loss in the catalyst activity.

Obermayer *et al.* [127] have reported the combination of iron oxide nanoparticle catalyst encapsulated within a mesoporous aluminosilicate support and a TEMPO co-catalyst for aerobic oxidation of benzyl alcohol in continuous flow conditions. A fixed bed catalyst cartridge was employed in an automated flow set-up. Initial experiments from this configuration were accompanied by high pressure drop along the catalyst bed and low product yields. The catalyst was diluted with silica gel to circumvent the pressure drop problem, but this resulted in reduction of the active catalyst sites and hence a lower substrate: catalyst ratio and a further reduction in product yield. Further experiments were carried out by operating the reactor in a semi-batch mode and complete conversions were observed for the reaction. This indicates that the reaction can be carried under flow conditions, by increasing the length of the catalyst bed, to increase the residence time of the reaction mixture. The catalyst bed was found to deactivate due to the deposition of reaction by-products, which was overcome by increasing the concentration of the co-catalyst to shift the reaction equilibrium towards the desired product. Overall, the low reaction volumes and low oxygen gas pressures greatly improved the safety of the otherwise dangerous reaction scheme.

5.3. Membrane reactors

Membrane reactors are one of the earliest examples of achieving process intensification by combining reaction and separation steps in a single unit. The membrane reactor can be operated in three configurations: (i) selective removal of products from the reactor, (ii) controlled addition of reactants to the reaction mixture and (iii) improve contact between the reactant and catalyst (catalytic membranes) [114b,128] Flow through catalytic membrane reactor is a popular configuration for heterogeneous catalytic transformations due to high catalyst activity. The catalyst is present inside the membrane pores resulting in convective flow of reactants intensifying the contact between the catalyst and the reactants [128,129]. In traditional fixed bed reactor, the reaction rate is often limited by pore diffusion resistance. In addition to providing high product selectivity and yield, they also minimise catalyst losses compared to traditional homogeneous catalyst systems [129]

Bahadorikhalili *et al.* [129a] have developed a flow through catalytic membrane reactor to overcome the challenges associated with separation of reactant feed and mass transfer limitations with conventional membrane reactors (Scheme 34). The catalyst system consisted of palladium immobilised on a silica coated iron oxide core shell nanoparticles. The catalyst was used as an active filler for the preparation of polyethersulfone/palladium nanoparticle catalytic membrane through phase inversion method. This catalyst was incorporated in a flow through membrane reactor to investigate Heck and Sonogashira coupling reactions. Excellent reaction yield were obtained, which was comparable to reports from flow processes and even higher in some cases. The study also demonstrated the reusability of the catalytic membrane with no fouling for ten consecutive runs. In difference to the traditional methods for the two reaction schemes, this study used water as a solvent and milder reaction conditions, hence reducing the negative environmental impacts. The PES/NP membrane could be tuned easily to increase the surface hydrophilicity, resulting in improved reaction yields.

5.4. Enzymatic catalysis

Enzymes are macromolecules which are advantageous due to their high specificity, selectivity and stability towards organic and biochemical reactions and that too under mild conditions. Enzymes are popularly used in processes, such as redox reactions, (trans)-esterification processes, hydrolysis and enantioselective synthesis but their high cost, difficulty in reuse, recycling and availability restricts their usage. With the progress of magnetic nano particle as substrate for enzymes, facilitated the use of enzymes for catalytic applications. Enzymes are very active biomolecules, which can serve as highly specific and efficient catalysts. Many enzyme nanomimics which have been produced from

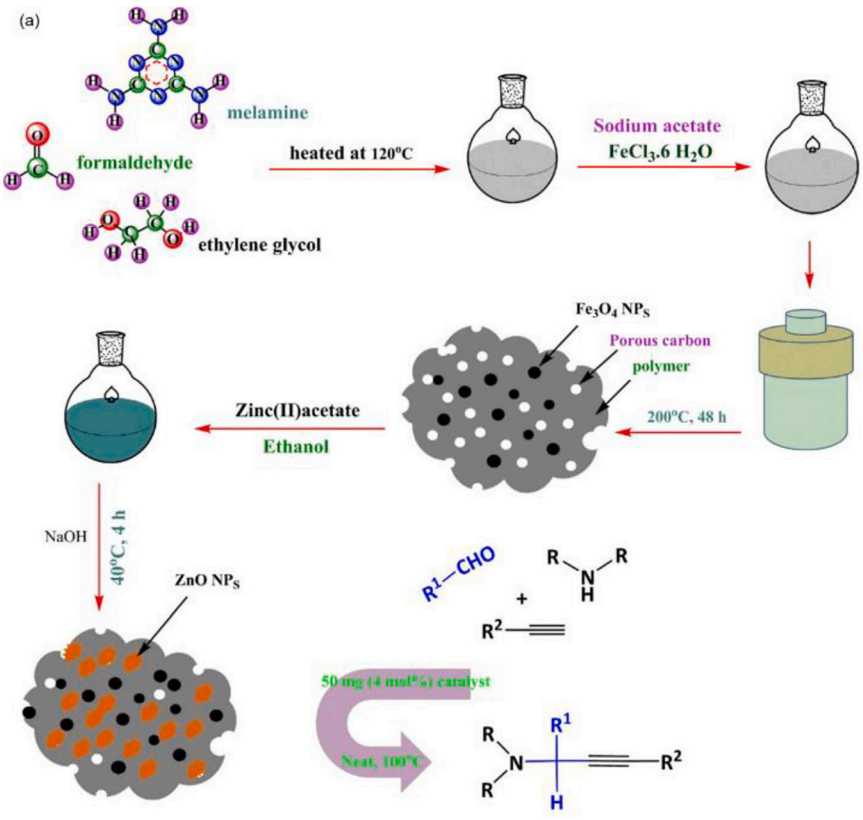

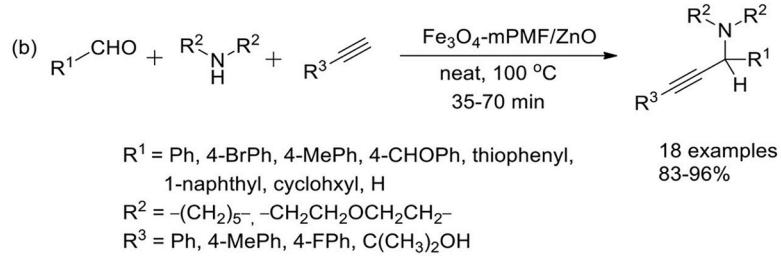

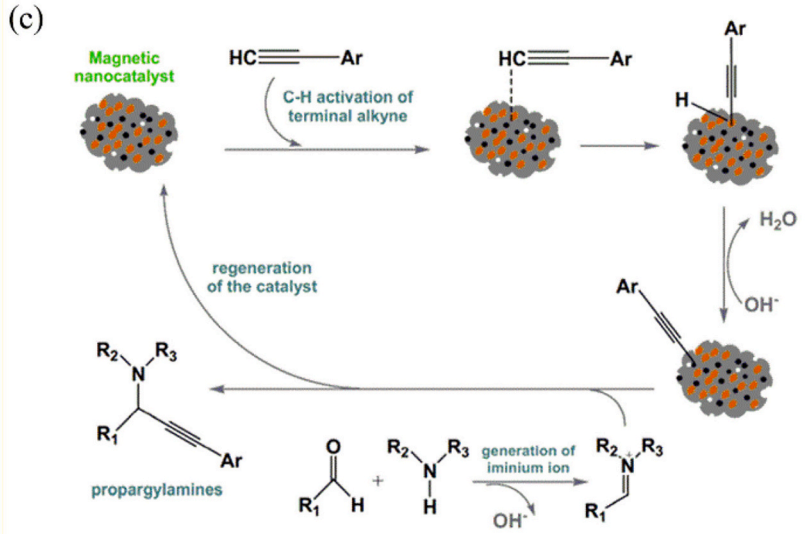

Scheme 28. (a) Synthesis of Fe_3O_4-mPMF/ZnO nanocomposite; (b) Synthesis of propargylic amines using Fe_3O_4-mPMF/ZnO nanocomposite; (c) Plausible reaction mechanism. Adopted from ref. [106]

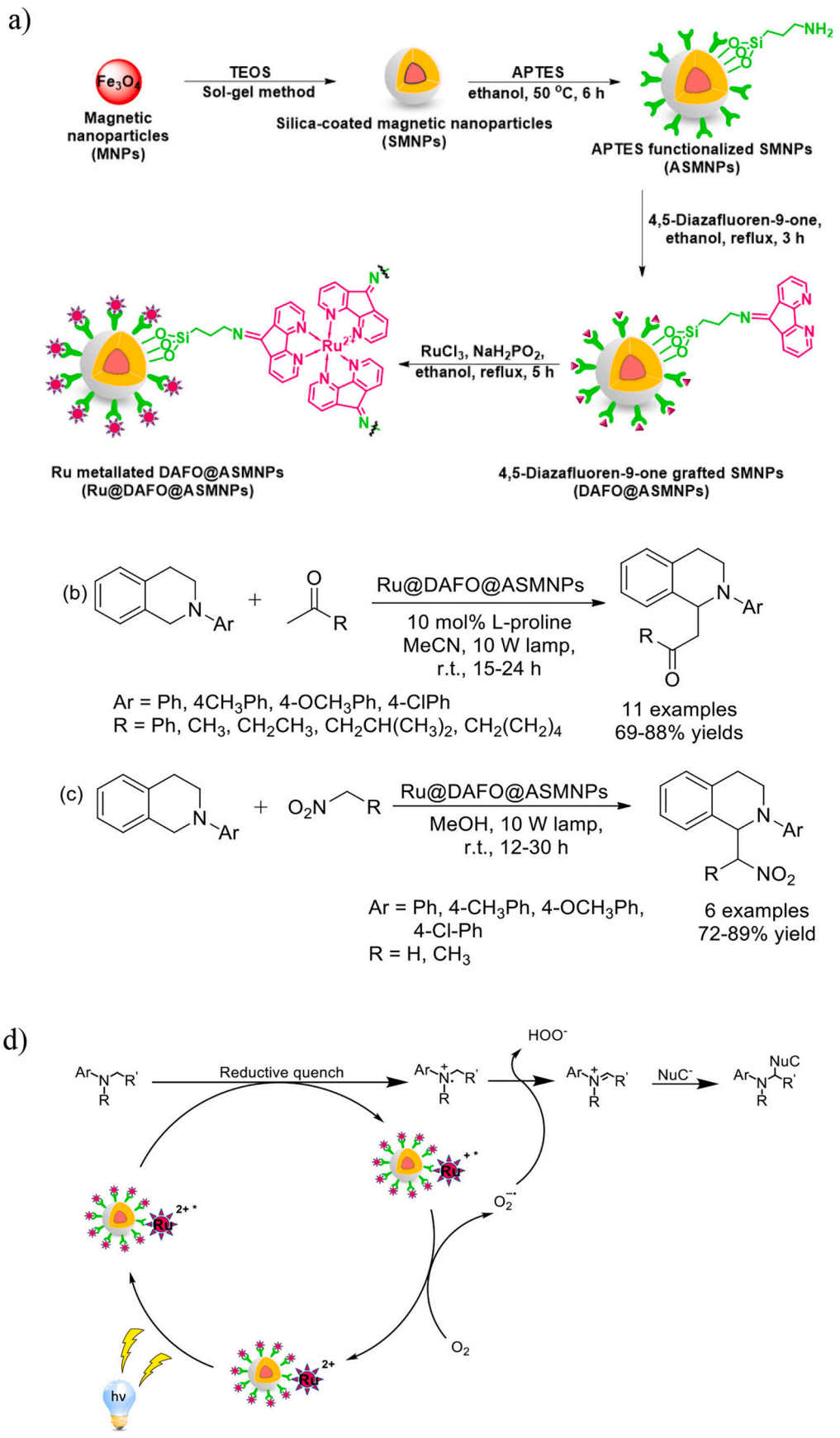

Scheme 29. (a) Synthetic illustration of magnetic Ru@DAFO@ASMNPs photocatalyst; A magnetic Ru@DAFO@ASMNPs photocatalyst assisted (b) Mannich reaction (c) Nitro-Mannich reaction and (d) Plausible reaction mechanism of Ru@DAFO@ASMNPs mediated cross-dehydrogenative coupling reaction. Reproduced with permission from Royal Society of Chemistry from ref. [109]

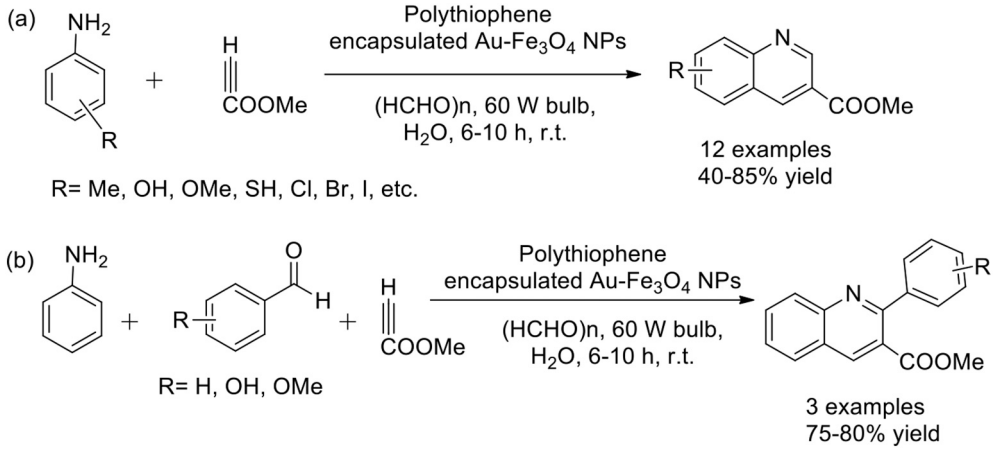

Scheme 30. Polythiophene encapsulated Au-Fe_3O_4 NPs (0.5 mol%, i.e. 300 μL of 4:Au-Fe_3O_4 in Water/THF, 7/3) under Photocatalytic conditions (Irradiation of 60 W Tungsten Filament Bulb) assisted (a) photocatalytic C(sp^2)-H activation reaction between anilines, methyl propiolate and paraformaldehyde; (b) photocatalytic C (sp^2)-H activation reaction between anilines, methyl propiolate and substituted benzaldehydes.

nanoparticles showed specific catalytic activities [130]. Enzymes can be attached to the surface of magnetic nanoparticles or beads through the use of EDC coupling [131] and these nanocomposites can then be used for a range of reactions for the production of useful pharmaceuticals and organic materials [132] as well as other applications in fields such as sensing [133] for proteomic sample preparation and peptidomic analysis [134].

Magnetic nanoparticle supported catalysis has shown tremendous success in last few years. Many studies have been reported for utilisation of MNP supported enzymes for production at industrial level. In one recent work magnetic nanoparticles by Huizhou *et al.* were produced in the presence of gum Arabic through precipitation [135] then Lipase derived from Candida rugosa was bound on it. The resultant enzyme supported on MNP was utilized for the multi-step synthesis of ethyl-isovalerate with 80% conversion rate. β- fructanfuranosidase immobilised over chitosan stabilised MNP were used for the production of fructo-oligosaccarides from sucrose [136]. Peijun *et al.* [137] utilised nanocomposites supported on functionalized magnetic iron oxides [138] bound with lipase extracted from Yarrowia lipolytica on carbon nanotubes for highly effective chiral resolution of (*R,S*)-1-Phenyl ethanol in heptane.

A lot of researches have been focussed on utilization of MNP supported enzymatic catalysis for organic transformations such as hydrolysis reactions and enzymatic esterification [139]. MNPs coated with an inorganic oxide, such as silica for example Fe_3O_4@SiO_2 serves a strong substrate to immobilize enzymes and is reported for production of biodiesel with excellent yields [140]. Fe_3O_4@SiO_2 also served as covalent substrate for lipase extracted from Candida antarctica (CALB) and is utilized for catalytic synthesis of biodiesel from cooking oil with almost 100% conversion [141]. In another study magnetic nanoparticles were used for immobilization of lipase from cephalosporin Pseudomonas for catalytic synthesis of biodiesel from waste edible oil [142]. Wang *et al.* [143] have thoroughly discussed the catalytic importance of MNPs for green synthesis of biodiesel. The effort will be definitely instructive for the future research avenues in the field of all emerging areas involving magnetic nanoparticle catalyzed synthesis. Trichoderma reesei cellulase was covalently immobilized on chitosan-coated magnetic nanoparticles using glutaraldehyde as a coupling agent and was utilized for hydrolysis of carboxymethylcellulose [144]. *N*-methylglucamine based calix [4] arene magnetic nanoparticles enhanced the enantioselective synthesis of S-Naproxen with yield greater than 98% when used with Candida rugosa lipase (CRL) encapsulated within a chemically inert sol–gel support (Scheme 35) [145].

A number of studies on enzymes for C—H bonds functionalization has also been reported [146]. Davies *et al.* [147] briefly reviewed the catalytic methods for C—H functionalization in organic transformations such as hydroxylation to hydroalkylation. They specified the role of dehydratases to convert glycerol to 3-hydroxypropionaldehyde, FAD-dependent hydroxylases and halogenases for aromatic hydroxylation, xylene monooxygenases (TMO and XMO) catalysed aromatic and benzylic hydroxylation and haem enzymes for aliphatic hydroxylation. Zhang *et al.* [148] evaluated the activity of amine-functionalized SiO_2@Fe_3O_4 NPs supported α-amylase in the hydrolysis of starch. Bovine Carbonic anhydrase (CA) immobilized on (octa(aminophenyl)-silsesquioxane)-modified Fe_3O_4/SiO_2 NPs [149] *via* covalent bonding have shown satisfactory sequestration of CO_2. Other magnetic substrates like alpha chymotrypsin-coated Fe_3O_4, gum Arabic (a surfactant) coated Fe_3O_4 NPs, β-cyclodextrin@SiO_2 were also reported [150]. A magnetically separable nano biocatalyst composing of a covalently immobilized enzyme (chloroperoxidase, CPO) on iron oxides MNP and core shell of polymer has been reported for enantioselective sulfoxidation of thioanisole to result into (*R*)-methyl phenyl sulfoxide [151]. Chen *et al.* [152] have shown activity of immobilized lipases on zirconia modified by a carboxylic surfactant and found significant improvement towards asymmetric reactions in organic media.

In lieu of the above researches carried out in field of enzymatic catalysis, it is noteworthy that the in-spite of an extensive research reports utilizing potential of enzymes and of magnetic nano particle towards greener synthesis, biosensing, biofuel production and organic transformation leading to cleaner derivatives; to the best of our knowledge, researches focussing on potential of enzymes immobilized MNPs are not significantly reported so far for CH bond functionalization. CH bond activation either *via* enzymatic catalysis on various substrates or magnetic nano particle catalysed are reported. Thus, looking into the potential of MNPs and enzymes towards C—H bond functionalization; there is need to explore MNP based enzymatic catalysis. Coating or encapsulation of active MNPs and utilizing them as substrate for enzyme could result into considerable potentialities for further research and could also minimize the toxicity of MNPs.

5.5. Regioselective synthesis

The C—H functionalization or activation by transition metals are of significant importance in organic chemistry due to their highly versatile applications for the synthesis of polymers, pharmaceuticals, feedstock chemicals and natural products [153]. Regioselectivity is an important concern in organic synthesis for development of desired product in good yields. Magnetically recoverable nanoparticles have recently attracted considerable attention in this regard due to their good catalytic efficiency to produce products selectively. Numerous magnetic

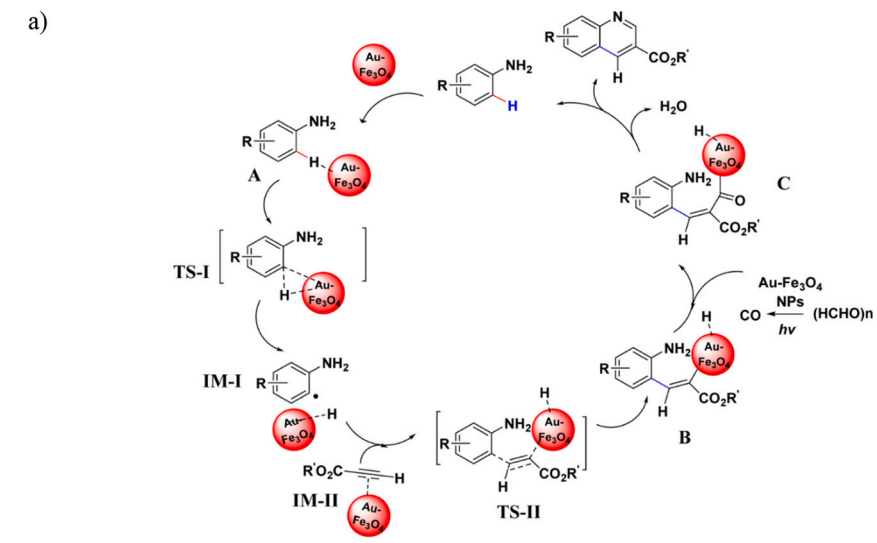

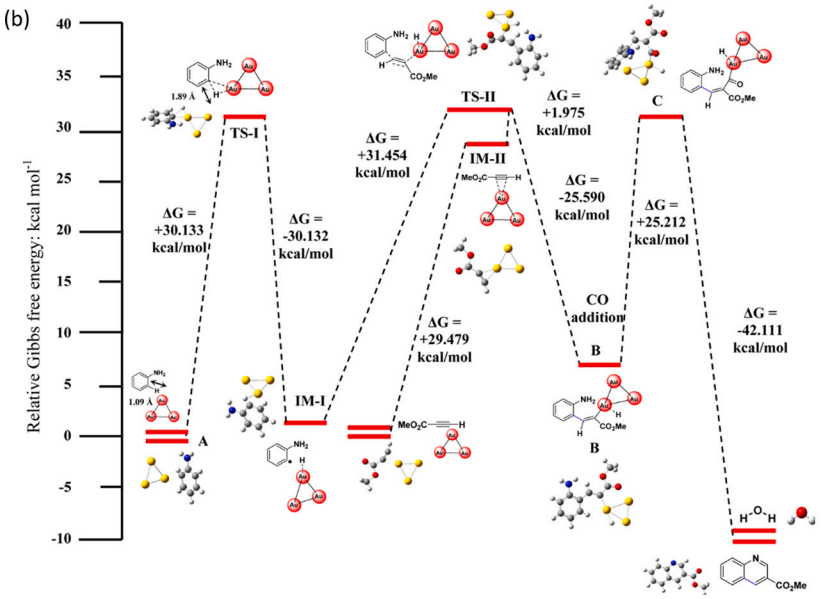

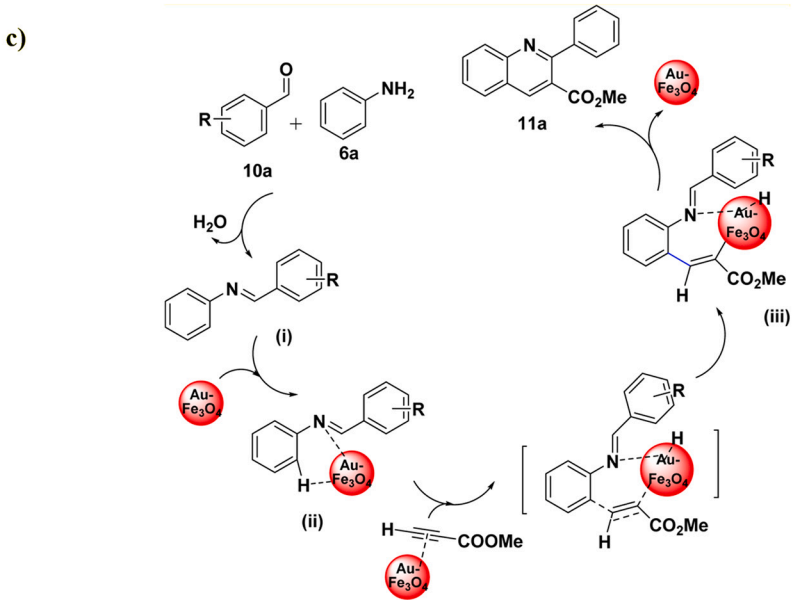

Scheme 31. (a) Probable reaction mechanism for synthesis of Quinoline through C(sp^2)-H activation between substituted anilines, alkynes and paraformaldehyde (R= substituents and R'= Me/Et) catalyzed by Polythiophene Encapsulated Au-Fe_3O_4 NPs (0.5 mol%, i.e. 300 μL of 4: Au-Fe_3O_4 in Water/THF, 7/3) under Photocatalytic conditions (Irradiation of 60 W Tungsten Filament Bulb). (b) Plausible reaction mechanism for the synthesis of Quinolines derivatives *via* C(sp^2)-H activation reaction between anilines, alkynes and paraformaldehyde catalyzed by 4: Au-Fe_3O_4 NPs and (c) Plausible reaction mechanism of Quinoline synthesis through C(sp^2)-H activation reactions between anilines, alkynes and substituted aromatic aldehydes (R=substituents) catalyzed by Polythiophene encapsulated Au-Fe_3O_4 NPs (0.5 mol%, i.e., 300 L of 4:Au-Fe_3O_4 in water/THF, 7/3) under photocatalytic conditions (Irradiation of 60 W Tungsten filament bulb). Reproduced with permission from ref [110], American Chemical Society.

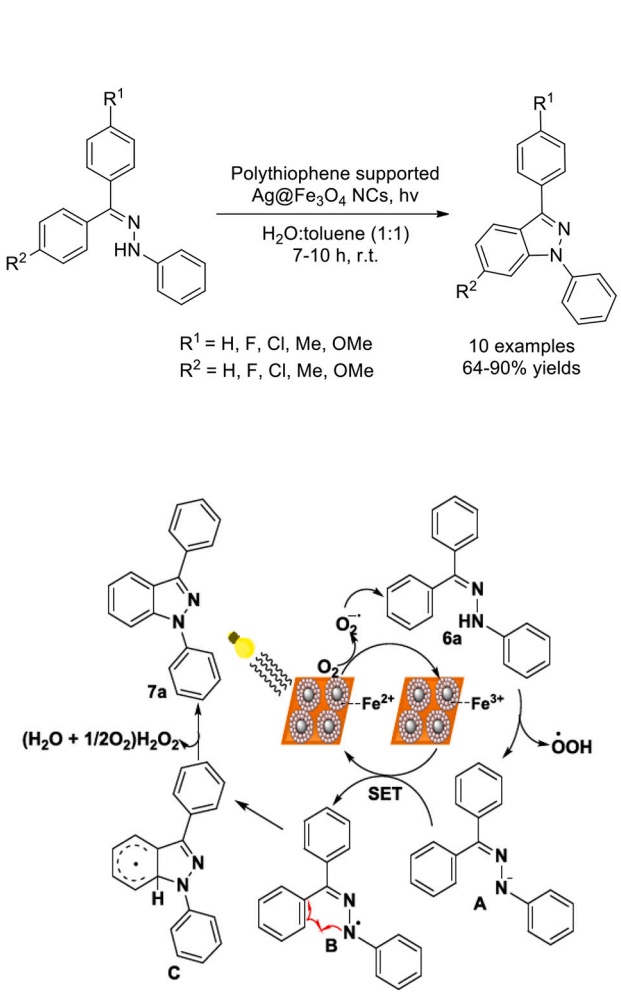

Scheme 32. (a) Polythiophene supported Ag@Fe_3O_4 NCs mediated photocatalytic dehydrogenative coupling of phenylhydrazones and (b) Probable reaction mechanism of dehydrogenative coupling of phenylhydrazones *via* polythiophene supported Ag@Fe_3O_4 NCs as photocatalyst. Reproduced with permission from ref [111], American Chemical Society.

nanoparticles have been employed for regioselective synthesis of various organic compounds. Magnetic iron oxide nanoparticles, especially magnetite (Fe_3O_4) and maghemite (γ-Fe_2O_3), have attracted much attention because of their unique properties and potentials.

A group of chemists have synthesized Fe_3O_4 [154] and then surface modification with SiO_2 was achieved by reaction of tetra ethyl orthosilicate (TEOS) followed by refluxing in an inert atmosphere of nitrogen with urea-based ligand in dry toluene for 24 h. The synthesized MNPs (Fe_3O_4@SiO_2@ $(CH_2)_3$-Urea-Triazole) [155] were then separated, washed with *n*-hexane and air-dried and finally, $CoCl_26H_2O$ was added to a mixture of the prepared MNPs. C—H functionalization (sulfenylation of ortho phenols/naphthols) was then performed stirring a mixture of phenol, pivalic anhydride, K_2CO_3 in DMSO at room temperature for around 20 to 120 min followed by stirring at 90 °C for one day with further addition of MNPs, Cs_2CO_3, PPh_3, $K_2S_2O_8$, thiophenol and DMSO (Scheme 36). The composite showed regioselective *ortho*-sulfenylation of free phenols and naphthols by employing pivalic anhydride as a directing group (DG), $K_2S_2O_8$ and PPh_3 as an oxidant and additive, respectively

Scheme 36b elucidates plausible mechanistic pathway for the Fe_3O_4@SiO_2-UT@Co^{II} catalysed reaction of thiols with phenols and naphthols wherein pivalic anhydride acts as the directing group. The cobalt coordinates with the oxygen atom (II) and paves the way towards radical mediated directed ortho-metalation leading to the formation of intermediate III. Intermediate III then affords IV through aromatization and reduction of cobalt in the presence of $K_2S_2O_8$. Intermediate IV then reacts with thiols to form V which further undergoes reductive elimination followed by RS immigration to yield VI which finally produces the anticipated product along with the regeneration of the catalyst.

In summary, it could be concluded that regioselectivity is of paramount importance in organic synthesis which go hand in hand with green synthesis and magnetic nanoparticles significantly influences both avenues. Thus, regioselective synthesis must be explored with magnetically recyclable nanoparticles for more substrate to obtain a variety of desired products.

5.6. *Enantioselective synthesis*

Since the last decade, asymmetric catalysis has garnered immense recognition for synthesizing optically active pharmaceutical as well as biologically significant motifs with high efficiency [156]. Nevertheless, the difficulty in recovering the metal catalyst poses a serious challenge to the chemists working in this direction. Within this context, the utilization of magnetic nanoparticles as solid support for mediating asymmetric catalysis has proven to be a more rational solution that permits facile separation and recyclability [157].

The direct asymmetric aldol reaction between ketones and aldehydes renders a facile access to chiral organic compounds of great significance in synthetic organic chemistry. In this perspective, Yin and co-workers judiciously grafted *L*-proline on imidazolium based ionic liquid modified magnetic nanoparticles (catalyst 1) (Scheme 37a) and further employed it as a catalytic entity in asymmetric aldol reaction of cycloalkanones and aliphatic ketones (such as acetone) with aromatic aldehydes in water [158]. The synthesized catalyst demonstrated high activity in terms of product yield (upto 96%), diastereoselectivity (dr; 88/12) and enantioselectivity (ee; 85%) (Scheme 37b). Alternatively, authors also prepared ionic liquid free proline immobilized on magnetic silica (catalyst 2) (Scheme 37c) and compared its catalytic efficacy in the concerned reaction which was found to be very slow and further no chiral induction was observed. The high catalytic performance in case of PILMC catalyst was further attributed to the ionic liquid moiety that promoted superior diffusion of hydrophobic reagents toward the active catalytic sites and simultaneously worked as a stabilizing agent for the enamine intermediate formed during the reaction. Further, the catalyst possessing magnetic characteristics could be reused for multiple cycles and without any appreciable decline in its activity.

Pericas and co-workers designed and reported the immobilization of a second-generation MacMillan imidazolidin-4-one based organocatalyst onto 1% DVB Merrifield resin (PS) (termed as catalyst A) and Fe_3O_4 nanoparticles (catalyst B) [159]. The catalytic efficacy of the developed material was further investigated in the asymmetric Friedal-Crafts alkylation of indoles with α,β-unsaturated aldehydes (Scheme 38). Though both the fabricated materials exhibited facile recoverability and recyclability, the polystyrene based catalyst exhibited superior activity and stereoselectivity which was further attributed to the polymeric nature of PS that delivered favorable microenvironment to the active sites thereby resulting in enhanced reactivity and enantioselectivity.

On similar grounds, Dash *et al.* utilized copper assisted Huisgen cycloaddition for immobilizing enantiopure butyl-imidazolidin-4-one onto magnetic nanosupport (MNP-A, MNP-B) at two distinct anchoring sites and Merrifield resin support (PS) [160]. The synthesized catalysts were employed as catalytic entities in the alkylation of indoles with α,β-unsaturated aldehydes furnishing desired organic products in high yields along with good enantioselectivities (Scheme 39). The magnetic nanosupport with functionalization at the *O*-aryl residue demonstrated comparatively higher catalytic performance than the magnetic nanosupport with functionalization at the amide nitrogen. Further, the PS supported catalyst showed highest catalytic activity in

Table 11
Comparison of catalytic activity of polythiophene supported Ag@Fe_3O_4 nanoclusters with other catalysts documented in literature for C—H functionalization/C-N bond formation.

S. No.	Catalyst	Catalyst loading	Ligand/base /oxidant	Solvent	Temperature	Time	Yield
1.	Polythiophene supported Ag@Fe_3O_4 NCs	0.01 mol	-	H_2O:Toluene	Visible light	7-10 h	64-90%
2.	Acr^+ - Mes ClO_4^-, $Co(dmgH)_2PyCl$	3 mol%	-	CH_3CN	Blue LED (3W) under nitrogen atmosphere	24 h	35-89%
3.	$Pd(OAc)_2$	0.89 mmol	Di(2-pyridyl)ketone, H_2O_2	CH_3CN, MeOH, THF or AcOH	60°-80°C	3-12 h	82-98%
4.	$[RhCp^*Cl_2]_2$	5 mol%	2-methylquinoline, PhCOONa, Ag_2CO_3	Toluene	90°C under nitrogen atmosphere	16 h	44-88%
5.	CuI or $Cu(OTf)_2$	10 mol%	$PhI(OTFA)_2$	DCE	100 °C	10 h	32-85%
6.	$Pd(CH_3CN)_2Cl_2$	10 mol%	Chloranil	1,4-dioxane	80 °C	24 h	27-98%
7.	$Ru(bpy)_3Cl_2.6H_2O$	2 mol%	TEMPO, K_2CO_3	$CHCl_3$	Blue LED (3W)	5-24 h	51-86%
8.	Pd/bis-sulfoxide, Co(salophen)	2.5-5 mol%	DHBQ, TBAA, O_2	TBME	45 °C	72 h	52-96%
9.	$Pd(OAc)_2$	10 mol%	O_2	DMSO/toluene	80 °C-120 °C	24 h	36-95%
10.	$Pd(OAc)_2$	20 mol%	$Cu(OAc)_2$, O_2	DMSO	120 °C	8-10 h	63-87%
11.	$Ir(ppy)_2$ (dtbbpy)PF_6	2 mol%	NaClO	1,4-dioxane	White LED (5W)	1 h	45-91%
12.	Copper(II)2-ethylhexanoate	20 mol%	Dess-Martin periodinane	DMSO	110 °C	1 h	70-87%
13.	$Cu(OAc)_2$	15 mol%	Ag_2CO_3	m-Xylene	140 °C	24 h	68-91%
14.	$[Ir(dFppy)_2phen]PF_6$, $Pd(OAc)_2$	10 mol%	Molecular O_2	DMSO	80 °C, Blue LED (7W)	8-16 h	75-94%
15.	$Pd(OAc)_2$	10 mol%	$Ce(SO_4)_2$, DMF, MsOH	DCM	120 °C	48 h	30-74%

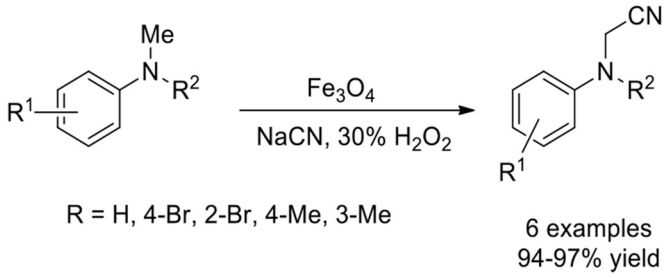

Scheme 33. Fe_3O_4 catalysed α-cyanation of amines.

the concerned reaction due to the high loading of the catalyst, yet its recycling efficiency was found to be significantly low in comparison to the magnetic nanocatalysts.

He and co-workers fabricated magnetic nanoparticles (Fe_3O_4@SiO_2) supported cinchona alkaloids (quinine and quinidine) based chiral organocatalysts as catalytic entities in the asymmetric Michael addition of 1,3-dicarbonyls and maleimides [161]. The catalyst was synthesized through a step-by-step assembly strategy wherein 3-mercaptopropyltrimethoxysilane was employed as a linking agent between cinchona alkaloid and Fe_3O_4@SiO_2. The primary step involved the coupling between equimolar quinine and 3-mercaptopropyltrimethoxysilane under UV irradiations which was further immobilized onto Fe_3O_4@SiO_2 nanoparticles *via* sol-gel approach. The obtained quinine functionalized

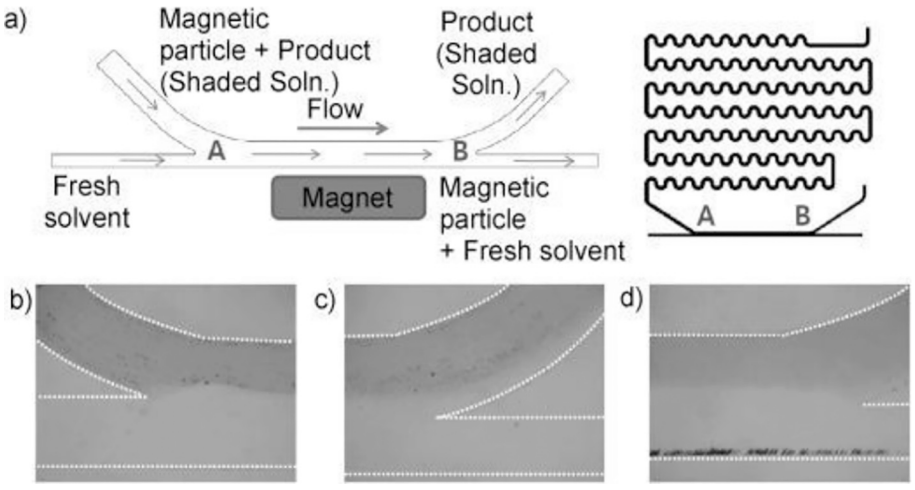

Fig. 4. (a) Initial microfluidic separator design for continuous recovery of magnetic particle from product solution; (b) Captured image at part A: shaded solution is the product solution and black dots are magnetic particles. Captured image at part B in the; (c) absence and d) presence of a magnetic field. Adopted from ref [120]

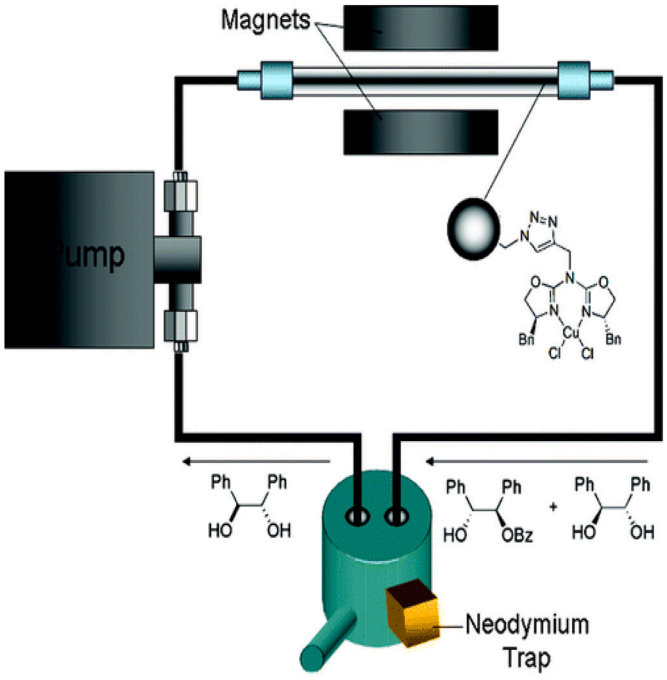

Fig. 5. Representation of a closed circuit type reactor for the asymmetric monobenzoylation of racemic diol (±)-1 catalyzed by azabis(oxazoline)–copper(II) complexes tagged to magnetic nanobeads. Adopted from ref. [124]

Fe_3O_4@SiO_2 nanoparticles were further modified with triethoxypropylsilane to avoid any potential interference of residual hydroxyl moieties present on the surface of MNPs (Scheme 40a). It was further observed that both quinine as well as quinidine modified MNPs could effectively catalyze the asymmetric Michael addition reaction with high enantioselectivity (up to 93% ee) (Scheme 40b). Further, the catalyst being magnetic in nature could be consecutively reused for three cycles without any appreciable loss of activity.

Another research group led by Li *et al.* delineated the synthesis of a Fe_3O_4 nanoparticle supported copper(I) pybox as catalytic entity in the enantioselective direct addition reaction of terminal alkynes with imines to form propargylamines [162]. Catalyst synthesis step involved the *N*-arylation reaction between APTES functionalized silica coated Fe_3O_4 nanoparticles and 4-bromo-substituted phenyl-pybox ligand in the presence of CuBr/BINOL (1,12-binaphthyl-2,22-diol) to generate compound 1 which after stirring in dichloromethane solution of $(CuOTf)_2$ toluene yielded the desired Fe_3O_4 nanoparticle supported copper(I) pybox catalyst (Scheme 41a). Further, the catalyst being versatile in nature successfully resulted in the generation of six optically active propargyl amines in excellent yields (80-93%) and high enantioselectivity (84-92%). Besides, recyclability experiments revealed that the catalyst was efficiently reused for six cycles without undergoing any obvious decline in efficiency and enantioselectivity.

6. Toxicology of MNPs

Nanotechnology has become the next step in science where engineering is integrated with biology, chemistry, medicine and physics to develop functional materials, devices, and systems by altering matters at the atomic/molecular scale [12a]. While these nanotechnologies offer several benefits, nanoparticles (NPs) can have side effects and can be toxic [163]. Even though various types of NPs and their applications are continuing to increase, studies to characterise their effects after exposure and potential toxicity are quite limited. Given the efficient delivery of many biologically active compounds, size-dependent intrinsic magnetic properties, ability to function on a cellular and molecular level and wide usage in the field of biomedical engineering, magnetite NPs

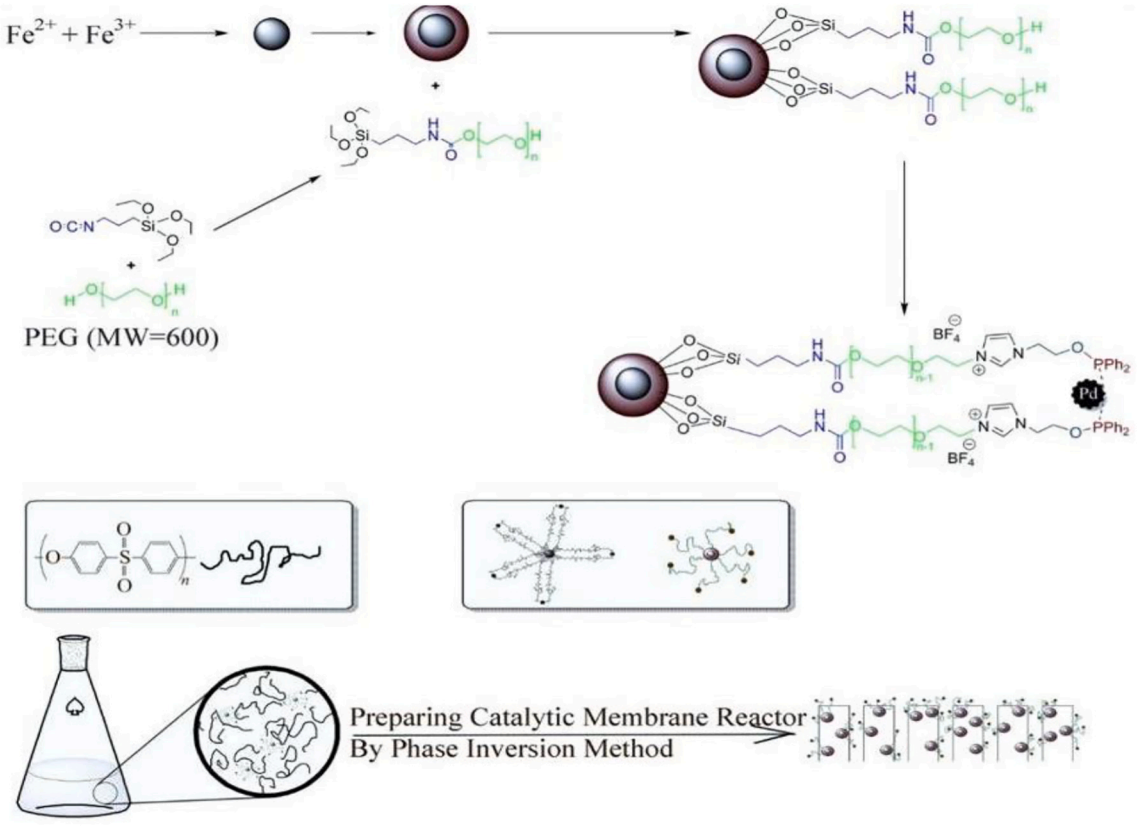

Scheme 34. Preparation of the catalytic membrane. Adopted from ref [129a].

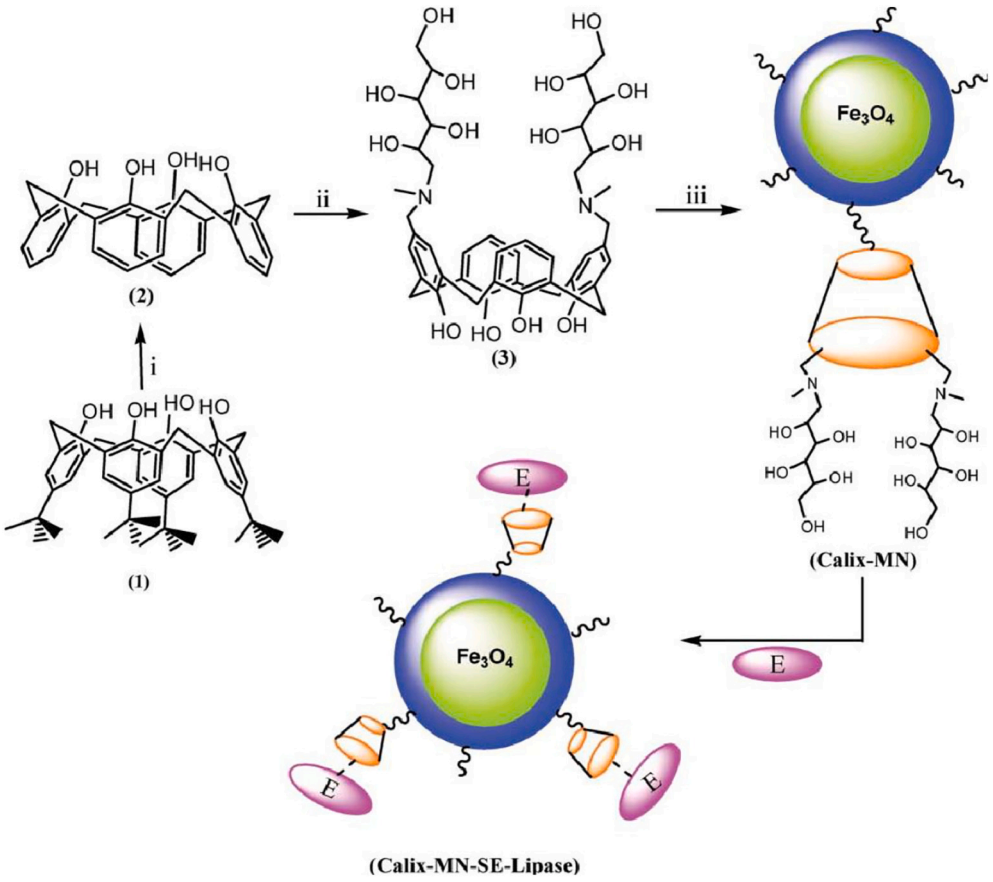

Scheme 35. The sol–gel encapsulation procedure of Calix-MN-SE-Lipase. Reaction conditions: (i) $AlCl_3$, phenol, toluene; (ii) *N*-methylglucamine, formaldehyde, CH_3COOH, THF; (iii) EPPTMS-MN, K_2CO_3, CH_3CN. Adopted from ref. [145]

(MNPs) are being studied extensively [164].

The important factor that determines toxicity and the biocompatibility of MNPs is the nature of the magnetically responsive components, such as magnetite, iron, nickel, and cobalt, and the final size of the particles, their core, and the coatings. Iron oxide NPs such as magnetite (Fe_3O_4) or its oxidized form maghemite (γ-Fe_2O_3) are commonly employed in the area of biomedical engineering [165,166]. Highly magnetic materials such as Co and Ni are susceptible to oxidation and hence are considered toxic [167,168]. For *in vivo* biomedical applications, MNPs should be made of a non-toxic and non-immunogenic material, as they need to remain in the blood circulation after injection and to pass through the capillary systems of organs and tissues. To overcome the toxic effects, studies have started to focus on developing encapsulation of MNPs with polyesters such as PLGA, a synthetic copolymer of lactic acid (α-hydroxy propanoic acid) and glycolic acid (hydroxy acetic acid), as they are biocompatible, biodegradable and less toxic [169].

Recently, superparamagnetic iron oxide nanoparticles (SPIONs) have started to receive much attention in drug and biomolecule delivery systems and magnetic resonance imaging (MRI). However, we cannot rule out the toxic side-effects that are associated with the exposure to SPIONs. Studies have shown that exposure to SPIONs has been associated with toxic effects [170] such as vascular endothelial and pulmonary inflammation, impaired mitochondrial membrane function leading to the formation of apoptotic bodies, leakage of lactate dehydrogenase due to cell membrane damage and increased production of reactive oxygen species (ROS) leading to DNA damage and chromosome condensation (Fig. 6) [171]. Hence, there is a need to address biocompatibility and biosafety concerns that are associated with the use of SPIONs in a wide variety of biomedical applications.

Studies have shown that properties such as the type of coating, the size of the nanoparticle, and the concentrations of MNPs are important in terms of determining the cytotoxicity. Materials such as polyvinylpyrrolidone (PVP), dextran, PEGylated starch, citrate and silicon have been used for surface coating of SPION [172]. A BT-474 cell line study showed that larger nanoparticles (dextran-SPION) had less cytotoxicity and, at higher concentration (above 100 μg/ml), PVP-SPIONs decreased cell viability [173]. In a recent study in dopaminergic neuronal PC12 cells, treatment with SPIONs reduced the cell viability and resulted in the decrease of nerve fibre density [174]. Several strategies have been implemented to minimise the toxicity due to exposure to SPIONS. A study used a combination of an external magnetic field and the composite particles of PLGA with the SPIONs (SPION-PLGA particles) for protein delivery to bone-marrow derived primary dendritic cells, where SPION-PLGA particles exhibited superparamagnetic property which showed low cytotoxicity [175]. In another study [176], the SPIONs were non-toxic up to 100 μg/ml *in vitro* for NT2 cell line after coating the surface of SPION with poly (ethylene glycol)-grafted polyethylenimine (mPEG-co-PEI) shell, where PEI increased the gene transfection efficiency and PEG methyl ether reduced the cytotoxicity. Furthermore, a study where SPIONs were synthesized by thermal decomposition of iron (III) acetylacetonate $Fe(acac)_3$ and functionalized with dihexadecyl phosphate (DHP) *via* phase transfer did not show a significant cytotoxicity suggesting that SPION-DHP might hold a great potential for biological applications [177]. By using a simple conjugation approach [178], where ferumoxides (FE) contrast agent was attached to the fixable fluorescent dextrans (FL FE) and mixed with protamine sulfate (Pro), toxicity was significantly reduced in cells which proves that FL FE-Pro complex might provide the ability to monitor cells by MRI in a less toxic way compared to other chemical conjugation methods [179].

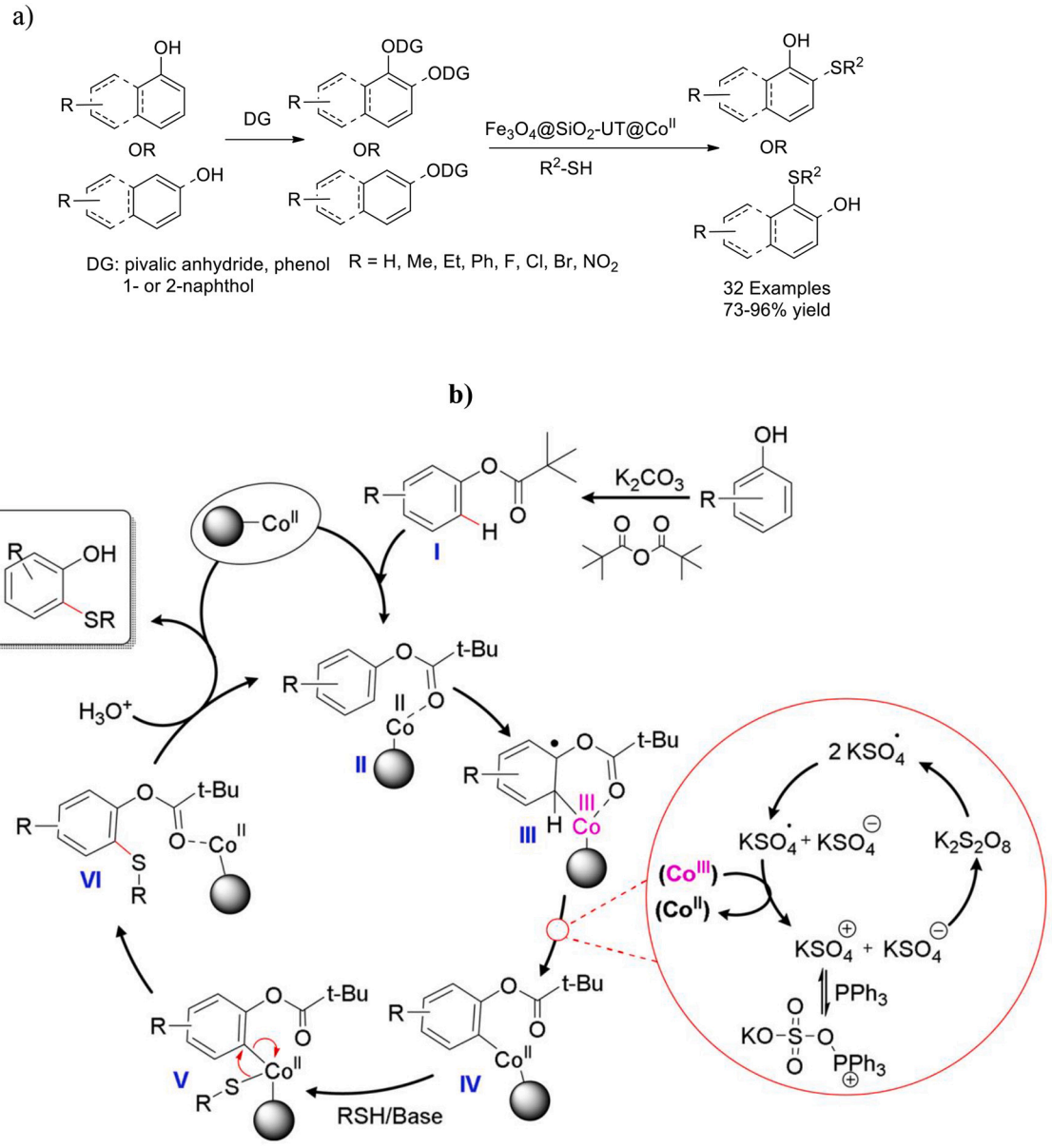

Scheme 36. (a) *O*-sulfenylation of free phenols and naphthols and (b) Plausible catalytic cycle for *ortho*-regioselective sulfenylation of phenols and naphtols. Adopted from ref [155]

Another interesting area of research where MNPs are used include ribonucleic acid (RNA) interference-based silencing of cancer-related gene expression [180]. Recent studies have focused on using SPIONs as vehicles for short-interfering RNA (siRNA) [181], as the SPION-siRNA conjugates are non-toxic, biocompatible, stable, and amenable to specific targeting and can cross tight junction of endothelial cells in blood brain barrier [182]. As a therapeutic strategy against HIV and other infectious diseases, SPIONs are also used as an RNA delivery system into target cells. Chitosan coated SPIONs were optimized as a system for delivering siRNA against HIV-1 tat to HEK293 cells, where the NPs showed no considerable toxicity on the cells [183]. NPs comprised of nanoengineered complexes are now being used as reporters for many physiological processes and have enabled targeted delivery of a range of safer therapeutics for applications such as cardiovascular diseases [184].

Recent studies have identified specific cytotoxic effects associated with cardiovascular system upon exposure to different MNPs. An animal study has shown that ultra-small SPIONs that are composed of magnetite Fe_3O_4 with <1.0% stabilizing ligands of PEG lead to adverse effects on myocardium, DNA damage and increase of cardiac oxidative stress [185]. Besides iron oxide nanoparticles, nano-sized zerovalent iron particles have also been shown to produce toxic effects relating to pulmonary and cardiovascular systems, where increased levels of oxidative stress in human cultured endothelial and epithelial cell lines were identified [186]. The toxic effects of SPIONS have also been studied and reported in plants. After exposure to SPION, toxic effects such as growth inhibition, ROS formation, decrease in chlorophyll content and photosynthesis inhibition were identified in the aquatic plant *Lemma gibba* [187]. Furthermore, in the microalgae, *Chlorella vulgaris* and *Pseudokirchneriella subcapitata*, the toxicity of nano-Fe_3O_4 and nano-Fe_2O_3 was shown to result in ROS formation and deterioration of photosynthetic activities [188]. Upon exposure to SPION, a recent study in the microalga, *Chlamydomonas reinhardtii*, has demonstrated a toxic response consisting of a decrease in metabolic activity, increased ROS formation and alterations in the mitochondrial membrane potential [189].

In summary, majority of the animal and human cell line studies have reported increased levels of oxidative stress as one of the important

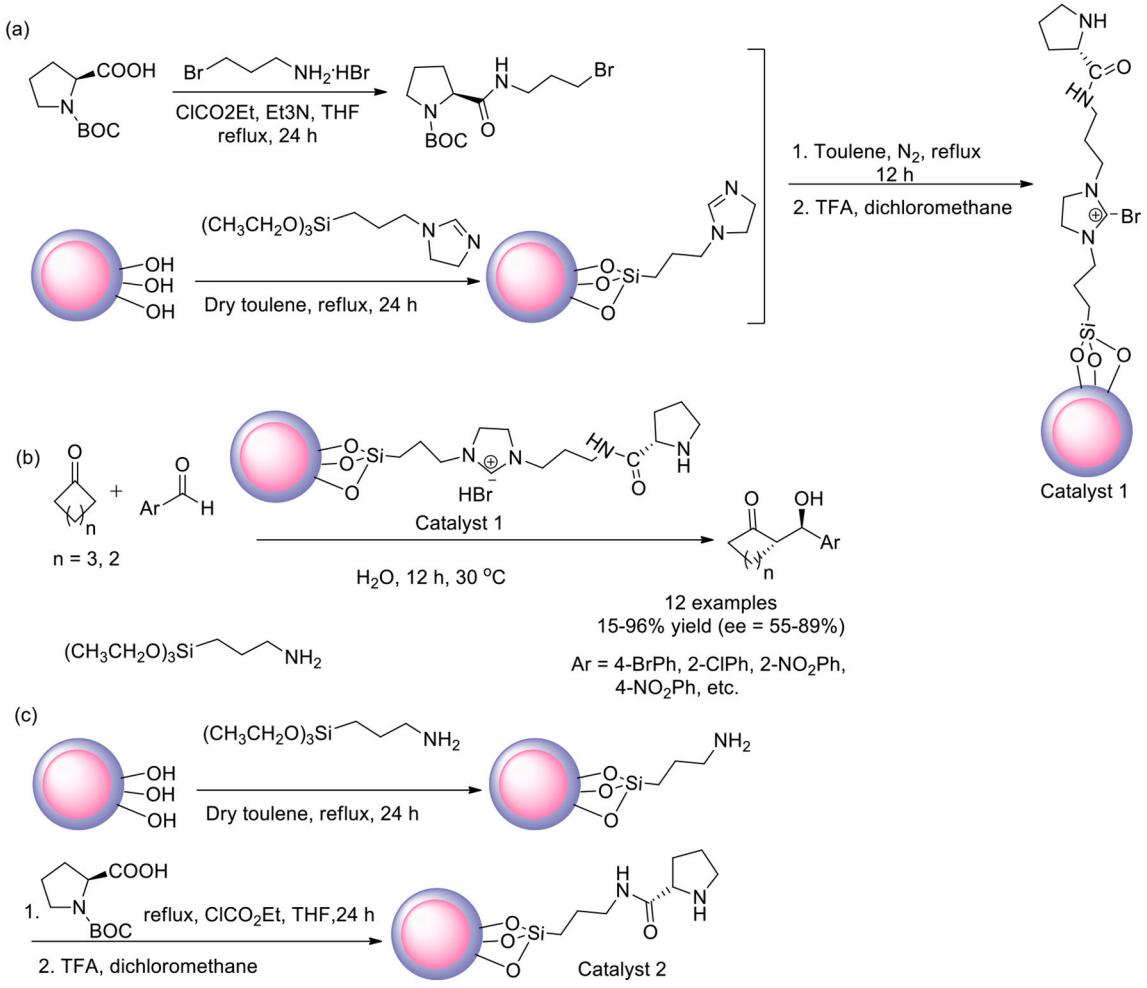

Scheme 37. (a) Preparation of *L*-proline on imidazolium based ionic liquid modified magnetic nanoparticles catalyst; (b) *L*-proline on imidazolium based ionic liquid modified magnetic nanoparticles catalyzed direct asymmetric aldol reaction between cycloalkanones and aromatic aromatic aldehydes; (c) Preparation of ionic liquid free proline immobilized on magnetic silica catalyst.

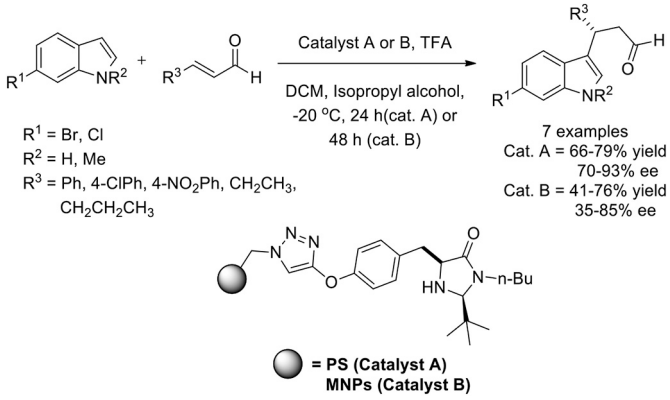

Scheme 38. Immobilized 2nd generation MacMillan catalyst mediated asymmetric Friedal-Crafts alkylation of indoles with α,β-unsaturated aldehydes.

mechanisms by which MNPs induce cytotoxicity. Hence, oxidative stress and the generation of ROS might be the main factor leading to the other changes in intracellular signalling pathways resulting in apoptosis. However, as the current data on the toxicity of MNPs are very limited, further mechanistic studies are required to understand the pathways leading to the cytotoxic effects. Given the information about toxic effects of MNPs, despite the great potential for biomedical applications, their impact on human health should further be investigated and taken into special consideration before wide-spread use.

7. Conclusion

The field of C—H activation that exploit the ubiquity of C(sp^3)–H and C(sp^2)–H bonds for C-C and C-heterobond formation has witnessed striking advancements with the advent of innovative recyclable and magnetically retrievable nanocatalysts that are here to rule for hundreds and thousands of years without any doubt with their majestic capabilities in promoting sustainable synthesis. In fact, with effective utilization of the nanocatalysts, the sales of global market have already reached USD 2,900 which is expected to grow exponentially within few years. The distinctive properties of the magnetic nanocatalysts including low toxicity, more abundance, economic viability and most importantly the prospects of recovering the catalysts with a greener, solvent-free, rapid magnetic separation technique have rendered them the material of choice for expediting a notable number of industrially significant reactions by leveraged C—H activation. The review aimed to revisit all the magnetic catalysts being employed at the laboratory as well as industrial level for aiding in the construction of diverse array of C-C as well as C-hetero bond formations. Apart from focusing on the recent approaches involved extensively in the design of the magnetite nanoparticles, their subsequent surface modification strategies including the covalent immobilization methodology and the direct one-pot synthesis of the metal loaded MNPs have also been given due consideration which are

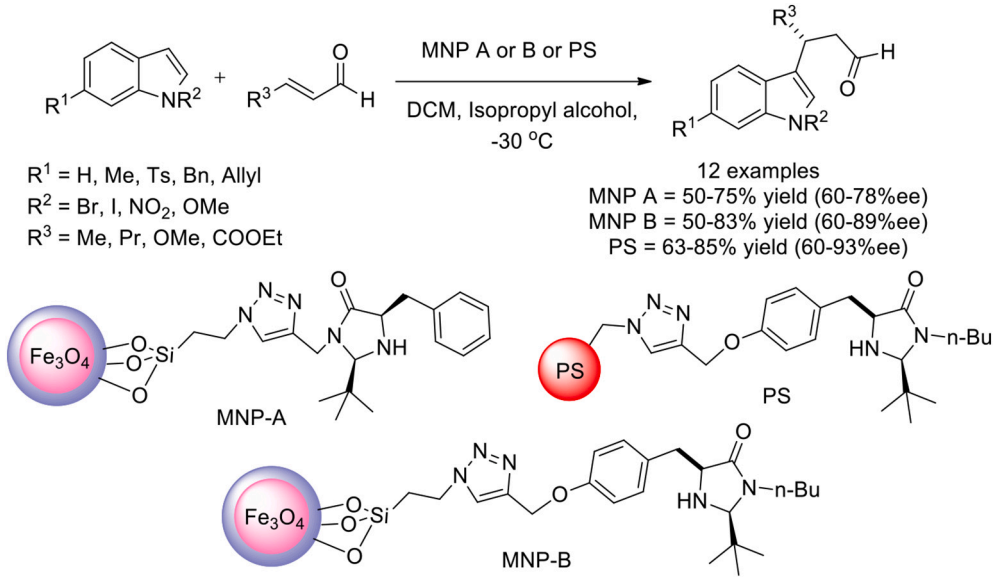

Scheme 39. Magnetic nanoparticles and polymer supported imidazolidinone catalysts for enantioselective Friedal-Crafts alkylation of indoles.

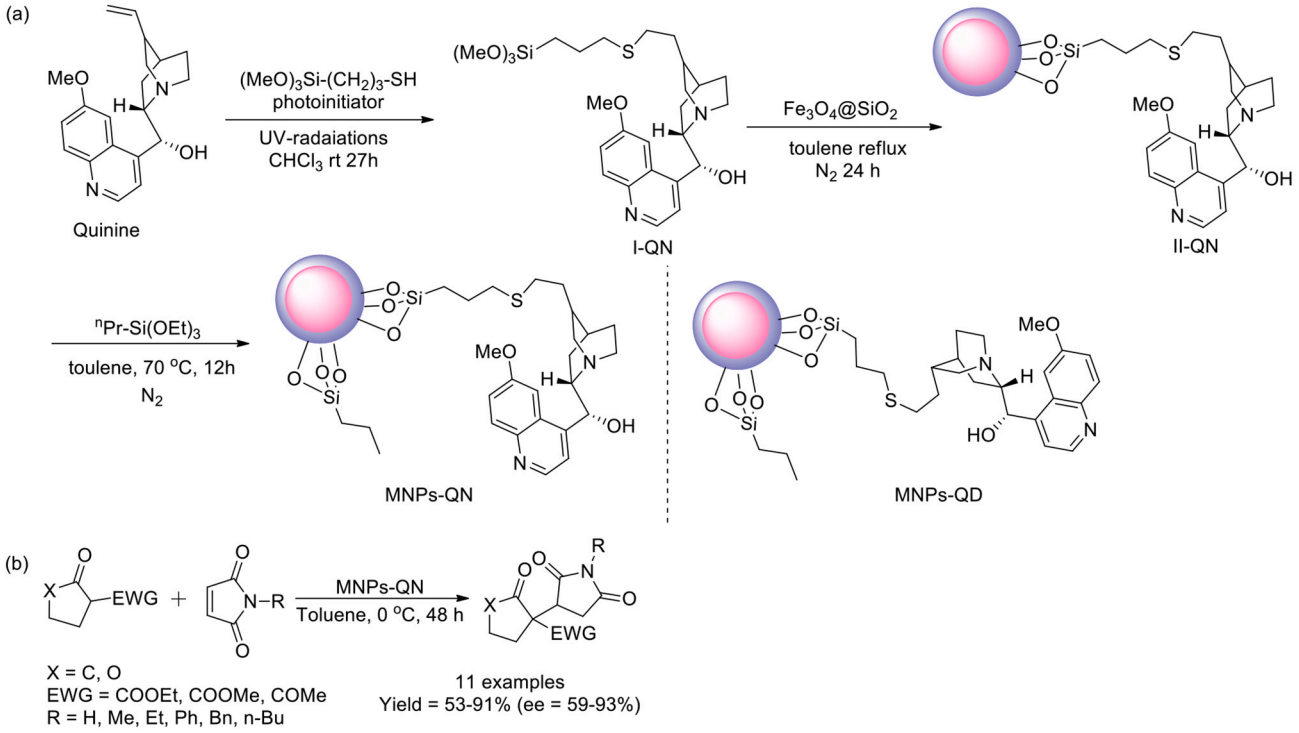

Scheme 40. (a) Preparation of MNPs-QN organocatalyst; (b) MNPs-QN organocatalyst for asymmetric Michael addition of 1,3-dicarbonyls and maleimides.

anticipate to benefit the researchers interested in working in this highly propitious area. Exclusive light has also been thrown on the use of different types of micro as well as macro reactors that enhance the applicability of these catalysts for multi-phase heterogeneous reactions. Lastly, a critical assessment based on the toxicity of the MNPs has also been presented which have divulged that further research needs to be conducted in evaluation of the toxic aspects associated, especially while directing attention to the biomedical applications. The area of magnetic C—H activation presents enormous scope to resolve some real environmental/industrial challenges on the horizon as well. For instance, competent photocatalysts are being designed for the rapid degradation of emerging contaminants that have shown promising efficacy in wastewater treatment. Also, regioselective catalysts are also being innovated and utilized for direct C—H functionalization of important bioactive molecules. However, certain barriers still impede the large scale applicability of these protocols for instance lack of mechanistic understanding at the nanoscale which can be resolved with theoretical understanding with the aid of more competent computational softwares and simulations. The synthesis of ideal nanostructures, understanding their dynamics and bringing these to the labscale also pose a grand challenge. For realistic industrial applications, it is crucial to develop stable and robust MNPs in an economical and scalable way that can bear the reaction conditions experienced in heterogeneous catalysis. In view of large scale applicability and long term benefits, one needs to focus on

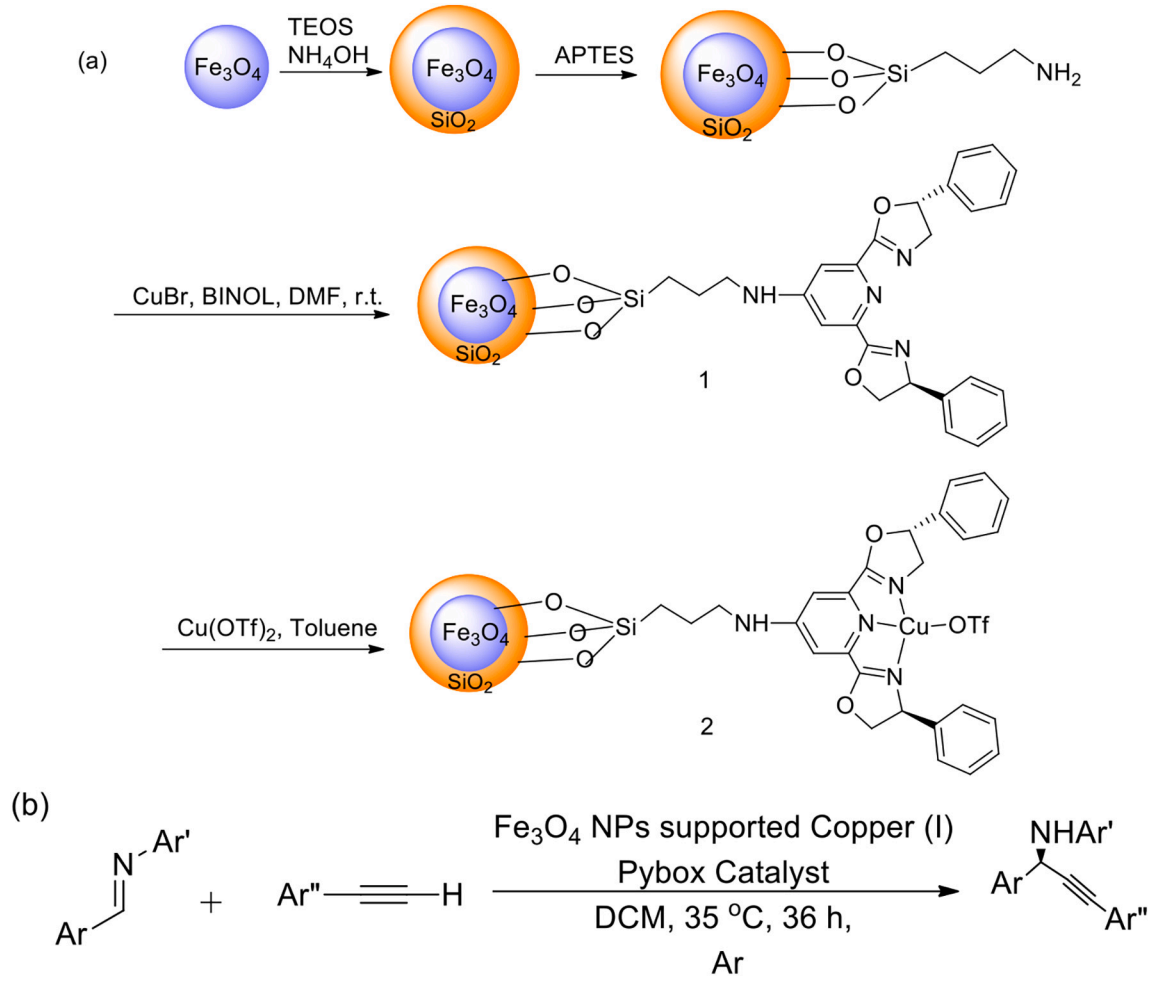

Scheme 41. (a) Synthesis of Fe_3O_4 NPs-Supported Copper(I) Pybox Catalyst and (b) Application of the catalyst in the Enantioselective Direct-Addition Reactions of Terminal Alkynes to Imines

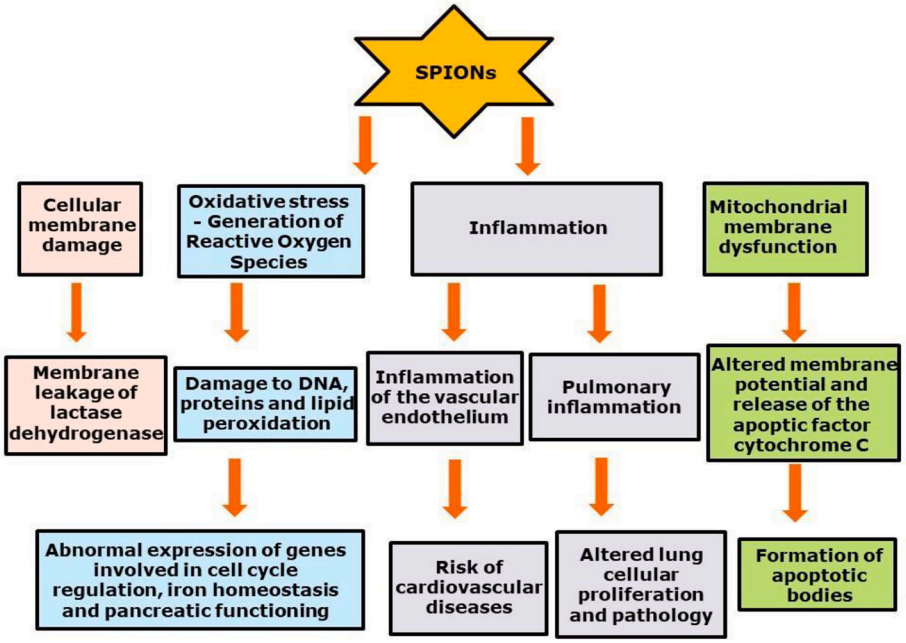

Fig. 6. Toxic effects induced by SPIONs. Exposure to SPION could lead to toxic effects such as cellular membrane damage, increased production of reactive oxygen species, impaired mitochondrial function and inflammation.

the synthetic strategies that could ultimately aid in strong metal-support interactions and assure long term stability as well as activity. Continuous flow MW reactors have also been tried on a limited scale, and this idea is interesting for mass scale production, but more investigation is needed to check the efficiency of the reactor for synthesizing a wide variety of supported nanocatalysts with durable properties. Also, efforts need to be directed towards the automated recycling of the magnetic nanocatalysts in order to demonstrate their utility as support materials in parallel and high throughput synthesis. Future direction of research can be projected towards the correct exploitation of theoretical and experimental methods simultaneously for more outcome based realistic bent results that will ultimately help us in transitioning towards the final door of sustainability.

Declaration of Competing Interest

The authors declare that they have no known competing financial interests.

Data availability

Data will be made available on request.

Acknowledgements

The authors would like to thank British Council for providing grant for INDO-UK Collaborative workshop and this research output is an outcome of the same. One of the authors would also like to express gratitude to SERB for providing fund to Dr. Prashant Kumar under the scheme of Teacher Associateship for Research Excellence (TARE) (File number TAR/2021/000201).

References

[1] T. Dalton, T. Faber, F. Glorius, C–H Activation: toward sustainability and applications, ACS Cent. Sci. 7 (2) (2021) 245–261, https://doi.org/10.1021/acscentsci.0c01413.

[2] (a) A. Kate, L.K. Sahu, J. Pandey, M. Mishra, P.K. Sharma, Green catalysis for chemical transformation: The need for the sustainable development, Curr. Res. Green Sustain. Chem. 5, 100248 (2022), https://doi.org/10.1016/j.crgsc.2021.100248;
(b) G. Rothenberg, Catalysis: Concepts and Green Applications, John Wiley & Sons, 2017;
(c) R.A. Sheldon, I. Arends, U. Hanefeld, Green Chemistry and Catalysis, John Wiley & Sons, 2007.

[3] (a) R.N. Baig, R.S. Varma, Organic synthesis *via* magnetic attraction: benign and sustainable protocols using magnetic nanoferrites, Green Chem. 15 (2013) 398–417, https://doi.org/10.1039/C2GC36455G;
(b) R. Taheri-Ledari, A. Maleki, Magnetic nanocatalysts utilized in the synthesis of aromatic pharmaceutical ingredients, New J. Chem. 45 (2021) 4135–4146, https://doi.org/10.1039/D0NJ06022D;
(c) R.S. Varma, Nano-catalysts with magnetic core: sustainable options for greener synthesis, Sustain. Chem. Process 2 (2014) 1–8, https://doi.org/10.1186/2043-7129-2-11;
(d) S. Yadav, R. Dixit, S. Sharma, S. Dutta, B. Arora, P. Rana, R.K. Sharma, Unlocking the catalytic potency of a magnetic responsive CoFe2O4/Ni-BTC MOF composite for the sustainable synthesis of tri- and tetra-substituted imidazoles, Mater. Chem. Front. 5 (2021) 7343–7355, https://doi.org/10.1039/D1QM00904D.

[4] (a) M.V. Kirillova, C.I. Santos, W. Wu, Y. Tang, A.M. Kirillov, Mild oxidative C−H functionalization of alkanes and alcohols using a magnetic core-shell Fe3O4@mSiO2@Cu4 nanocatalyst, J. Mol. Catal. A Chem. 426 (2017) 343–349, https://doi.org/10.1016/j.molcata.2016.06.028;
(b) D. Pla, M. Gomez, Metal and metal oxide nanoparticles: a lever for C–H functionalization, ACS Catal. 6 (2016) 3537–3552, https://doi.org/10.1021/acscatal.6b00684;
(c) P. Kumar, S. Dutta, S. Kumar, V. Bahadur, E.V. Van der Eycken, K. S. Vimaleswaran, V.S. Parmar, B.K. Singh, Aldehydes: magnificent acyl equivalents for direct acylation, Org. Biomol. Chem. 18 (2020) 7987–8033, https://doi.org/10.1039/d0ob01458c;
(d) P. Kumar, R.S.K. Lalji, M. Gupta, V.S. Parmar, B.K. Singh, Palladium-catalyzed decarboxylative synthesis of 5*H*-Benzo[4,5][1,3]oxazino[2,3-*a*] isoindole-5,11(6a*H*)-Diones using 2-Phenyl-4*H*-Benzo[*d*][1,3]oxazin-4-Ones and α-oxo carboxylic acids, Adv. Synth. Catal. 362 (2019) 552–560, https://doi.org/10.1002/adsc.201901142;
(e) M. Gupta, S. Kumar, P. Kumar, A.K. Singh, V. Bahadur, B.K. Singh, *N*-Directed Pd-Catalyzed Direct ortho-Acetoxylation and ortho-tert-Butoxylation of 2-Phenyl-4*H*-benzo[*d*][1,3]oxazin-4-ones *via* C-H Activation, ChemistrySelect 4 (2019) 13992–13997, https://doi.org/10.1002/slct.201902755;
(f) P. Kumar, M. Gupta, V. Bahadur, V.S. Parmar, B.K. Singh, Radical-induced, palladium-catalyzed C–H activation: an approach to functionalize 4*H*-Benzo[*d*][1,3]oxazin-4-one derivatives by using toluenes, aldehydes, and benzyl alcohols, Eur. J. Org. Chem. 1552-1558 (2018), https://doi.org/10.1002/ejoc.201800263;
(g) M. Gupta, P. Kumar, V. Bahadur, K. Kumar, B.K. Singh, Metal-free, regioselective, dehydrogenative cross-coupling between formamides/aldehydes and coumarins by C–H functionalization, Eur. J. Org. Chem. 896-900 (2018), https://doi.org/10.1002/ejoc.201701764.

[5] (a) R.H. Crabtree, A. Lei, Introduction: CH Activation, Chem. Rev. 117 (2017) 8481–8482, https://doi.org/10.1021/acs.chemrev.7b00307;
(b) S. Santoro, S.I. Kozhushkov, L. Ackermann, L. Vaccaro, Heterogeneous catalytic approaches in C–H activation reactions, Green Chem. 18 (2016) 3471–3493, https://doi.org/10.1039/C6GC00385K.

[6] (a) R.K. Sharma, S. Dutta, S. Sharma, Quinoline-2-carboimine copper complex immobilized on amine functionalized silica coated magnetite nanoparticles: a novel and magnetically retrievable catalyst for the synthesis of carbamates *via* C–H activation of formamides, Dalton Trans. 44 (2015) 1303–1316, https://doi.org/10.1039/C4DT03236E.(b) H. Veisi, L. Mohammadi, S. Hemmati, T. Tamoradi, P. Mohammadi, In situ immobilized silver nanoparticles on rubia tinctorum extract-coated ultrasmall iron oxide nanoparticles: an efficient nanocatalyst with magnetic recyclability for synthesis of propargylamines by A3 coupling reaction. ACS omega 4, 13991-14003 (2019). https://doi.org/10.1021/acsomega.9b01720.
(c) H. Veisi, A. Sedrpoushan, B. Maleki, M. Hekmati, M. Heidari, S. Hemmati, Palladium immobilized on amidoxime-functionalized magnetic Fe3O4 nanoparticles: a highly stable and efficient magnetically recoverable nanocatalyst for sonogashira coupling reaction. Appl. Organomet. Chem. 29, 834-839 (2015). https://doi.org/10.1002/aoc.3390.

[7] (a) B.G. Hashiguchi, S.M. Bischof, M.M. Konnick, R.A. Periana, Designing catalysts for functionalization of unactivated C–H bonds based on the CH activation reaction, Acc. Chem. Res. 45 (2012) 885–898, https://doi.org/10.1021/ar200250r;
(b) C.J. Jones, D. Taube, V.R. Ziatdinov, R.A. Periana, R.J. Nielsen, J. Oxgaard, W.A. Goddard III, Selective oxidation of methane to methanol catalyzed, with C-H activation, by homogeneous, Cationic Gold. Angew. Chem. 116 (2004) 4726–4729, https://doi.org/10.1002/ange.200461055;
(c) N. Van Velthoven, S. Waitschat, S.M. Chavan, P. Liu, S. Smolders, J. Vercammen, D.E. De Vos, Single-site metal–organic framework catalysts for the oxidative coupling of arenes via C–H/C–H activation, Chem. Sci. 10 (2019) 3616–3622, https://doi.org/10.1039/C8SC05510F.

[8] (a) T. Gensch, M.N. Hopkinson, F. Glorius, J. Wencel-Delord, Mild metal-catalyzed C–H activation: examples and concepts, Chem. Soc. Rev. 45 (2016) 2900–2936, https://doi.org/10.1039/C6CS00075D;
(b) K.M. Altus, J.A. Love, The continuum of carbon–hydrogen (C–H) activation mechanisms and terminology, Commun. Chem. 4 (2021) 1–11, https://doi.org/10.1038/s42004-021-00611-1.

[9] (a) L.H. Reddy, J.L. Arias, J. Nicolas, P. Couvreur, Magnetic nanoparticles: design and characterization, toxicity and biocompatibility, pharmaceutical and biomedical applications, Chem. Rev. 112 (2012) 5818–5878, https://doi.org/10.1021/cr300068p;
(b) J. Gao, H. Gu, B. Xu, Multifunctional Magnetic Nanoparticles: Design, Synthesis, and Biomedical Applications, Acc. Chem. Res. 42 (2009) 1097–1107, https://doi.org/10.1021/ar9000026.

[10] C.W. Lim, I.S. Lee, Magnetically recyclable nanocatalyst systems for the organic reactions, Nano Today 5 (2010) 412–434, https://doi.org/10.1016/j.nantod.2010.08.008.

[11] (a) R. Hudson, Y. Feng, R.S. Varma, A. Moores, Bare magnetic nanoparticles: sustainable synthesis and applications in catalytic organic transformations, Green Chem. 16 (2014) 4493–4505, https://doi.org/10.1039/C4GC00418C;
(b) R.S. Varma, Greener and sustainable trends in synthesis of organics and nanomaterials, ACS Sustain. Chem. Eng. 4 (11) (2016) 5866–5878, https://doi.org/10.1021/acssuschemeng.6b01623.

[12] (a) R.K. Sharma, S. Dutta, S. Sharma, R. Zboril, R.S. Varma, M.B. Gawande, Fe3O4 (iron oxide)-supported nanocatalysts: synthesis, characterization and applications in coupling reactions, Green Chem. 18 (2016) 3184–3209, https://doi.org/10.1039/C6GC00864J;
(b) A.G. Niculescu, C. Chircov, A.M. Grumezescu, Magnetite nanoparticles: synthesis methods–A comparative review, Methods 199 (2021) 16–27, https://doi.org/10.1016/j.ymeth.2021.04.018.

[13] F.N. Sayed, V. Polshettiwar, Facile and sustainable synthesis of shaped iron oxide nanoparticles: effect of iron precursor salts on the shapes of iron oxides, Sci. Rep. 5 (2015) 1–14, https://doi.org/10.1038/srep09733.

[14] Y. Wang, I. Nkurikiyimfura, Z. Pan, Sonochemical synthesis of magnetic nanoparticles, Chem. Eng. Commun. 202 (2015) 616–621, https://doi.org/10.1080/00986445.2013.858039.

[15] R. Abu-Much, A. Gedanken, Sonochemical synthesis under a magnetic field: structuring magnetite nanoparticles and the destabilization of a colloidal magnetic aqueous solution under a magnetic field, J. Phys. Chem. C 112 (2008) 35–42, https://doi.org/10.1021/jp075637k.

[16] T. Togashi, S. Takami, K. Kawakami, H. Yamamoto, T. Naka, K. Sato, T. Adschiri, Continuous hydrothermal synthesis of 3,4-dihydroxyhydrocinnamic acid-modified magnetite nanoparticles with stealth-functionality against

immunological response, J. Mater. Chem. 22 (2012) 9041–9045, https://doi.org/10.1039/C2JM30325F.
[17] Y. Zhong, L. Yu, Z.F. Chen, H. He, F. Ye, G. Cheng, Q. Zhang, Microwave-assisted synthesis of Fe3O4 nanocrystals with predominantly exposed facets and their heterogeneous UVA/fenton catalytic activity, ACS Appl. Mater. Interfaces 9 (2017) 29203–29212, https://doi.org/10.1021/acsami.7b06925.
[18] J.J. Lenders, C.L. Altan, P.H. Bomans, A. Arakaki, S. Bucak, G. de With, N. A. Sommerdijk, A bioinspired coprecipitation method for the controlled synthesis of magnetite nanoparticles, Cryst. Growth Des. 14 (2014) 5561–5568, https://doi.org/10.1021/cg500816z.
[19] Y.P. Yew, K. Shameli, M. Miyake, N. Kuwano, N.B.B.A. Khairudin, S.E. B. Mohamad, K.X. Lee, Green synthesis of magnetite (Fe3O4) nanoparticles using seaweed (Kappaphycus alvarezii) extract, Nanoscale Res. Lett. 11 (2016) 1–7, https://doi.org/10.1186/s11671-016-1498-2.
[20] W. Li, X. Cai, S. Ma, X. Zhan, F. Lan, Y. Wu, Z. Gu, Synthesis of amphipathic superparamagnetic Fe3O4 Janus nanoparticles via a moderate strategy and their controllable self-assembly, RSC Adv. 6 (2016) 40450–40458, https://doi.org/10.1039/C6RA04648G.
[21] Y. Li, F. Ma, X. Su, L. Shi, B. Pan, Z. Sun, Y. Hou, Ultra-large-scale synthesis of Fe3O4 nanoparticles and their application for direct coal liquefaction, Ind. Eng. Chem. Res. 53 (2014) 6718–6722, https://doi.org/10.1021/ie500216c.
[22] S. Liu, B. Yu, S. Wang, Y. Shen, H. Cong, Preparation, surface functionalization and application of Fe3O4 magnetic nanoparticles, Adv. Colloid Interface Sci. 281 (2020) 102165, https://doi.org/10.1016/j.cis.2020.102165.
[23] H.L. Ding, Y.X. Zhang, S. Wang, J.M. Xu, S.C. Xu, G.H. Li, Fe3O4@SiO2 core/shell nanoparticles: the silica coating regulations with a single core for different core sizes and shell thicknesses, Chem. Mater. 24 (2012) 4572–4580, https://doi.org/10.1021/cm302828d.
[24] R.K. Sharma, Y. Monga, A. Puri, G. Gaba, Magnetite (Fe3O4) silica based organic–inorganic hybrid copper(II) nanocatalyst: a platform for aerobic *N*-alkylation of amines, Green Chem. 15 (2013) 2800–2809, https://doi.org/10.1039/C3GC40818C.
[25] Y. Li, Z. Zhang, J. Shen, M. Ye, Hierarchical nanospheres based on Pd nanoparticles dispersed on carbon coated magnetite cores with a mesoporous ceria shell: a highly integrated multifunctional catalyst, Dalton Trans. 44 (2015) 16592–16601, https://doi.org/10.1039/C5DT01805F.
[26] R.N. Baig, M.N. Nadagouda, R.S. Varma, Arbon-coated magnetic palladium: applications in partial oxidation of alcohols and coupling reactions, Green Chem. 16 (2014) 4333–4338, https://doi.org/10.1039/C4GC00748D.
[27] I. Robinson, L.D. Tung, S. Maenosono, C. Wälti, N.T. Thanh, Synthesis of core-shell gold coated magnetic nanoparticles and their interaction with thiolated DNA, Nanoscale 2 (2010) 2624–2630, https://doi.org/10.1039/C0NR00621A.
[28] M.E.F. Brollo, R. López-Ruiz, D. Muraca, S.J. Figueroa, K.R. Pirota, M. Knobel, Compact Ag@Fe3O4 Core-shell nanoparticles by means of single-step thermal decomposition reaction, Sci. Rep. 4 (2014) 1–6, https://doi.org/10.1038/srep06839.
[29] L. De Matteis, R. Fernandez-Pacheco, L. Custardoy, M.L. Garcia-Martin, J.M. de la Fuente, C. Marquina, M.R. Ibarra, Influence of a silica interlayer on the structural and magnetic properties of Sol–Gel TiO2-coated magnetic nanoparticles, Langmuir 30 (2014) 5238–5247, https://doi.org/10.1021/la500423e.
[30] Z.C. Wu, W.P. Li, C.H. Luo, C.H. Su, C.S. Yeh, Rattle-type Fe3O4@CuS developed to conduct magnetically guided photoinduced hyperthermia at first and second NIR biological windows, Adv. Funct. Mater. 25 (2015) 6527–6537, https://doi.org/10.1002/adfm.201503015.
[31] F. Mi, X. Chen, Y. Ma, S. Yin, F. Yuan, H. Zhang, Facile synthesis of hierarchical core–shell Fe3O4@MgAl–LDH@Au as magnetically recyclable catalysts for catalytic oxidation of alcohols, Chem. Commun. 47 (2011) 12804–12806, https://doi.org/10.1039/C1CC15858A.
[32] X. Cui, S. Belo, D. KrŘger, Y. Yan, R.T. de Rosales, M. Jauregui-Osoro, P. J. Blower, Aluminium hydroxide stabilised MnFe2O4 and Fe3O4 nanoparticles as dual-modality contrasts agent for MRI and PET imaging, Biomaterials 35 (2014) 5840–5846, https://doi.org/10.1016/j.biomaterials.2014.04.004.
[33] I. Karimzadeh, H.R. Dizaji, M. Aghazadeh, Development of a facile and effective electrochemical strategy for preparation of iron oxides (Fe3O4 and γ-Fe2O3) nanoparticles from aqueous and ethanol mediums and in situ PVC coating of Fe3O4 superparamagnetic nanoparticles for biomedical applications, J. Magn. Magn. 416 (2016) 81–88, https://doi.org/10.1016/j.jmmm.2016.05.015.
[34] M.B. Gawande, Y. Monga, R. Zboril, R.K. Sharma, Silica-decorated magnetic nanocomposites for catalytic applications, Coord. Chem. Rev. 288 (2015) 118–143, https://doi.org/10.1016/j.ccr.2015.01.001.
[35] M. Bystrzejewski, S. Cudziło, A. Huczko, H. Lange, G. Soucy, G. Cota-Sanchez, Carbon encapsulated magnetic nanoparticles for biomedical applications: Thermal stability studies, Biomol. Eng. 24 (2007) 555–558, https://doi.org/10.1016/j.bioeng.2007.08.006.
[36] M. Barrow, A. Taylor, P. Murray, M.J. Rosseinsky, D.J. Adams, Design considerations for the synthesis of polymer coated iron oxide nanoparticles for stem cell labelling and tracking using MRI, Chem. Soc. Rev. 44 (2015) 6733–6748, https://doi.org/10.1039/C5CS00331H.
[37] M. Neamtu, C. Nadejde, V.D. Hodoroaba, R.J. Schneider, L. Verestiuc, U. Panne, Functionalized magnetic nanoparticles: Synthesis, characterization, catalytic application and assessment of toxicity, Sci. Rep. 8 (2018) 1–11, https://doi.org/10.1038/s41598-018-24721-4.
[38] F. Gao, An overview of surface-functionalized magnetic nanoparticles: preparation and application for wastewater treatment, ChemistrySelect 4 (2019) 6805–6811, https://doi.org/10.1002/slct.201900701.
[39] (a) R.K. Sharma, Y. Monga, S. Sharma, M. Yadav, S. Dutta, R. Gaur, G. Arora, World Scientific 4, 2019, https://doi.org/10.1142/q0221;
(b) S. Dutta, S. Sharma, A. Sharma, R.K. Sharma, Fabrication of core–shell-structured organic–inorganic hybrid nanocatalyst for the expedient synthesis of polysubstituted oxazoles via tandem oxidative cyclization pathway, ACS Omega 2 (2017) 2778–2791, https://doi.org/10.1021/acsomega.7b00382.
[40] (a) D.M.A. Neto, L.S. da Costa, F.L. de Menezes, L.M. Fechine, R.M. Freire, J. C. Denardin, P.B. Fechine, A novel amino phosphonate-coated magnetic nanoparticle as MRI contrast agent, Appl. Surf. Sci. 543 (2021) 148824, https://doi.org/10.1016/j.apsusc.2020.148824;
(b) S. Yu, G.M. Chow, Carboxyl group (–CO2H) functionalized ferrimagnetic iron oxide nanoparticles for potential bio-applications, J. Mater. Chem. 14 (2004) 2781–2786, https://doi.org/10.1039/B404964K;
(c) H. Mahmoudi, A.A. Jafari, S. Saeedi, H. Firouzabadi, Sulfonic acid-functionalized magnetic nanoparticles as a recyclable and eco-friendly catalyst for atom economical Michael addition reactions and bis indolyl methane synthesis, RSC Adv. 2015 (5) (2015) 3023–3030, https://doi.org/10.1039/C4RA11605D;
(d) L. Shiri, H. Narimani, M. Kazemi, Sulfamic acid immobilized on amino-functionalized magnetic nanoparticles: a new and active magnetically recoverable catalyst for the synthesis of *N*-heterocyclic compounds, Appl. Organomet. Chem. 32 (2018), e3999, https://doi.org/10.1002/aoc.3999.
[41] B. Chen, S. Chen, H.A. Bandal, R. Appiah-Ntiamoah, A.R. Jadhav, H. Kim, Cobalt nanoparticles supported on magnetic core-shell structured carbon as a highly efficient catalyst for hydrogen generation from NaBH4 hydrolysis, Int. J. Hydrog. Energy 43 (2018) 9296–9306, https://doi.org/10.1016/j.ijhydene.2018.03.193.
[42] R.K. Sharma, S. Dutta, S. Sharma, Nickel(II) complex covalently anchored on core shell structured SiO2@Fe3O4 nanoparticles: a robust and magnetically retrievable catalyst for direct one-pot reductive amination of ketones, New J. Chem. 40 (2016) 2089–2101, https://doi.org/10.1039/C5NJ02495A.
[43] C. Sappino, L. Primitivo, M. De Angelis, M.O. Domenici, A. Mastrodonato, I. B. Romdan, Functionalized magnetic nanoparticles as catalysts for enantioselective henry reaction, ACS Omega 4 (2019) 21809–21817, https://doi.org/10.1021/acsomega.9b02683.
[44] A. Najafpoor, R. Norouzian-Ostad, H. Alidadi, T. Rohani-Bastami, M. Davoudi, F. Barjasteh-Askari, J. Zanganeh, Effect of magnetic nanoparticles and silver-loaded magnetic nanoparticles on advanced wastewater treatment and disinfection, J. Mol. Liq. 303 (2020) 112640, https://doi.org/10.1016/j.molliq.2020.112640.
[45] (a) K.P. de Jong, Synthesis of Solid Catalysts, Wiley, 2009, https://doi.org/10.1002/9783527626854;
(b) J. Regalbuto, Catalyst Preparation: Science and Engineering, CRC Press, 2007;
(c) G. Ertl, H. Knözinger, J. Weitkamp, Preparation of Solid Catalysts, Wiley, 1999.
[46] P. Munnik, P.E. de Jongh, K.P. de Jong, Recent developments in the synthesis of supported catalysts, Chem. Rev. 115 (2015) 6687–6718, https://doi.org/10.1021/cr500486u.
[47] S.N. Shelke, S.R. Bankar, G.R. Mhaske, S.S. Kadam, D.K. Murade, S.B. Bhorkade, R.S. Varma, Iron oxide-supported copper oxide nanoparticles (Nanocat-Fe-CuO): magnetically recyclable catalysts for the synthesis of pyrazole derivatives, 4-methoxyaniline, and ullmann-type condensation reactions, ACS Sustain. Chem. Eng. 2 (2014) 1699–1706, https://doi.org/10.1021/sc500160f.
[48] S. Wang, Z. Zhang, B. Liu, Catalytic conversion of fructose and 5-hydroxymethylfurfural into 2,5-furandicarboxylic acid over a recyclable Fe3O4–CoOx magnetite nanocatalyst, ACS Sustain. Chem. Eng. 3 (2015) 406–412, https://doi.org/10.1021/sc500702q.
[49] P. Koley, S. Chandra Shit, B. Joseph, S. Pollastri, Y.M. Sabri, E.L. Mayes, J. Mondal, Leveraging Cu/CuFe2O4-catalyzed biomass-derived furfural hydrodeoxygenation: a nanoscale metal–organic-framework template is the prime key, ACS Appl. Mater. Interfaces 12 (2020) 21682–21700, https://doi.org/10.1021/acsami.0c03683.
[50] M.M. Natile, A. Glisenti, New NiO/Co3O4 and Fe2O3/Co3O4 nanocomposite catalysts: synthesis and characterization, Chem. Mater. 15 (2003) 2502–2510, https://doi.org/10.1021/cm031019e.
[51] S. Gaur, S. Johansson, F. Mohammad, C.S. Kumar, J.J. Spivey, Catalytic activity of titania-supported core–shell Fe3O4@Au nano-catalysts for CO oxidation, J. Phys. Chem. C 116 (2012) 22319–22326, https://doi.org/10.1021/jp3045725.
[52] S.M. Louie, J.M. Pettibone, Research highlights: engineering nanomaterial-based technologies for environmental applications, Environ. Sci. Nano 3 (2016) 11–14, https://doi.org/10.1039/C6EN90001A.
[53] L.M. Rossi, N.J. Costa, F.P. Silva, R. Wojcieszak, Magnetic nanomaterials in catalysis: advanced catalysts for magnetic separation and beyond, Green Chem. 16 (2014) 2906–2933, https://doi.org/10.1039/C4GC00164H.
[54] Y. Zhu, K. Loo, H. Ng, C. Li, L.P. Stubbs, F.S. Chia, M. Tan, S.C. Peng, Magnetic nanoparticles supported second generation Hoveyda-Grubbs catalyst for metathesis of unsaturated fatty acid esters, Adv. Synth. Catal. 351 (2009) 2650–2656, https://doi.org/10.1002/adsc.200900370.
[55] S.E.G. Garrido, J. Francos, V. Cadierno, J.M. Basset, V. Polshettiwar, Chemistry by nanocatalysis: first example of a solid-supported RAPTA complex for organic reactions in aqueous medium, ChemSusChem 4 (2011) 104, https://doi.org/10.1002/cssc.201000280.
[56] P.D. Stevens, J. Fan, H.M. Gardimalla, M. Yen, Y. Gao, Superparamagnetic nanoparticle-supported catalysis of suzuki cross-coupling reactions, Org. Lett. 7 (2005) 2085–2088, https://doi.org/10.1021/ol050218w.

[57] M.J. Jin, D.H. Lee, A practical heterogeneous catalyst for the suzuki, sonogashira, and stille coupling reactions of unreactive aryl chlorides, Angew. Chem., Int. Ed. 49 (2010) 1119–1122, https://doi.org/10.1002/anie.200905626.

[58] R.B. Nasir Baig, R.S. Varma, A highly active and magnetically retrievable nanoferrite–DOPA–copper catalyst for the coupling of thiophenols with aryl halides, Chem. Commun. 48 (2012) 2582–2584, https://doi.org/10.1039/C2CC17283F.

[59] M. Masteri-Farahani, N. Tayyebi, A new magnetically recoverable nanocatalyst for epoxidation of olefins, J. Mol. Catal. A. Chem. 348 (2011) 83–87, https://doi.org/10.1016/j.molcata.2011.08.007.

[60] J. Sun, G. Yu, L. Liu, Z. Li, Q. Kan, Q. Huo, J. Guan, Core–shell structured Fe3O4@SiO2 supported cobalt(II) or copper(II) acetylacetonate complexes: magnetically recoverable nanocatalysts for aerobic epoxidation of styrene, Catal. Sci. Technol. 4 (2014) 1246–1252, https://doi.org/10.1039/C4CY00017J.

[61] S.M. Sadeghzadeh, Recyclable gold(III) dipyridine complex immobilized on Fe3O4 magnetic nanoparticles: synthesis of 2,6-dihydro[2,1-*a*]isoindole under mild conditions, RSC Adv. 4 (2014) 43315–43320, https://doi.org/10.1039/C4RA07107G.

[62] R. Gupta, M. Yadav, R. Gaur, G. Arora, R.K. Sharma, A straightforward one-pot synthesis of bioactive *N*-aryl oxazolidin-2-ones via a highly efficient Fe3O4@SiO2-supported acetate-based butylimidazolium ionic liquid nanocatalyst under metal- and solvent-free conditions, Green Chem. 19 (2017) 3801–3812, https://doi.org/10.1039/C7GC01414G.

[63] H. Woo, D. Kim, J.C. Park, J.W. Kim, S. Park, J.M. Lee, K.H. Park, A new hybrid nanocatalyst based on Cu-doped Pd–Fe3O4 for tandem synthesis of 2-phenylbenzofurans, J. Mater. Chem. A 3 (2015) 20992–20998, https://doi.org/10.1039/C5TA05111H.

[64] H. Woo, K. Lee, J.C. Park, K.H. Park, Facile synthesis of Pd/Fe3O4/charcoal bifunctional catalysts with high metal loading for high product yields in Suzuki–Miyaura coupling reactions, New J. Chem. 38 (2014) 5626–5632, https://doi.org/10.1039/C4NJ01329H.

[65] V. Panwar, P. Kumar, A. Bansal, S.S. Ray, S.L. Jain, PEGylated magnetic nanoparticles (PEG@Fe3O4) as cost effective alternative for oxidative cyanation of tertiary amines *via* C-H activation, Appl. Catal. A: Gen. 498 (2015) 25–31, https://doi.org/10.1016/j.apcata.2015.03.018Get.

[66] P. Majumdar, A. Pati, M. Patra, R.K. Behera, A.K. Behera, Acid hydrazides, potent reagents for synthesis of oxygen-, nitrogen-, and/or sulfur-containing heterocyclic rings, Chem. Rev. 114 (2014) 2942–2977, https://doi.org/10.1021/cr300122t.

[67] P.N. Kalaria, S.C. Karad, D.K. Raval, A review on diverse heterocyclic compounds as the privileged scaffolds in antimalarial drug discovery, Eur. J. Med. Chem. 158 (2018) 917–936, https://doi.org/10.1016/j.ejmech.2018.08.040.

[68] R. Goel, V. Luxami, K. Paul, Imidazo[1,2-*a*]pyridines: promising drug candidate for antitumor therapy, Curr. Top. Med. Chem. 16 (2016) 3590–3616.

[69] A.K. Bagdi, S. Santra, K. Monir, A. Hajra, Synthesis of imidazo[1,2-*a*]pyridines: a decade update, Chem. Commun. 51 (2015) 1555–1575, https://doi.org/10.1039/C4CC08495K.

[70] J. Lee, J. Chung, S.M. Byun, B.M. Kim, C. Lee, Direct catalytic C–H arylation of imidazo[1,2-a]pyridine with aryl bromides using magnetically recyclable Pd–Fe3O4 nanoparticles, Tetrahedron 69 (2013) 5660–5664, https://doi.org/10.1016/j.tet.2013.04.031.

[71] F.M. Moghaddam, G. Tavakoli, F. Latifi, B. Saeednia, α-Arylation of oxindoles using recyclable metal oxide ferrite nanoparticles: Comparison between the catalytic activities of nickel, cobalt and copper ferrite nanoparticles, Catal. Commun. 75 (2016) 37–41, https://doi.org/10.1016/j.catcom.2015.11.020.

[72] S.V. Céspedes, K.M. Chepiga, N. Möller, A.H. Schäfer, F. Glorius, Direct C–H arylation of heteroarenes with copper impregnated on magnetite as a reusable catalyst: evidence for CuO nanoparticle catalysis in solution, ACS Catal. 6 (2016) 5954–5961, https://doi.org/10.1021/acscatal.6b01288.

[73] M. Shariatipour, A. Salamatmanesh, M. Jadidinejad, A. Heydari, Imidazole-aryl coupling reaction *via* C-H bond activation catalyzed by palladium supported on modified magnetic reduced graphene oxide in alkaline deep eutectic solvent, Catal. Commun. 135 (2020) 105890, https://doi.org/10.1016/j.catcom.2019.105890.

[74] L. Zhang, P. Li, C. Liu, J. Yang, M. Wang, L. Wang, A highly efficient and recyclable Fe3O4 magnetic nanoparticle immobilized palladium catalyst for the direct C-2 arylation of indoles with arylboronic acids, Catal. Sci. Technol. 4 (2014) 1979–1988, https://doi.org/10.1039/C4CY00040D.

[75] D. Enders, J.P. Shilvock, Some recent applications of α-amino nitrile chemistry, Chem. Soc. Rev. 29 (2000) 359–373, https://doi.org/10.1039/A908290E.

[76] (a) C.S. Yeung, V.M. Dong, Catalytic dehydrogenative cross-coupling: forming carbon−carbon bonds by oxidizing two carbon−hydrogen bonds, Chem. Rev. 111 (2011) 1215, https://doi.org/10.1021/cr100280d;
(b) C.L. Sun, B.J. Li, Z.J. Shi, Direct C−H transformation *via* iron catalysis, Chem. Rev. 111 (2011) 1293–1314, https://doi.org/10.1021/cr100198w.

[77] (a) J.M. Allen, T. Lambert, Tropylium ion mediated α-cyanation of amines, J. Am. Chem. Soc. 133 (2011) 1260–1262, https://doi.org/10.1021/ja109617y;
(b) S.I. Murahashi, T. Nakae, H. Terai, N. Komiya, Ruthenium-catalyzed oxidative cyanation of tertiary amines with molecular oxygen or hydrogen peroxide and sodium cyanide: sp3 C−H bond activation and carbon−carbon bond formation, J. Am. Chem. Soc. 2008 (130) (2008) 11005–11012, https://doi.org/10.1021/ja8017362;
(c) S.I. Murahashi, N. Komiya, H. Terai, T. Nakae, Aerobic ruthenium-catalyzed oxidative cyanation of tertiary amines with sodium cyanide, J. Am Chem. Soc. 125 (2003) 15312–15313, https://doi.org/10.1021/ja0390303;
(d) S. Singhal, S.L. Jain, B. Sain, Heterogeneously catalyzed oxidative cyanation of tertiary amines with sodium cyanide/hydrogen peroxide using polymer-supported Iron (II) phthalocyanines as catalyst, Adv. Synth. Catal. 352 (2010) 1338–1344, https://doi.org/10.1002/adsc.201000007.

[78] S. Verma, R.B.N. Baig, C. Han, M.N. Nadagouda, R.S. Varma, Magnetic graphitic carbon nitride: its application in the C–H activation of amines, Chem. Commun. 51 (2015) 15554–15557, https://doi.org/10.1039/C5CC05895C.

[79] J. Tsuji, Transition metal reagents and catalysts: innovations in organic synthesis, John Wiley & Sons, Ltd, 2000.

[80] R. Chinchilla, C. Najera, The sonogashira reaction: a booming methodology in synthetic organic chemistry, Chem. Rev. 107 (2007) 874–922, https://doi.org/10.1021/cr050992x.

[81] H. Doucet, J.C. Hierso, Palladium-based catalytic systems for the synthesis of conjugated enynes by sonogashira reactions and related alkynylations, Angew. Chem. Int. Ed. 46 (2007) 834–871, https://doi.org/10.1002/anie.200602761.

[82] H. Huang, H. Jiang, K. Chen, H. Liu, Efficient iron/copper cocatalyzed alkynylation of aryl iodides with terminal alkynes, J. Org. Chem. 73 (2008) 9061–9064, https://doi.org/10.1021/jo801942h.

[83] N. Panda, A.K. Jena, S. Mohapatra, Ligand-free Fe-Cu cocatalyzed cross-coupling of terminal alkynes with aryl halides, Chem. Lett. 40 (2011) 956–958, https://doi.org/10.1246/cl.2011.956.

[84] H. Firouzabadi, N. Iranpoor, M. Gholinejad, J. Hoseini, Magnetite (Fe3O4) nanoparticles-catalyzed Sonogashira– Hagihara reactions in ethylene glycol under ligand-free conditions, Adv. Synth. Catal. 353 (2011) 125–132, https://doi.org/10.1002/adsc.201000390.

[85] M. Gholinejad, A. Neshat, F. Zareh, C. Nájera, M. Razeghi, A. Khoshnood, Palladium supported on bis(indolyl)methane functionalized magnetite nanoparticles as an efficient catalyst for copper-free Sonogashira-Hagihara reaction, Appl. Catal. A: Gen. 525 (2016) 31–40, https://doi.org/10.1016/j.apcata.2016.06.041.

[86] D. Firuzabadi Fa, Z. Asadi, F. Panahi, Immobilized NNN Pd-complex on magnetic nanoparticles: efficient and reusable catalyst for Heck and Sonogashira coupling reactions, RSC Adv. 6 (2016) 101061–101070, https://doi.org/10.1039/C6RA22535G.

[87] W. Li, X. Jia, B. Zhang, L. Tian, X. Li, H. Zhang, Q. Zhang, Fabrication of PEI grafted Fe3O4/SiO2/P(GMA-co-EGDMA) nanoparticle anchored palladium nanocatalyst and its application in Sonogashira cross-coupling reactions, New J. Chem. 39 (2015) 2925–2934, https://doi.org/10.1039/C4NJ02117G.

[88] N.T.S. Phan, H.V. Le, Superparamagnetic nanoparticles-supported phosphine-free palladium catalyst for the Sonogashira coupling reaction, J. Mol. Catal. A Chem. 334 (2011) 130–138, https://doi.org/10.1016/j.molcata.2010.11.009.

[89] A. Elhampour, N. Firouzeh, H.T. Nahzomi, V. Mohagheghi, Magnetic nanoparticle-supported tetrazole-functionalized palladium catalyst: synthesis, DFT study and application for Sonogashira and Heck cross-coupling reactions, Res. Chem. Intermed. 43 (2017) 6737–6761, https://doi.org/10.1007/s11164-017-3018-0.

[90] M. Esmaeilpour, A.R. Sardarian, J. Javidi, Synthesis and characterization of Schiff base complex of Pd(II) supported on superparamagnetic Fe3O4@SiO2 nanoparticles and its application as an efficient copper- and phosphine ligand-free recyclable catalyst for Sonogashira–Hagihara coupling reactions, J. Organomet. Chem. 749 (2014) 233–240, https://doi.org/10.1016/j.jorganchem.2013.10.011.

[91] S. Sobhani, Z. Zeraatkar, F. Zarifi, Pd complex of an NNN pincer ligand supported on γ-Fe2O3@SiO2 magnetic nanoparticles: a new catalyst for Heck, Suzuki and Sonogashira coupling reactions. New J. Chem. 9 (2015) 7076–7085, https://doi.org/10.1039/C5NJ00344J.

[92] (a) H.J. Mann, Moricizine: a new class I antiarrhythmic, Clin. Pharmacy 9 (1990) 842–852;
(b) A.L. Dopp, J.M. Miller, J.E. Tisdale, Effect of drugs on defibrillation capacity, Drugs 68 (2008) 607–630, https://doi.org/10.2165/00003495-200868050-00004;
(c) C.E. Stafstrom, S. Grippon, P. Kirkpatrick, Ezogabine (retigabine), Nature Rev. Drug Discovery 10 (2011) 729–730, https://doi.org/10.1038/nrd3561;
(d) S.M. Clarke, F.M. Mulcahy, Efavirenz therapy in drug users, HIV Med. 1 (2000) 15–17, https://doi.org/10.1046/j.1468-1293.2000.00004.x;
(e) R. Konrad, J.L. Jarogniew, B. Barbara, C. Roman, J.C. Stanislaw, Clinical utility of adjunctive retigabine in partial onset seizures in adults, Ther. Clin. Risk Manage. 8 (2012) 7–14, https://doi.org/10.2147/TCRM.S22605.

[93] (a) S. Ozaki, Recent advafnces in isocyanate chemistry, Chem. Rev. 72 (1972) 457–496, https://doi.org/10.1021/cr60279a002;
(b) L. Pasguato, G. Modena, L. Cotarca, P. Delgu, J. Mantovami, Conversion of bis(trichloromethyl) carbonate to phosgene and reactivity of triphosgene, diphosgene, and phosgene with methanol, J. Org. Chem. 65 (2000) 8224–8228, https://doi.org/10.1021/jo000820u;
(c) J.S. Nowick, N.A. Powell, T.M. Nguyen, G.J. Noronha, An improved method for the synthesis of enantiomerically pure amino acid ester isocyanates, J. Org. Chem. 57 (1992) 7364–7366, https://doi.org/10.1021/jo00052a069;
(d) R.A. Batey, V. Santhakumar, C.Y. Ishii, S.D. Taylor, An efficient new protocol for the formation of unsymmetrical tri- and tetrasubstituted ureas, Tetrahedron Lett. 39 (1998) 6267–6270, https://doi.org/10.1016/S0040-4039(98)01330-6.

[94] (a) E.V. Vinogradova, N.H. Park, B.P. Fors, S.L. Buchwald, Palladium-catalyzed synthesis of N-Aryl carbamates, Org. Lett. 15 (2013) 1394–1397, https://doi.org/10.1021/ol400369n;
(b) D.F. Niu, L. Zhang, L.P. Xiao, Y.W. Luo, J.X. Lu, Nickel-catalyzed coupling of CO2 and amines: improved synthesis of carbamates, Appl. Organomet. Chem. 21 (2007) 941–944, https://doi.org/10.1002/aoc.1314.

[95] (a) F. Shi, Y. Deng, First gold(I) complex-catalyzed oxidative carbonylation of amines for the syntheses of carbamates, Chem. Commun. 5 (2001) 443–444, https://doi.org/10.1039/B009575N;

(b) Z.H. Guan, H. Lei, M. Chen, Z.H. Ren, Y. Bai, Y.Y. Wanga, Palladium-catalyzed carbonylation of amines: switchable approaches to carbamates and *N, N′*-disubstituted ureas, Adv. Synth. Catal. 354 (2012) 489–496, https://doi.org/10.1002/adsc.201100545;
(c) H. Zhou, F. Shi, X. Tian, Q. Zhang, Y. Deng, Synthesis of carbamates from aliphatic amines and dimethyl carbonate catalyzed by acid functional ionic liquids, J. Mol. Catal. A: Chem. 271 (2007) 89–92, https://doi.org/10.1016/j.molcata.2007.02.017.

[96] (a) J. Shang, S. Li, X. Ma, L. Lua, Y. Deng, A new route of CO2 catalytic activation: syntheses of N-substituted carbamates from dialkyl carbonates and polyureas, Green Chem. 14 (2012) 2899–2906, https://doi.org/10.1039/C2GC36043H;
(b) R.N. Salvatore, S.I. Shin, A.S. Nagle, K.W. Jung, Efficient carbamate synthesis via a three-component coupling of an amine, CO2, and alkyl halides in the presence of Cs2CO3 and tetrabutylammonium iodide, J. Org. Chem. 66 (2001) 1035–1037, https://doi.org/10.1021/jo001140u;
(c) K.N. Singh, Mild and convenient synthesis of organic carbamates from amines and carbon dioxide using tetraethylammonium superoxide, Synth. Commun. 37 (2007) 2651–2654, https://doi.org/10.1080/00397910701465149;
(d) A. Ion, C.V. Doorslaer, V. Parvulescu, P. Jacobsa, D.D. Vos, Green synthesis of carbamates from CO2, amines and alcohols, Green Chem. 10 (2008) 111–116, https://doi.org/10.1039/B711197E.

[97] (a) S. Yoganathan, S.J. Miller, *N*-methylimidazole-catalyzed synthesis of carbamates from hydroxamic acids via the lossen rearrangement, Org. Lett. 15 (2013) 602–605, https://doi.org/10.1021/ol303424b;
(b) O. Kreye, S. Wald, M.A.R. Meiera, Introducing catalytic lossen rearrangements: sustainable access to carbamates and amines, Adv. Synth. Catal. 355 (2013) 81–86, https://doi.org/10.1002/adsc.201200760;
(c) X. Huang, J.W. Keillor, Preparation of methyl carbamates *via* a modified Hofmann rearrangement, Tetrahedron Lett. 38 (1997) 313–316, https://doi.org/10.1016/S0040-4039(96)02341-6.

[98] K. Lauder, A. Toscani, N. Scalacci, D. Castagnolo, Synthesis and reactivity of propargylamines in organic chemistry, Chem. Rev. 117 (2017) 14091–14200, https://doi.org/10.1021/acs.chemrev.7b00343.

[99] X. Huo, J. Liu, B. Wang, H. Zhang, Z. Yang, X. She, P. Xi, A one-step method to produce graphene–Fe3O4 composites and their excellent catalytic activities for three-component coupling of aldehyde, alkyne and amine, J. Mater. Chem. A 1 (2013) 651–656, https://doi.org/10.1039/C2TA00485B.

[100] A.T. Nguyen, L.T. Pham, N.T.S. Phan, T. Truong, Efficient and robust superparamagnetic copper ferrite nanoparticle-catalyzed sequential methylation and C–H activation: aldehyde-free propargylamine synthesis, Catal. Sci. Technol. 4 (2014) 4281–4288, https://doi.org/10.1039/C4CY00753K.

[101] M. Tajbakhsh, M. Farhang, S.M. Baghbanian, R. Hosseinzadeh, M. Tajbakhsh, Nano magnetite supported metal ions as robust, efficient and recyclable catalysts for green synthesis of propargylamines and 1,4-disubstituted 1,2,3-triazoles in water, New J. Chem. 39 (2015) 1827–1839, https://doi.org/10.1039/C4NJ01866D.

[102] A. Elhampour, M. Malmir, E. Kowsari, F. Boorboor Ajdari, F. Nemati, Ag-doped nano magnetic γ-Fe2O3@DA core–shell hollow spheres: an efficient and recoverable heterogeneous catalyst for A3 and KA2 coupling reactions and [3+2] cycloaddition, RSC Adv. 6 (2016) 96623–96634, https://doi.org/10.1039/C6RA18810A.

[103] Z. Zarei, B. Akhlaghinia, Zn(II) anchored onto the magnetic natural hydroxyapatite (ZnII/HAP/Fe3O4): as a novel, green and recyclable catalyst for A3-coupling reaction towards propargylamine synthesis under solvent-free conditions, RSC Adv. 6 (2016) 106473–106484, https://doi.org/10.1039/C6RA20501A.

[104] A.M. Munshi, M. Shi, S. Thomas, M. Saunders, M. Spackman, K.S. Iyer, Nicole M. Smith, Magnetically recoverable Fe3O4@Au-coated nanoscale catalysts for the A3-coupling reaction, Dalton Trans. 46 (2017) 5133–5137, https://doi.org/10.1039/C7DT00058H.

[105] S. Sadjadi, M. Malmirb, M.M. Heravi, A green approach to the synthesis of Ag doped nano magnetic γ-Fe2O3@SiO2-CD core–shell hollow spheres as an efficient and heterogeneous catalyst for ultrasonic-assisted A3 and KA2 coupling reactions, RSC Adv. 7 (2017) 36807–36818, https://doi.org/10.1039/C7RA04635A.

[106] Z. Shahamat, F. Nemati, A. Elhampour, One-pot synthesis of propargylamines using magnetic mesoporous polymelamine formaldehyde/zinc oxide nanocomposite as highly efficient, eco-friendly and durable nanocatalyst: optimization by DOE approach, Mol. Divers. 24 (2020) 691–706, https://doi.org/10.1007/s11030-019-09977-w.

[107] S. Zhu, D. Wang, Photocatalysis: basic principles, diverse forms of implementations and emerging scientific opportunities, Adv. Energy Mater. 7 (2017) 1700841, https://doi.org/10.1002/aenm.201700841.

[108] (a) S. Yadav, R. Dixit, S. Sharma, S. Dutta, K. Solanki, R.K. Sharma, Magnetic metal–organic framework composites: structurally advanced catalytic materials for organic transformations, Mater. Advan. 2 (2021) 2153–2187, https://doi.org/10.1039/D0MA00982B;
(b) R.K. Sharma, S. Yadav, S. Sharma, S. Dutta, A. Sharma, Expanding the horizon of multicomponent oxidative coupling reaction via the design of a unique, 3D copper isophthalate MOF-based catalyst decorated with mixed spinel CoFe2O4 nanoparticles, ACS Omega 3 (2018) 15100–15111, https://doi.org/10.1021/acsomega.8b02061;
(c) S. Yadav, S. Sharma, S. Dutta, A. Sharma, A. Adholeya, R.K. Sharma, Harnessing the untapped catalytic potential of a CoFe2O4/Mn-BDC hybrid MOF composite for obtaining a multitude of 1,4-disubstituted 1,2,3-triazole scaffolds, Inorg. Chem. 59 (2020) 8334–8344, https://doi.org/10.1021/acs.inorgchem.0c00752.

[109] P. Rana, R. Gaur, R. Gupta, G. Arora, A. Jayashree, Sharma, Cross-dehydrogenative C(sp3)–C(sp3) coupling *via* C–H activation using magnetically retrievable ruthenium-based photoredox nanocatalyst under aerobic conditions, Chem. Commun. 55 (2019) 7402–7405, https://doi.org/10.1039/C9CC02386K.

[110] M. Kaur, S. Pramanik, M. Kumar, V. Bhalla, Polythiophene-encapsulated bimetallic Au-Fe3O4 nano-hybrid materials: a potential tandem photocatalytic system for nondirected C(sp2)–H activation for the synthesis of quinoline carboxylates, ACS Catal. 7 (2017) 2007–2021, https://doi.org/10.1021/acscatal.6b02681.

[111] R. Chopra, M. Kumar, V. Bhalla, Fabrication of polythiophene-supported Ag@Fe3O4 nanoclusters and their utilization as photocatalyst in dehydrogenative coupling reactions, ACS Sustain. Chem. Engin. 6 (2018) 7412–7419, https://doi.org/10.1021/acssuschemeng.7b04891.

[112] H. Kaur, M. Kaur, P.K. Walia, M. Kumar, V. Bhalla, Encapsulating Au-Fe3O4 nanodots into AIE-active supramolecular assemblies: ambient visible-light harvesting "Dip-Strip" photocatalyst for C−C/C−N bond formation reactions, Chem. Asian J. 14 (2019) 809–813, https://doi.org/10.1002/asia.201801556.

[113] (a) C.G. Frost, L. Mutton, Heterogeneous catalytic synthesis using microreactor technology, Green Chem. 12 (2010) 1687–1703, https://doi.org/10.1039/C0GC00133C;
(b) V. Hessel, D. Kralisch, N. Kockmann, T. Noël, Q. Wang, Novel process windows for enabling, accelerating, and uplifting flow chemistry, ChemSusChem 6 (2013) 746–789, https://doi.org/10.1002/cssc.201200766.

[114] (a) P. Shivaprasad, E.A.C. Emanuelsson, Process intensification of immobilized enzyme reactors, in: A. Górak, A. Stankiewicz (Eds.), Intensification of Biobased Processes, 2018, pp. 249–267;
(b) R. Munirathinam, J. Huskens, W. Verboom, Supported catalysis in continuous-flow microreactors, Adv. Synth. Catal. 357 (2015) 1093–1123, https://doi.org/10.1002/adsc.201401081.

[115] S. Govaerts, A. Nyuchev, T. Noel, Pushing the boundaries of C–H bond functionalization chemistry using flow technology, J. Flow Chem. 10 (2020) 13–71, https://doi.org/10.1007/s41981-020-00077-7.

[116] R.N. Baig, R.S. Varma, Magnetically retrievable catalysts for organic synthesis, Chem. Commun. 49 (2013) 752–770, https://doi.org/10.1039/C2CC35663E.

[117] (a) S. Santoro, F. Ferlin, L. Ackermann, L. Vaccaro, C–H functionalization reactions under flow conditions, Chem. Soc. Rev. 48 (2019) 2767–2782, https://doi.org/10.1039/C8CS00211H;
(b) T. Noël, Y. Su, V. Hessel, Beyond organometallic flow chemistry: the principles behind the use of continuous-flow reactors for synthesis, Organomet. Flow Chem. 57 (2015) 1–41, https://doi.org/10.1007/3418_2015_152.

[118] K. Tadele, S. Verma, M.N. Nadagouda, M.A. Gonzalez, R.S. Varma, A rapid flow strategy for the oxidative cyanation of secondary and tertiary amines *via* C-H activation, Sci. Rep. 7 (2017) 16311, https://doi.org/10.1038/s41598-017-16410-5.

[119] T.H. Rehm, A. Bogdan, C. Hofmann, P. Löb, Z.B. Shifrina, D.G. Morgan, L. M. Bronstein, Proof of concept: magnetic fixation of dendron-functionalized iron oxide nanoparticles containing palladium nanoparticles for continuous-flow suzuki coupling reactions, ACS Appl. Mater. Interfaces 7 (2015) 27254–27261, https://doi.org/10.1021/acsami.5b08466.

[120] C.P. Park, D.P. Kim, A microchemical system with continuous recovery and recirculation of catalyst-immobilized magnetic particles, Angew. Chem. 122 (2010) 6977–6981, https://doi.org/10.1002/ange.201002490.

[121] S.K. Lee, X. Liu, V.S. Cabeza, K.F. Jensen, Synthesis, assembly and reaction of a nanocatalyst in microfluidic systems: a general platform, Lab on a Chip 12 (2012) 4080–4084, https://doi.org/10.1039/C2LC40186J.

[122] J. Wegner, S. Ceylan, C. Friese, A. Kirschning, Facile oxidations under flow conditions in fixed-bed reactors, Eur. J. Org. Chem. (2010) 4372–4375, https://doi.org/10.1055/s-0030-1258824.

[123] L. Miao, Y.Z. Zhu, H.F. Wang, Nickel-decorated Fe3O4 nanoparticles as recyclable magnetic self-stirring nanocatalysts for microreactions, ACS Sustain. Chem. Engin. 5 (2017) 1864–1870, https://doi.org/10.1021/acssuschemeng.6b02581.

[124] A. Schätz, R.N. Grass, Q. Kainz, W.J. Stark, O. Reiser, Cu(II)−Azabis(oxazoline) complexes immobilized on magnetic Co/C nanoparticles: kinetic resolution of 1,2-diphenylethane-1,2-diol under batch and continuous-flow conditions, Chem. Mater. 22 (2010) 305–310, https://doi.org/10.1021/cm9019099.

[125] T. Zhang, X. Zhang, X. Yan, L. Kong, G. Zhang, H. Liu, J. Qiu, K.L. Yeung, Synthesis of Fe3O4@ZIF-8 magnetic core–shell microspheres and their potential application in a capillary microreactor, Chem. Eng. J. 228 (2013) 398–404, https://doi.org/10.1016/j.cej.2013.05.020.

[126] Z.A. Narei, B. Shafiee, A.R. Khosropour, Synergic effect of nano-catalyst and continuous flow system: Dakin–West reaction catalyzed by Nafion-H@SPIONs in a microreactor, RSC Adv. 5 (2015) 20132–20137, https://doi.org/10.1039/C4RA15466E.

[127] D. Obermayer, A.M. Balu, A.A. Romero, W. Goessler, R. Luque, C.O. Kappe, Nanocatalysis in continuous flow: supported iron oxide nanoparticles for the heterogeneous aerobic oxidation of benzyl alcohol, Green Chem. 15 (2013) 1530–1537, https://doi.org/10.1039/C3GC40307F.

[128] T. Westermann, T. Melin, Flow-through catalytic membrane reactors—Principles and applications, Chem. Eng. Process.: Process Intensif 48 (2009) 17–28, https://doi.org/10.1016/j.cep.2008.07.001.

[129] (a) S. Bahadorikhalili, H. Mahdavi, Palladium magnetic nanoparticle-polyethersulfone composite membrane as an efficient and versatile catalytic membrane reactor, Polym. Adv. Technol. 29 (2018) 1138–1149, https://doi.org/10.1002/pat.4225;

(b) K.V. Plakas, A. Mantza, S.D. Sklari, V.T. Zaspalis, A.J. Karabelas, Heterogeneous Fenton-like oxidation of pharmaceutical diclofenac by a catalytic iron-oxide ceramic microfiltration membrane, Chem. Eng. J. 373 (2019) 700–708, https://doi.org/10.1016/j.cej.2019.05.092.
[130] H. Wei, E. Wang, Nanomaterials with enzyme-like characteristics (nanozymes): next-generation artificial enzymes, Chem. Soc. Rev. 42 (2013) 6060–6093, https://doi.org/10.1039/C3CS35486E.
[131] D. Horak, J. Kucerova, L. Korecka, B. Jankovicova, J. Palarcik, P. Mikulasek, Z. Bílkova, New monodisperse magnetic polymer microspheres biofunctionalized for enzyme catalysis and bioaffinity separations, Macromol. Biosci. 12 (2012) 647–655, https://doi.org/10.1002/mabi.201100393.
[132] H.H.P. Yiu, M.A. Keane, Enzyme–magnetic nanoparticle hybrids: new effective catalysts for the production of high value chemicals, J. Chem. Technol. Biotechnol. 87 (2012) 583–594, https://doi.org/10.1002/jctb.3735.
[133] (a) S.A. Ansari, Q. Husain, Potential applications of enzymes immobilized on/in nano materials: A review, Biotechnol. Adv. 30 (2012) 512–523, https://doi.org/10.1016/j.biotechadv.2011.09.005;
(b) J. Garcia, Y. Zhang, H. Taylor, O. Cespedes, E.W. Michael, D. Zhou, Multilayer enzyme-coupled magnetic nanoparticles as efficient, reusable biocatalysts and biosensors, Nanoscale 3 (2011) 3721–3730, https://doi.org/10.1039/C1NR10411J.
[134] Y. Li, X. Zhang, C. Deng, Functionalized magnetic nanoparticles for sample preparation in proteomics and peptidomics analysis, Chem. Soc. Rev. 42 (2013) 8517–8539, https://doi.org/10.1039/C3CS60156K.
[135] I. Mahmood, I. Ahmad, G. Chen, L. Huizhou, A surfactant-coated lipase immobilized in magnetic nanoparticles for multicycle ethyl isovalerate enzymatic production, Biochem. Eng. J. 73 (2013) 72–79, https://doi.org/10.1016/j.bej.2013.01.017.
[136] S.C. Chen, D.C. Sheu, K.J. Duan, Production of fructooligosaccharides using β-fructofuranosidase immobilized onto chitosan-coated magnetic nanoparticles, J. Taiwan Inst. Chem. Eng. 45 (2014) 1105–1110, https://doi.org/10.1016/j.jtice.2013.10.003.
[137] H. Tan, W. Feng, P. Ji, Lipase immobilized on magnetic multi-walled carbon nanotubes, Bioresour. Technol. 115 (2012) 172–176, https://doi.org/10.1016/j.biortech.2011.10.066.
[138] W.J. Goh, V.S. Makam, J. Hu, L. Kang, M. Zheng, S.L. Yoong, C.N.B. Udalagama, G. Pastorin, Iron oxide filled magnetic carbon nanotube–enzyme conjugates for recycling of amyloglucosidase: toward useful applications in biofuel production process, Langmuir 28 (2012) 16864–16873, https://doi.org/10.1021/la303046m.
[139] (a) A. Dayal, K. Loos, M. Noto, S.W. Chang, C. Spagnoli, K.V.P.M. Shafi, A. Ulman, M. Cowman, R.A. Gross, Activity of Candida rugosa Lipase Immobilized on γ-Fe2O3 magnetic nanoparticles, J. Am. Chem. Soc. 125 (2003) 1684–1685, https://doi.org/10.1021/ja021223n;
(b) S.H. Huang, M.H. Liao, D.H. Chen, Direct binding and characterization of lipase onto magnetic nanoparticles, Biotechnol. Prog. 19 (2003) 1095–1100, https://doi.org/10.1021/bp025587v;
(c) X. Gao, K.M.K. Yu, K.Y. Tam, S.C. Tsang, Colloidal stable silica encapsulated nano-magnetic composite as a novel bio-catalyst carrier, Chem. Commun. 24 (2003) 2998–2999, https://doi.org/10.1039/B310435D.
[140] K. Ullah, M. Ahmad, S. Sultana, L.K. Teong, V.K. Sharma, A.Z. Abdullah, M. Zafar, Z. Ullah, Experimental analysis of di-functional magnetic oxide catalyst and its performance in the hemp plant biodiesel production, Appl. Energy 113 (2014) 660–669, https://doi.org/10.1016/j.apenergy.2013.08.023.
[141] R.M. Mehrasbi, J. Mohammadi, M. Peyda, M. Mohammadi, Covalent immobilization of Candida antarctica lipase on core-shell magnetic nanoparticles for production of biodiesel from waste cooking oil, Renew. Energy 101 (2017) 593–602, https://doi.org/10.1016/j.renene.2016.09.022.
[142] C.Y. Yu, L.Y. Huang, I. Lee, S.L. Kuan, Optimized production of biodiesel from waste cooking oil by lipase immobilized on magnetic nanoparticles, Inter. J. Mole. Sci. 14 (2013) 24074–24086, https://doi.org/10.3390/ijms141224074.
[143] A. Wang, P. Sudarsanam, Y. Xu, H. Zhang, H.S. Yang Li, Functionalized magnetic nanosized materials for efficient biodiesel synthesis via acid–base/enzyme catalysis, Green Chem. 22 (2020) 2977–3012.
[144] S.J. Sanchez, L.H. Jose Martınez, P.S. Ceniceros, G. Lopez, H. Saade, M.A. Medina-Morales, R.R. Gonzalez, C.N. Aguilar, A. Ilyina, Cellulases immobilization on chitosan-coated magnetic nanoparticles: application for Agave Atrovirens lignocellulosic biomass hydrolysis, Bioprocess. Biosyst. Eng. 40 (2017) 9–22, https://doi.org/10.1007/s00449-016-1670-1.
[145] S. Sayin, E. Yilmaz, M. Yilmaz, Improvement of catalytic properties of Candida Rugosalipase by sol–gel encapsulation in the presence of magnetic calix[4] arenenanoparticles, Org. Biomol. Chem. 9 (2011) 4021–4024, https://doi.org/10.1039/C1OB05115F.
[146] J.C. Lewis, P.S. Coelho, F.H. Arnold, Enzymatic functionalization of carbon–hydrogen bonds, Chem. Soc. Rev. 40 (2011) 2003–2021, https://doi.org/10.1039/C0CS00067A.
[147] M.L. Davies Huw, J. Du Bois, J.Q. Yu, Tionalization in organic synthesis, Chem. Soc. Rev. 40 (2011) 1855–1856, https://doi.org/10.1039/C1CS90010B.
[148] Q. Zhang, X. Han, B. Tang, Preparation of a magnetically recoverable biocatalyst support on monodisperse Fe3O4 nanoparticles, RSC Adv. 3 (2013) 9924–9934, https://doi.org/10.1039/C3RA40192H.
[149] M. Vinoba, M. Bhagiyalakshmi, S.K. Jeong, S.C. Nam, Y. Yoon, Carbonic anhydrase immobilized on encapsulated magnetic nanoparticles for CO2 sequestration, Chem. Eur. J. 18 (2012) 12028–12034, https://doi.org/10.1002/chem.201201112.
[150] (a) J. Mukherjee, M.N. Gupta, Alpha chymotrypsin coated clusters of Fe3O4nanoparticles for biocatalysis in low water media, Chem. Cent. J. 6 (2012) 133, https://doi.org/10.1186/1752-153X-6-133;
(b) M. Iram, A. Ishfaq, C. Guo, H. Liu, A surfactant-coated lipase immobilized in magnetic nanoparticles for multicycle ethyl isovalerate enzymatic production, Bio. Eng. J. 73 (2013) 72–79, https://doi.org/10.1016/j.bej.2013.01.017;
(c) E. Ozyilmaza, S. Sayina, M. Arslanb, M. Yilmaz, Improving catalytic hydrolysis reaction efficiency of sol–gel-encapsulated Candida rugosa lipase with magnetic β-cyclodextrin nanoparticles, Colloid. Surf. B: Biointerfaces 113 (2014) 182–189, https://doi.org/10.1016/j.colsurfb.2013.08.019.
[151] W. Wang, Y. Xu, D.I.C. Wang, Z. Li, Recyclable nanobiocatalyst for enantioselective sulfoxidation: facile fabrication and high performance of chloroperoxidase-coated magnetic nanoparticles with iron oxide core and polymer shell, J. Am. Chem. Soc. 131 (2009) 12892–12893, https://doi.org/10.1021/ja905477j.
[152] Y.Z. Chen, C.T. Yang, C.B. Ching, R. Xu, Immobilization of lipases on hydrophobilized zirconia nanoparticles: highly enantioselective and reusable biocatalysts, Langmuir 24 (2008) 8877–8884, https://doi.org/10.1021/la801384c.
[153] (a) J. Wencel, F. Glorius, C–H bond activation enables the rapid construction and late-stage diversification of functional molecules, Nat. Chem. 5 (2013) 369–375, https://doi.org/10.1038/nchem.1607;
(b) J. Yamaguchi, A.D. Yamaguchi, K. Itami, C-H bond functionalization: emerging synthetic tools for natural products and pharmaceuticals, Angew. Chem. Int. Ed. 51 (2012) 8960–9009, https://doi.org/10.1002/anie.201201666;
(c) D.J. Schipper, K. Fagnou, Direct arylation as a synthetic tool for the synthesis of thiophene-based organic electronic materials, Chem. Mater. 23 (2011) 1594–1600, https://doi.org/10.1021/cm103483q.
[154] M.A. Zolfigol, R. Ayazi-Nasrabadi, S. Baghery, Synthesis of the first nanomagnetic particles with semicarbazide-based acidic ionic liquid tag: an efficient catalyst for the synthesis of 3,3′-(arylmethylene)bis(4-hydroxycoumarin) and 1-carbamato-alkyl-2-naphthol derivatives under mild and green conditions, Appl. Organomet. Chem. 30 (2016) 500–509, https://doi.org/10.1002/aoc.3461.
[155] S. Khaef, A. Rostami, V. Khakyzadeh, M.A. Zolfigolb, A. Taherpoura Avat, M. Yarie, Regioselective Ortho-C-H sulfenylation of free phenols catalyzed by Co (II)-immobilized on silica-coated magnetic nanoparticles, Mol. Catal. 484 (2020) 110772, https://doi.org/10.1016/j.mcat.2020.110772.
[156] (a) T.G. Saint-Denis, R.Y. Zhu, G. Chen, Q.F. Wu, J.Q. Yu, Enantioselective C (sp3)–H bond activation by chiral transition metal catalysts, Science 359 (2018) 6377, https://doi.org/10.1126/science.aao4798;
(b) M.I. Lapuh, S. Mazeh, T. Besset, Chiral transient directing groups in transition-metal-catalyzed enantioselective C–H bond functionalization, ACS Catal. 10 (2020) 12898–12919, https://doi.org/10.1021/acscatal.0c03317.
[157] R.B.N. Baig, M.N. Nadagouda, R.S. Varma, Magnetically retrievable catalysts for asymmetric synthesis, Coord. Chem. Rev. 287 (2015) 137–156, https://doi.org/10.1016/j.ccr.2014.12.017.
[158] Y. Kong, R. Tan, L. Zhao, D. Yin, L-Proline supported on ionic liquid-modified magnetic nanoparticles as a highly efficient and reusable organocatalyst for direct asymmetric aldol reaction in water, Green Chem. 15 (2013) 2422–2433, https://doi.org/10.1039/C3GC40772A.
[159] S. Ranjbar, P. Riente, C. Rodríguez-Escrich, J. Yadav, K. Ramineni, M.A. Pericas, Polystyrene or magnetic nanoparticles as support in enantioselective organocatalysis? A case study in friedel–crafts chemistry, Org. Lett. 18 (2016) 1602–1605, https://doi.org/10.1021/acs.orglett.6b00462.
[160] S. Pagoti, T. Ghosh, J. Dash, Synthesis of magnetic nanoparticles and polymer supported imidazolidinone catalysts for enantioselective Friedel-crafts alkylation of indoles, ChemistrySelect 1 (2016) 386–4391, https://doi.org/10.1002/slct.201600995.
[161] S.X. Cao, J.X. Wang, Z.J. He, Magnetic nanoparticles supported cinchona alkaloids for asymmetric Michael addition reaction of 1,3-dicarbonyls and maleimides, Chin. Chem. Lett. 29 (2018) 201–204, https://doi.org/10.1016/j.cclet.2017.06.022.
[162] T. Zeng, L. Yang, R. Hudson, G. Song, A.R. Moores, C.J. Li, Fe3O4 nanoparticle-supported copper(I) pybox catalyst: magnetically recoverable catalyst for enantioselective direct-addition of terminal alkynes to imines, Org. Lett. 13 (2011) 442–445, https://doi.org/10.1021/ol102759w.
[163] P.C. Ray, H. Yu, P.P. Fu, Toxicity and environmental risks of nanomaterials: challenges and future needs, J. Environ. Sci. Health C Environ. Carcinog. Ecotoxicol Rev. 27 (2009) 1–35, https://doi.org/10.1080/10590500802708267.
[164] (a) C. Sun, J.S. Lee, M. Zhang, Magnetic nanoparticles in MR imaging and drug delivery, Adv. Drug Deliv. Rev. 60 (2008) 1252–1265, https://doi.org/10.1016/j.addr.2008.03.018;
(b) A. Akbarzadeh, M. Samiei, S. Davaran, Magnetic nanoparticles: preparation, physical properties, and applications in biomedicine, Nanoscale Res. Lett. 7 (2012) 144, https://doi.org/10.1186/1556-276X-7-144;
(c) Z.R. Stephen, F.M. Kievit, M. Zhang, Magnetite nanoparticles for medical MR imaging, Mater Today (Kidlington) 14 (2011) 330–338, https://doi.org/10.1016/S1369-7021(11)70163-8;
(d) R. Mayne, J. Whiting, A. Adamatzky, Toxicity and applications of internalised magnetite nanoparticles within live paramecium caudatum cells, BioNanoSci. 8 (2018) 90–94, https://doi.org/10.1007/s12668-017-0425-z.
[165] L.L. Muldoon, M. Sandor, K.E. Pinkston, E.A. Neuwelt, Imaging, distribution, and toxicity of superparamagnetic iron oxide magnetic resonance nanoparticles in the rat brain and intracerebral tumor, Neurosurgery 57 (2005) 785–796, https://doi.org/10.1093/neurosurgery/57.4.785.

[166] D.E. Sosnovik, M. Nahrendorf, R. Weissleder, Molecular magnetic resonance imaging in cardiovascular medicine, Circulation 115 (2007) 2076–2086, https://doi.org/10.1161/CIRCULATIONAHA.106.658930.
[167] X. Peng, L. Manna, W. Yang, J. Wickham, E. Scher, A. Kadavanich, A.P. Alivisatos, Shape control of CdSe nanocrystals, Nature 404 (2000) 59–61, https://doi.org/10.1038/35003535.
[168] H.S. Choi, W. Liu, P. Misra, E. Tanaka, J.P. Zimmer, B. Itty Ipe, M.G. Bawendi, J. V. Frangioni, Renal clearance of quantum dots, Nat. Biotechnol 25 (2007) 1165–1170. https://doi.org/10.1038/nbt1340.
[169] S.J. Lee, J.R. Jeong, S.C. Shin, J.C. Kim, Y.H. Chang, Y.M. Chang, J.D. Kim, Nanoparticles of magnetic ferric oxides encapsulated with poly(D,L latide-co-glycolide) and their applications to magnetic resonance imaging contrast agent, J. Magn. Magn. Mater. 272-276 (2004) 2432–2433, https://doi.org/10.1016/j.jmmm.2003.12.416.
[170] (a) H.A. Jeng, J. Swanson, Toxicity of metal oxide nanoparticles in mammalian cells, J. Environ Sci Health A Tox Hazard Subst Environ Eng. 41 (2006) 2699–2711, https://doi.org/10.1080/10934520600966177;
(b) N. Singh, G.J. Jenkins, R. Asadi, S.H. Doak, Potential toxicity of superparamagnetic iron oxide nanoparticles (SPION), Nano Rev. 1 (2010), https://doi.org/10.3402/nano.v1i0.5358;
(c) B. Ankamwar, T.C. Lai, J.H. Huang, R.S. Liu, M. Hsiao, C.H. Chen, Y.K. Hwu, Biocompatibility of Fe3O4 nanoparticles evaluated by in vitro cytotoxicity assays using normal, glia and breast cancer cells, Nanotechnology 21 (2010) 75102, https://doi.org/10.1088/0957-4484/21/7/075102.
[171] N. Singh, Conference scene - nanotoxicology: health and environmental impacts, Nanomedicine (Lond) 4 (2009) 385–390, https://doi.org/10.2217/nnm.09.20.
[172] Y.X. Wang, S.M. Hussain, G.P. Krestin, Superparamagnetic iron oxide contrast agents: physicochemical characteristics and applications in MR imaging, Eur. Radiol. 11 (2001) 2319–2331, https://doi.org/10.1007/s003300100908.
[173] M. Aliakbari, E. Mohammadian, A. Esmaeili, Z. Pahlevanneshan, Differential effect of polyvinylpyrrolidone-coated superparamagnetic iron oxide nanoparticles on BT-474 human breast cancer cell viability, Toxicol In Vitro 54 (2019) 114–222, https://doi.org/10.1016/j.tiv.2018.09.018.
[174] Y. Liu, J. Li, K. Xu, J. Gu, L. Huang, L. Zhang, N. Liu, J. Kong, M. Xing, L. Zhang, L. Zhang, Characterization of superparamagnetic iron oxide nanoparticle-induced apoptosis in PC12 cells and mouse hippocampus and striatum, Toxicol. Lett. 292 (2018) 151–161, https://doi.org/10.1016/j.toxlet.2018.04.033.
[175] C. Saengruengrit, P. Ritprajak, S. Wanichwecharungruang, A. Sharma, G. Salvan, D.R. Zahn, N. Insin, The combined magnetic field and iron oxide-PLGA composite particles: Effective protein antigen delivery and immune stimulation in dendritic cells, J. Colloid. Interface Sci. 520 (2018) 101–111, https://doi.org/10.1016/j.jcis.2018.03.008.
[176] Z. Sadeghi, P. Maleki, F. Shahabi, S.A.M. Bondarkhilli, M. Masoumi, M. Taheri, M. Mohammadi, J. Raheb, Surface modification of superparamagnetic iron oxide (SPION) and comparison of cytotoxicity effect of mPEG2000-PEI-SPION and mPEG750-PEI-SPION on the human embryonic carcinoma stem cell, NTERA2 cell line, Hum. Antibodies 28 (2020) 159–167, https://doi.org/10.3233/HAB-200403.
[177] A.A. Mieloch, M. Zurawek, M. Giersig, N. Rozwadowska, J.D. Rybka, Bioevaluation of superparamagnetic iron oxide nanoparticles (SPIONs) functionalized with dihexadecyl phosphate (DHP), Sci. Rep. 10 (2020) 2725, https://doi.org/10.1038/s41598-020-59478-2.
[178] J.H. Lee, B. Schneider, E.K. Jordan, W. Liu, J.A. Frank, Synthesis of complexable fluorescent superparamagnetic iron oxide nanoparticles (FL SPIONs) and cell labeling for clinical application, Adv. Mater. 20 (2008) 2512–2516, https://doi.org/10.1002/adma.200800223.
[179] J.A. Frank, S.A. Anderson, H. Kalsih, E.K. Jordan, B.K. Lewis, G.T. Yocum, Methods for magnetically labeling stem and other cells for detection by in vivo magnetic resonance imaging, Cytotherapy 6 (2004) 621–625, https://doi.org/10.1080/14653240410005267-1.
[180] (a) S. Dey, T.K. Maiti, Superparamagnetic nanoparticles and RNAi-mediated gene silencing: evolving class of cancer diagnostics and therapeutics, J. Nanomater. (2012) 129107, https://doi.org/10.1155/2012/129107;
(b) Y. Chen, G. Lian, C. Liao, W. Wang, L. Zeng, C. Qian, K. Huang, X.J. Shuai, Characterization of polyethylene glycol-grafted polyethylenimine and superparamagnetic iron oxide nanoparticles (PEG-g-PEI-SPION) as an MRI-visible vector for siRNA delivery in gastric cancer in vitro and in vivo, J. Gastroenterol 48 (2013) 809–821, https://doi.org/10.1007/s00535-012-0713-x.
[181] C.D. Novina, P.A. Sharp, The RNAi revolution, Nature 430 (2004) 161–164, https://doi.org/10.1038/430161a.
[182] F. Cengelli, D. Maysinger, F. Tschudi-Monnet, X. Montet, C. Corot, A. Petri-Fink, H. Hofmann, L. Juillerat-Jeanneret, Interaction of Functionalized Superparamagnetic Iron Oxide Nanoparticles with Brain Structures, J. Pharmacol. Exp. Ther. 318 (2006) 108–116, https://doi.org/10.1124/jpet.106.101915.
[183] I.M. Vahid, M.M. Hossein, R. Pooneh, B. Azam, A. Ehsan, Modification of SPION nanocarriers for siRNA delivery: a therapeutic strategy against HIV infection, Vaccine Research 6 (2019) 43–49.
[184] P. Galvin, D. Thompson, K.B. Ryan, A. McCarthy, A.C. Moore, C.S. Burke, M. Dyson, B.D. MacCraith, Y.K. Gun'ko, M.T. Byrne, Y. Volkov, Nanoparticle-based drug delivery: case studies for cancer and cardiovascular applications, Cell. Mol. Life Sci. 69 (2012) 389–404, https://doi.org/10.1007/s00018-011-0856-6.
[185] A. Nemmar, S. Beegam, P. Yuvaraju, J. Yasin, S. Tariq, S. Attoub, B.H. Ali, Ultrasmall superparamagnetic iron oxide nanoparticles acutely promote thrombosis and cardiac oxidative stress and DNA damage in mice, Part Fibre Toxicol. 13 (2015) 22, https://doi.org/10.1186/s12989-016-0132-x.
[186] Z. Sun, L. Yang, Z. Sun, L. Yang, K.F. Chen, G.W. Chen, Y.P. Peng, J.K. Chen, G. Suo, J. Yu, W.C. Wang, C.H. Lin, Nano zerovalent iron particles induce pulmonary and cardiovascular toxicity in an in vitro human co-culture model, Nanotoxicology 10 (2016) 881–890, https://doi.org/10.3109/17435390.2015.1133861.
[187] L. Barhoumi, A. Oukarroum, L.B. Taher, L.S. Smiri, H. Abdelmelek, D. Dewez, Effects of superparamagnetic iron oxide nanoparticles on photosynthesis and growth of the aquatic plant Lemna gibba, Arch. Environ. Contam. Toxicol. 68 (2015) 510–520, https://doi.org/10.1007/s00244-014-0092-9.
[188] (a) L. Barhoumi, D. Dewez, Toxicity of superparamagnetic iron oxide nanoparticles on green alga chlorella vulgaris, Biomed. Res. Int. (2013) 647974, https://doi.org/10.1155/2013/647974;
(b) X. Chen, X. Zhu, R. Li, H. Yao, Z. Lu, X. Yang, Photosynthetic toxicity and oxidative damage induced by nano-Fe3O4 on chlorella vulgaris in aquatic environment, Open J. Ecol. 2 (2012) 21, https://doi.org/10.4236/oje.2012.21003.
[189] J. Hurtado-Gallego, G. Pulido-Reyes, M. González-Pleiter, G. Salas, F. Leganés, R. Rosal, F. Fernández-Piñas, Toxicity of superparamagnetic iron oxide nanoparticles to the microalga Chlamydomonas reinhardtii, Chemosphere 238 (2020) 124562, https://doi.org/10.1016/j.chemosphere.2019.124562.